Response to Reviewers
We would like to thank both the reviewers for the valuable comments and suggestions. We have tried to implement all the suggestions proposed by the reviewers and hope that the new version is structured in a better way to ease the readers and is suitable for publication in ACP.

Reviewer 1
Summary
The manuscript reports on an extensive set of simulations with the GISS-E2.1 Earth system model spanning both near past and future, which investigate the impact of changing anthropogenic aerosol emissions on Arctic climate. The study is interesting and in principle suitable for ACP, but in places I find the text quite hard to follow to the point that I am not sure whether the results support the conclusions. However, this is mainly due to the presentation of the results (both in text and figures), not the results themselves and I would be happy to review a revised version of the manuscript again.
Response: We thank the reviewer for the general positive response to the manuscript. We have restructured the manuscript, as well as the presentation of the results and discussion.

General comments
The terms used in the radiative forcing discussion are somewhat outdated. In AR5, the IPCC recommends moving from direct and indirect effects to using radiative forcing due to aerosol-radiation interactions (RFARI) and due to aerosol-cloud interactions (RFACI), together with their resulting rapid adjustments and the final effective radiative forcing (see chapter 7 of AR5). In order to keep up with this development, I strongly recommend rewriting the text with respect to this.
Response: The new version now is using the RF_{ARI} (Section 3.2)

Many parts of the results section contain long listings of changes of different quantities in the different scenarios for several time periods and are quite hard to follow. I'm wondering whether it would be more beneficial to organise these results in tables and rather concentrate on systematic or principle differences between the different simulations. For instance, if there is a systematic decrease in sulfate emissions in the ssp simulations, how does this translate into Arctic sulfate burdens, radiative forcings and temperatures and how are the results of the Eclipse simulations different from that?
Response: We thank the reviewer for the suggestion. We now have more tables in the manuscript and tried to focus more on the differences between different scenarios (Section 3.2). However, while we can directly connect the forcings to burdens of individual aerosol components, it is not possible to further extent this to climate impacts per species as this requires explicit sensitivity simulations.

In the Discussion section I am missing a discussion on how the biases that have been found in the model evaluation section may affect the modelled climate impacts in the future and if and how much that adds to the uncertainty of the results.
Response: We have now added the following sentence in section 3.1.2 (Lines 518-524): "Results show that both absorbing (BC) and scattering aerosols (OC and SO_4^{2-}) are underestimated by the GISS-E2.1 model, implying that these biases can partly cancel out their impacts on radiative forcing due to aerosol-radiation interactions. This, together with the very low biases in surface temperatures suggests that aerosols over the Arctic do not affect the Arctic climate and that the changes in Arctic climate are mainly driven by changes due to greenhouse gas concentrations.".

Specific comments

Abstract

• lines 30—32: add “In the simulations” to “Surface aerosol levels ... have been significantly underestimated”

Response: Sentence is changed to: “Results showed that the simulations have underestimated observed surface aerosol levels, in particular black carbon (BC) and sulfate (SO_4^{2-}), by more than 50%, with the smallest biases calculated for the atmosphere-only simulations, where winds are nudged to reanalysis data.” (Lines 31-33).

• line 32: “The nudged simulations” have not been defined at this point. I recommend changing this to “...when winds were nudged to reanalysis data”

Response: Done, see above response (Lines 33).

• line 34: A change from “fully coupled simulations” to “simulations where atmosphere and ocean where coupled’ or something similar might be better at this point.

Response: We have now phrased the sentence as following: “In addition, simulations, where atmosphere and ocean are fully-coupled, had slightly smaller biases in aerosol levels compared to atmosphere only simulations without nudging.” (Lines 35-37)

• lines 37—48: None of the simulation names have been introduced at this point (naturally) and it might therefore be hard for the potential reader to grasp the general message of the abstract. I therefore recommend to re-write this paragraph. In my opinion a “maximum vs minimum effect”-type of discussion would be easier to digest at this point.

Response: We have rewritten the paragraph accordingly (Lines 39-55).

• line 46: remove “both”

Response: Removed.

• line 46—47: Change “In 2050” to “By 2050”?

Response: Changed (Line 53).

• line 52: “while scenarios no or little…” – add “with”

Response: We have now rewritten this paragraph (Lines 57-60).

• line 53: “lead” --> “leads”

Response: See above response (Line 57).

Introduction

• line 71: “This contribution ... puts” or “These contributions ... put” ?

Response: Corrected accordingly (Line 77).

• lines 80 --- 85: “BC” and “SO42-” have already been defined.

Response: Corrected accordingly (Line 86-89).

• line 90: I’m not sure myself: Is BC depositing on snow and ice or is BC being deposited, e.g. can you use the active form here?

Response: Thanks for raising this. Indeed, the BC is deposited on snow. We have corrected this accordingly (Line 96).

• line 93: While you talk about the lifetime and vertical extent effects here, if I understand the model description correctly, these effects are not included in your simulation, or are they?
Response: These affects are taken into account in the model. Aerosols affect clouds via first indirect (CDNC) and semi-direct effects. We have now added the following text in lines 204-209: "The parameterization described by Menon and Rotstayn (2006) that we use only affects CDNC, not cloud droplet size, which is not explicitly calculated in GISS-E2.1. Following the change in CDNC, we do not stop the model from changing either LWP or precipitation rates, since the clouds code sees the different CDNC and responds accordingly. What we do not include is the 2nd indirect effect (autoconversion).".

• lines 111—112: Is that global emissions?
Response: "Global" is added (Line 125)

Materials and Methods
• line 169—174: Can you elaborate on how that works? If Everything except dust and sea salt is externally mixed, does that mean that the model assumes separate sulphate, nitrate, BC and OC particles? How do you then treat the sulphate and nitrate coating of the dust particles?
Response: Thanks for pointing this wrong phrase. We have now corrected this section (Lines 188-191).

• Even though SOA production in the model is described in Tsigaridis and Kanakidou, maybe you could describe it briefly here as well. In particular, what are the assumptions of how SOA formation affects OC concentrations. This is important, as you attribute higher OC concentrations to higher SOA formation, but it is not clear, how that is modelled. Do you have separate SOA tracers or does VOC oxidation lead directly to OC production in the atmosphere? In the former case, how do you convert SOA into OC. Am I right in assuming that OC from the emission inventories is emitted as particulate matter?
Response: We added the following in the text (Lines 196-202): "SOA is calculated from terpenes and other reactive volatile organic compounds (VOCs) using NOx-dependent calculations of the 2-product model, as described in Tsigaridis and Kanakidou (2007). Isoprene is explicitly used as a source, while terpenes and other reactive VOCs are lumped on a-pinene, taking into account their different reactivity against oxidation. The semi-volatile compounds formed can condense on all submicron particles except sea salt and dust. In the model, an OA to OC ratio of 1.4 used.". In addition, we now use OA instead of OC and explained this in lines 342-344 as: "The GISS-E2.1 ensemble has been evaluated against surface observations of BC, organic aerosols (sum of OC and secondary organic aerosols (SOA), referred as OA in the rest of the paper)…".

• line 178—180: How does that work? If the model treats the first indirect (i.e. aerosol concentrations affecting CDNC and (I guess) cloud droplet size), how do you stop the model from changing LWP and precipitation rates?
Response:We now added the following to the manuscript (Lines 204-209): "The parameterization described by Menon and Rotstayn (2006) that we use only affects CDNC, not cloud droplet size, which is not explicitly calculated in GISS-E2.1. Following the change in CDNC, we do not stop the model from changing either LWP or precipitation rates, since the clouds code sees the different CDNC and responds accordingly. What we do not include is the 2nd indirect effect (autoconversion)."

• line 186: I guess this is also just the first indirect effect?

Response: Yes. We have now clarified this (Line 215).

• Section 2.2.3: Do I understand this correctly: Eclipse emissions have been complemented in some sectors by using CEDS emissions, while CEDS emissions are entirely "original", or did you also have to complement CEDS emissions in some sectors?
Response: Yes this is correct. We have now slightly modified this section for clarity (Lines 282-290): "In the GISS-E2.1 Eclipse simulations, the non-methane volatile organic carbons (NMVOC) emissions are chemically speciated assuming the SSP2-4.5 VOC composition profiles. In the Eclipse simulations, biomass burning emissions are taken from the CMIP6 emissions, which have been pre-processed to include the agricultural waste burning emissions from the EclipseV6b dataset, while the rest of the biomass burning emissions are taken as the original CMIP6 biomass burning emissions. In addition to the biomass burning emissions, the aircraft emissions are also taken from the CMIP6 database to be used in the Eclipse simulations."

• Lines 284 – 288: You have been quite thorough in explaining the differences between the ECLIPSE scenarios, but the differences between the different CEDS scenarios is quite compact. What, for instance, does "lowNTCF" mean?
Scenario: We thank the reviewer to raise this. We have now described the different CMIP6 scenarios (Lines 316-331).

• Section 2.2.3: How do the emissions and concentrations of Greenhouse gases evolve in the simulations? Are they kept fixed to capture the aerosol effect, or do they change? In the latter case, please elaborate on how you separate the aerosol effects from the Greenhouse gas effects.
Response: All scenarios use the same prescribed global and annual mean GHG concentrations. We have now added this section to the manuscript (Lines 334-337): "We have employed prescribed global and annual mean greenhouse (CO_2 and CH_4) concentrations, where a linear increase in global mean temperature of 0.2 °C/decade from 2019 to 2050 was assumed, which are approximately in line with the simulated warming rates for the SSP2-4.5 scenario (AMAP, 2021).".

• Section 2.2.3: If emissions are provided at 0.5x0.5° resolution, but the model operates at 2x2.5° resolution, I'm guessing you re-grid the emissions somehow?
Response: Correct, we have now written this explicitly in the manuscript (Lines 281-282): "The Eclipse V6b and CEDS emissions on $0.5° \times 0.5°$ spatial resolution are regridded to $2° \times 2.5°$ resolution in order to be used in the various GISS-E2.1 simulations."

• lines 317—326: As a side note, it has become more and more common to co-locate modelling data and observations in time to reduce the effects of observational "data sparseness" mentioned here. I understand that this is probably out of scope of this study, but worth considering in the future.
Response: Thanks for the recommendations. We will consider this in future studies.

Results

• Figure 3: It would be quite beneficial to add the station names to the figure. Especially because some of the stations are discussed in the text.

Response:We have now added station numbers to Figure 3, instead of station names as this makes the plot very busy and messy. We have added the station numbers to the tables in the supplementary material.

• lines 395-398: Could these high bias outliers be a problem with the representativeness of the observations (e.g. too few data points, or quickly changing orography)? Trapper Creek, for instance, is right next to another, blue, point.
Response: Thanks for the suggestion. Yes, this can also be contributing to the biases due to large grid boxes in the model grid. We have also included this as a potential explanation to the bias (Lines 452-459): "Such underestimations at high latitudes have also been reported by many previous studies (e.g. Skeike et al., 2011; Eckhardt et al., 2015; Lund et al., 2017, 2018; Schacht et al., 2019; Turnock et al., 2020), pointing to a variety of reasons including uncertainties in emission inventories, errors in the wet and dry deposition schemes, the absence or underrepresentation of new aerosol formation processes, and the coarse resolution of global models leading to errors in emissions and simulated meteorology, as well as in representation of point observations in coarse model grid cells."

• lines 433—436: Later in the article (line 774) you state that a higher cloud fraction may lead to higher in-cloud SO4 production – please add this statement also here.
Response: We have now added this in lines 494-497: "The Eclipse_AMIP_NCEP simulation is biased higher (NMB=-53%) compared to the Eclipse_AMIP (NMB=-50%), probably due to higher cloud fraction simulated by the nudged version (see section 3.1.6), leading to higher in-cloud SO_4^{2-} production."

• Tables 3 and 4: Please consider breaking up these tables into two parts and displaying them in portrait mode. At least in electronic form it would make the manuscript easier to read.
Response: We have now divided these tables into two (Tables 3a and 3b).

• Why do the AMIP runs have such a high bias in SST, if SST is prescribed?
• lines 461—462: Is that due to model resolution? After all, SIC is prescribed, right?
Response: This is due to differences with datasets used in the model input and the dataset used to evaluate the model. This is now described in lines 223-225 and 529-531.

• lines 470—471: Do you mean the climatology of the cloud fraction for the entire year here?
Response: Yes, we have now added this to the sentence (Line 546)

• Figure 5a: I think here it would be worth mentioning that the seasonal trends in observed and modelled cloud fraction trends are reversed. Looking at panels b and c, it almost looks like the model produces to few water or mixed-phase clouds during the winter months, did I get this right?
Response: We have now re-written this sentence (Lines 539-543): "All simulations overestimate the climatological (1995-2014) mean total cloud fraction by 21% to 25% during the extended winter months (October through February), where the simulated seasonality is anti-correlated in comparison to AVHRR CLARA-A2 observations, whereas, a good correlation is seen during the summer months irrespective of the observational data reference."

• lines 474 – 478: This sentence is very hard to grasp: Less overestimation due to an underestimation? Do you mean to say that you trust AVHRR CLARA-A2 less than

CALIPSO, because CALIPSO does a better job at separating bright surfaces from clouds? Also, you could add in line 466 that there you compare to AVH*RR data.*
Response: We have rephrased this sentence as (Lines 549-557): "The evaluation against CALIPSO data however shows much smaller biases (NMB = +3% to +6%). This is because in comparison to CALIPSO satellite that carries an active lidar instrument (CALIOP), the CLARA-A2 dataset has difficulties in separating cold and bright ice/snow surfaces from clouds thereby underestimating the cloudiness during Arctic winters. Here both datasets are used for the evaluation as they provide different observational perspectives and cover the typical range of uncertainty expected from the satellite observations. Furthermore, while the CLARA-A2 covers the entire evaluation period in current climate scenario, CALIPSO observations are based on 10-year data covering the 2007-2016 period."

• Figure 6 and Section 6.2: I take it that by Arctic burden you mean the integral over all grid boxes between 60 and 90° north and over all vertical levels, but then using monthly averages? Why do you use the unit kTon in the text, but Tg in the figures?
Response: This is correct, but the burdens are by default written as output so we do not do these calculations as a postprocessing of the data. We do not use monthly averages in these results in the manuscript. The figure is corrected now to included kTons instead of Tg.

• line 533: What do you mean by "better resolved"?
Response: We have now rewritten this section. We have now changed this sentence as (Lines 660-662): "This largest OA burden in the Eclipse_AMIP_NCEP simulation is attributed to the largest biogenic SOA burden calculated in this scenario, as well as a better-simulated transport from source regions due to the nudged winds (Figure S1).".

• lines 541-542: If you term it "reduction", I guess the number should be positive...
Response: We have now corrected this throughout the text.

• line 549 and following: How has statistical significance been tested?
Response: We used Mann-Kendall trend analyses to calculate trends and statistical significance. We have now written this in Lines (626-627).

• line 554—555: See my comment in the Materials and Methods section. If OC is a separate tracer, you should explain somewhere, how a larger SOA production leads to larger OC concentrations. If it is what I think (i.e. you talk the sum of OC and SOA species), I suggest calling it something else. Maybe organic aerosol (OA) or organic matter (OM) would be suitable?
Response: We now use OA instead of OC and explained this in lines 341-343 and 429-430 as: "The GISS-E2.1 ensemble has been evaluated against surface observations of BC, organic aerosols (sum of OC and secondary organic aerosols (SOA), referred as OA in the rest of the paper)…".

• Figure S1: This links directly to the comment above. Without any explanation, it is not really understandable what you are showing here.
Response: Corrected, see above response.

• line 580: ...because CLE levels off earlier (no further legislation after this point?). The calculated trend cannot really be 2015—2050.
Response: We cannot understand the comment. The CLE scenario is between 2015 and 2050.

• Figure 7: What are you actually plotting here? From the explanation in the text (double call to the radiation code with and without aerosols) it sounds like you are showing the radiative effect due to aerosol-radiation interaction (REARI) (see Chapter 7.3.4.1 of the IPCC AR5), formerly termed the "direct radiative effect". A radiative forcing due to aerosol-radiation interaction (RFARI) would be the change in REARI relative to some reference point, e.g. preindustrial levels. Please elaborate.
Response: This is correct. The plot and the text show the RF_{ARI}.

• line 595 – 602: Why do you only talk about Eclipse here?
Response: We thank the reviewer for pointing this out. We have now rewritten this part in a new separate sub-section (3.2.4).

• 595 – 597: Why is that? This is quite a substantial difference – can this be explained by differences in aerosol burdens alone?
Response: This difference is due to the larger sea-ice concentration simulated with the coupled model, leading to brighter surfaces compared to the AMIP simulations. This brighter surface also amplifies the effect of more positive BC forcing effect due to larger BC burdens simulated in the coupled model. This is now added in Lines 713-718.

• line 601—602: What is the meaning of the third value here?
Response: We have rewritten this section so this does not exist anymore. They used to show the mean of all eclipse future simulations (CLE and MFR combined), CLE simulations, and MFR simulations, respectively.

• Figure 7: Why do the AMIP runs differ so much from the other simulations (2000—2015)? Also, there is visible difference between the black and brown lines (NINT_Cpl and CMIP6_Cpl_Hist?) in the anthropogenic aerosol radiative forcings, byt the same difference is not visible for the total aerosol radiative forcing – what is compensating for the difference here?
Response: For the differences between AMIP and coupled simulations, please see the response above (Lines 718-718 in the manuscript). Regarding the difference in Figure 7 in the net vs anthropogenic RF_{ARI} between the coupled NINT and the coupled OMA simulation is mainly driven by the dust and sea-salt RF_{ARI}. We have now explained this in the text (Lines 618-623).

• If SOA can contribute to OC and if SOA can originate from both natural and anthropogenic sources, how can you separate the anthropogenic contribution of OC to the radiative forcing?
Response: The model output includes speciated forcings for the anthropogenic, biomass burning, and SOA aerosols. We have now added the following sentence in the text (Lines 611-615): "The instantaneous forcings are calculated with a double call to the model's radiation code, with and without aerosols. The model outputs separate forcing diagnostics for anthropogenic and biomass burning BC and OC, as well as biogenic SOA, making it possible to attribute the forcing to individual aerosol species.".

• Figure 8: how are the speciated forcings calculated?
Response: GISS-E2.1 can calculate the RFARI by the double-call to the radiation code (Lines 611-615).

• lines 640—651: This appears to be exactly the same text as lines 604—615.
Response: We thank the reviewer for noticing this, we have now corrected this section.

• line 650: What is higher to what here?
Response: We have now rephrased this sentence (Lines 742-744): "Overall, the changes in the different aerosol species leads to a more negative aerosol forcing by mid-century (2030-2050) compared to the 1990-2010 period."

• line 656: "sinnulations" --> "simulations"
Response: Corrected.

• line 657: You use the term "anomaly" the first time here – how is this calculated and what do you mean by "aerosol forcing anomaly"?
Response: We have rewritten this section and this does not exist anymore.

• Figure 9: In the figure you show only the surface temperatures between 2020 and 2050, but you talk a lot about temperature trends in earlier times – is there a reason for this? Also, it would be much easier to follow the discussion, if the observed trends would be added to the figure.
Response: We have rewritten this part (Section 3.3.1). We have also added the observed values in the plot (now Figure 10).

• Lines 665 – 673 I can't really believe the numbers you give in this paragraph. A 10° C/decade increase in surface air temperature is huge, even for the Arctic. As a reference, in the Figure 9 you show the surface temperatures between 2020 and 2050, which change by about 1-2°C in three decades. Please check your calculations or provide a figure, if the numbers are correct.
Response: We thank the reviewer for pointing this error. We have now corrected this (lines 760-767).

• 698: "warnings" --> "warmings"?
Response: Corrected.

• Figure 10: How statistically robust are these spatial distributions? Looking only at the SSP results (panels c, d and e), it looks like the changes are not very systematic in many regions, which makes me wonder how noisy the results are.
We now plot the statistically-significant (student t-test) changes in the pots and it is highlighted in the text (Lines 778-779) and figure captions.

• line 702: Figure 9 does not show SST.
Response: Corrected.

• line 712: Do you mean "Greenland sea"?
Response: Yes, this is now modified in the text (Lines 783-784).

• line 736: Here and in some other places where you compare the means of two time periods, you could consider replacing "... is projected to decrease by ... compared to ..." with "... is projected to be ... lower than ..."
Response: We have modified the text as suggested by the reviewer.

• Figure 11: Even though I the discussion is generally about the entire Arctic region, in this figure I'm wondering if it would be better to "zoom in" to where the changes are actually happening.
Response: We have changed the figure as suggested by the reviewer (now Figure 12).

• line 748: "Figure S1" --> "Figure S3"
• line 751: "Figure S2" shows SST
• line 754: "Figures S3—S7" --> "Figures S4—S7"
Response: We have restructured these figures and removed S4-S7 as suggested by the other reviewer.

Summary and Conclusions
• line 773: Like in the abstract, I would try to avoid using the names of the individual simulations in the conclusions.
Response: Implemented the suggestion.

• line 808: add "future"
Response: Added.

• lines 815 – 818. There appears to be one "Eclipse" too much.
Response: Corrected.

• line 826 – 829: Could one interpret this as the melting of sea ice acting buffering the changes in surface air temperatures?
Response: This part has been changed and corrected (Lines 902-909).

Reviewer 2

This study reports results from an extensive set of simulations with the GISS-E2.1 and two different emission inventories used to investigate the recent past and projected future changes in Arctic aerosols and aerosol-induced climate impacts. I find the study interesting and suitable within the scope of ACP. However, I also think it needs substantial further improvements before it can be accepted for publication. In particular, I find parts of the manuscript difficult to follow (the most notable example being the section on radiative forcing) and in some cases the possible reasons behind particular results could be better discussed. A better description of the experiments is needed for readers not within the AMAP group and I'm missing some context with impact due to other emissions than aerosols and precursors. In the introduction, the authors could better motivate why their study is important and timely. Finally, the figures could be visually more appealing. I think that improving the structure and readability should be quite feasible and some additional efforts will make a much stronger manuscript.

Response: We thank the reviewer for the positive response to our manuscript. We have tried to implement the changes the reviewer has suggested here.

Specific comments:

Line 30: "have been"? As in historical or in previous modeling work?

Response: Modified the sentence as (Lines 31-33): "Results showed that the simulations have underestimated observed surface aerosol levels…".

Line 33: Why also for climate parameters? What is different in the experimental setup?

Response: we mean both concentrations and climate (meteorological) parameters were simulated better in the CMIP6 ensemble, the simulations are not different for the different parameters.

Lines 37 onwards: would be useful to have the RF over the 1990-2014 period as well to understand changes in the scenarios.

Response: We have rewritten this paragraph following suggestions from both reviewers (Lines 39-52).

Line 46-48: Still due to changes in aerosols only? Should be more clear from the abstract hos greenhouse gases are treated.

Response: Correct. We have now added the following sentence to the abstract (Lines 28-29), and in related section in the Materials and Methods; Lines 334-337): "… while global annual mean greenhouse gas concentrations were prescribed and kept fixed in all simulations.".

Line 50-54: Similarly to the above comment, the role of aerosols vs. other emissions is a bit unclear.

Response: Same as above response.

Line 78: "mostly" – what are the remaining effects?

Response: We have now extended this part as (Lines 84-85: "They mostly affect climate by altering the amount of solar energy absorbed by Earth, as well as changing the cloud properties and indirectly affecting the scattering of radiation,…".

Line 88: “warming effects”: here and in the following paragraphs I would suggest the authors be a bit more precise with regards to positive and negative RF versus warming/cooling, with the latter used only when actual temperature estimates are given. Furthermore, perhaps be clear whether it’s surface warming or general.
Response: We have tried to modify the overall text accordingly.

Line 88: what are these aerosols? OC or all species?
Response: We have added ”organics” (Line 94).

Line 90-104: the rapid adjustments from BC should be mentioned (ref to e.g. Stjern et al. 2017, Takemura 2019).

Stjern, C. W., Samset, B. H., Myhre, G., Forster, P. M., Hodnebrog, Ø. Andrews, T., … Voulgarakis, A. (2017). Rapid adjustments cause weak surface temperature response to increased black carbon concentrations. Journal of Geophysical Research: Atmospheres, 122, 11,462– 11,481. https://doi.org/10.1002/2017JD027326

Takemura, T., Suzuki, K. Weak global warming mitigation by reducing black carbon emissions. Sci Rep **9,** 4419 (2019). https://doi.org/10.1038/s41598-019-41181-6
Response: We have now added a short section on the rapid adjustments (Lines 144-146).

Line 109: “response through aerosols” – something strange with the language?
Response: We have rephrased the sentence as (Lines 115-117): “The impact of aerosols on the Arctic climate change is mainly driven by a response to remote forcings (Gagné et al., 2015; Sand et al., 2015; Westervelt et al., 2015).”.

Line 109-onwards: Somewhere this section should mention/discuss long-range transport. While forcing exerted remotely is an important factor, there is also a lot of literature on the source attribution of Arctic aerosols. Given that Arctic burdens are shown later, the LRT is relevant to understand to interpret changes in burden over time.
Response: We have now added a short section on long-range transport (Lines 117-124).

Line 111: is this per unit global sulfur emission?
Response: Global, added to the sentence (Line 125).

Line 131: I think this paper actually removed aerosols entirely? Relevant for the response.
Response: Correct, we have now added this to the sentence (Lines 146-149): “Samset et al. (2018), using a multi-model ensemble of ocean coupled Earth system models (ESMs), where aerosol emissions were either kept at present-day conditions, or anthropogenic emissions of SO_2, and fossil fuel BC and OC were set to zero, showed…”.

Section 2.2: perhaps reconsider the number of small paragraphs? It becomes a bit broken up and the first sentences of the section are repeated later.
Response: We have slightly modified the section accordingly.

Section: 2.3: this is probably clear to people who are familiar with the AMAP runs, but to me it’s very unclear how other emissions (CO2, etc.) are treated in these experiments. Which in turn makes results hard to interpret. I think experiments could be a bit better explained.
Response: We have now provided with explanations on the different emission scenarios (in lines 315-331) and AMAP experiments (Lines 334-337).

Line 303: when I think of IMPROVE, I don't exactly think of the Arctic. Perhaps it could be useful to give the number of stations in each network that are within the relevant region? (yes, there are SI tables, but to help the reader).
Response: The IMPROVE measurements that are in the Arctic (>60oN), are all in Alaska. Thus, we have changed the text to make that clear (replacing "United States" with "Alaska"). There were 5 measurement locations in Alaska, all associated with IMPROVE, but some obtained from their PIs since they were difficult to obtain from the general IMPROVE data portal. There were 6 measurement locations in Europe, though not all associated with the EMEP network, and 1 measurement location in Canada/CABM. We don't include the number of sites in the text next to the networks however, since it is somewhat complicated when obtaining measurements from individual PIs instead of the network portals, and we wouldn't want to be in error.

Section 2.4.1: In later tables and figures satellite observations of AOD are mentioned, but I can't see those described here? Please clarify.
Response: In this paper we used a combined product developed by Sogacheva et al. (2020) by merging AOD from various different satellite products. We did not use here individual satellite AOD products. There is very detailed information in Sogacheva et al. (2020) about how they do it, and it is very technical. We think it would be unnecessary to discuss the details of that here.

Line 383-384: I don't understand this sentence and relationship. Please consider rephrasing.
Response: We have rephrased this sentence as (Lines 434-436): "The monthly observed and simulated time series for each station are accumulated per species in order to get a full Arctic timeseries data, which also includes spatial variation, to be used for the evaluation of the model."

Section 3.1: In general, an indication of the interannual variation around the climatological mean would be very useful, at least for observations when this can be added to the figures.
Response: We have now updated the Figures 2,4, and 5 to include the interannual variation in the observations and simulations.

Section 3.1.1: perhaps discuss the seasonal differences in the underestimation better.
Response: We have now added some more explanation throughout the model evaluation section.

Moreover, I'm not convinced by the inclusion of individual ensemble members as separate experiments. I think it rather adds unnecessary complexity and, in addition given how briefly these results are discussed in the text, could rather be an average and a ± range. (This goes for climate variables as well.)
Response: We now present only the ensemble means of the individual experiments.

Line 423-430: From Figure 3, it seems that OC is very well captured. This seems worth describing and explaining. It surprises me that the seasonal cycle of the observations is so different from BC. Is it a dominance by biogenic SOA?
Response: We have now added the following explanation (Lines 485-491): "As can be seen in Figure S1, the OA levels are dominated by the biogenic SOA, compared to anthropogenic and biomass burning OA. While OC and BC are emitted almost from similar sources, this biogenic-dominated OA seasonality also explains why simulated BC seasonality is not as

well captured, suggesting the underestimations in the anthropogenic emissions of these species, in particular during the winter. "

Figure 2: Is this an average over all stations? Please be specific.
Response: As explained in lines 434-436, the figure shows the monthly observed and simulated time series for each station are accumulated per species in order to get a full Arctic timeseries data.

Figure 1: Needs improvement. Difficult to see different colors.
Response: We have tried to increase visibility in the figure.

Section 3.1.2: Is it possible to place the GISS model in context of other CMIP model's performance here? Is this a typical feature? Would be useful.
Response: There is already some discussion on this in later sections (3.3.1 and 3.3.2) for surface temperatures and sea-ice extent, however focusing on the projected changes rather than model evaluation. Comparing GISS-E2.1 with other CMIP6 models is out of the scope of this paper and requires large amount of analysis.

Lines 555 onwards: I find the discussion around the role of SOA hard to follow. So OC in figure 6 includes SOA? What is the OA-OC conversion factor? Furthermore, I think more explanation of why these differences exist is needed, rather than just attributing one to the other.
Response: We now use OA instead of OC, which is the sum of OC and SOA (Lines 341-343).

Section 3.2: use same unit as figure 6?
Response: We have changed figure unit to kTon to be consistent with the text.

Section 3.3: this section needs some improvement.

- I would recommend using terminology RFari and RFaci. I also don't think you need to keep saying TOA radiative forcing, that's in the definition. Will help improve readability as well.

Response: We now use RF_{ARI} throughout the text.

- The section is difficult to follow with the many different time periods used. For instance, lines 595-602 gives a set of numbers that are not quite different from the sum of the aerosol RF in Figure 8. Lines 595-602 seems to give the RF due to changes in aerosols from 1990 to 2010 and then from 2030 to 2050, but what but the RF due to the difference from 2010 – 2030 and 2050?

Response: We have now restructured this section by combining with the burdens for the individual aerosol species, provided extra tables and tried to focus on the differences in the text.

- Figure 8: RF is already a delta, a perturbation vs. a baseline, so it's not clear to me what this figure is showing.

Response: The figure shows the difference between the 2030-2050 mean and 1990-2010 RFARI values for the different aerosol species.

- Some RF numbers have a ± range, but it doesn't seem to be the case for the numbers in table 4.

Response: We now present the mean values in the text.

- Line 654: here the 2015-2050 forcing is also introduced. To me, this is a more relevant measure than the e.g. the forcing in 2050 relative to 2030 because in many cases, the emission changes are not that large from 2030 to 2050. At the very least, give this period in table 4 and hint to the reader at the beginning of the section that it will be mentioned. And why calculate this relative to 2015 and not 2010?

Response: We now present the results from the difference of 1990-2010 and the 2030-2050 means to focus more on the difference between the future and the past.

- At the beginning of the paper, you talk about how Arctic climate change is primarily due to remote forcing. For this reason, I think it would be useful to give the reader an idea of also the global mean RF. This can be done in the SI, but would also enable comparison with previous work.

Response: We now have a new section (Section 3.2.4) that focuses on the net aerosol forcing, where we also present briefly the global mean RF_{ARI}. We also present the global spatial distribution of the difference between the 1990-2010 and 2030-2050 mean RF_{ARI} in Figure S2 (lines 750-753).

- One or two figures of the geographical distribution of forcing would also be useful. Can be sub-panels of figure 7.

Response: We have added a new figure (Figure 8) showing the spatial distribution of the Arctic difference between the 1990-2010 and 2030-2050 mean RF_{ARI}

Line 667-671: the model gives a 10 degree per decade change compared to 2 degrees from the observations? That seems like a very noticeable difference that I don't think you can just mention briefly like this, but needs more attention. What does this imply for confidence in any of the projections?

Response: We thank the reviewer for noticing this error. We have now corrected this (Lines 758-767).

Line 698: Not sure lowNTCF has been defined anywhere?

Response: We have now defined all the different CMIP6 scenarios in section 2.3 (Lines 316-331).

Line 754-755: Here you have 3 big figures in the SI that hardly show anything but white map and then show that anything they do show is not really significant. I would perhaps reconsider the usefulness and need for these figures.

Response: We agree with the reviewer. We have removed these figures.

Figure S8: I'm not sure it's correct to refer to projected changes as anomalies? And, is the isoprene plot referred to anywhere in the text? This is important for the discussion about SOA burden.

Response: We have rewritten this part and now we do not use this term anymore.

Line 765: 1990-2014? But RF was discussed based on 1990-2010? Please clarify.

Response: This only defines the simulation period, which is from 1990 to 2050. The analyses are conducted in the manuscript focuses on the differences between the 1990-2010 and 2030-2050 periods.

Present and future aerosol impacts on Arctic climate change in the GISS-E2.1 Earth system model

Ulas Im[1,2,*], Kostas Tsigaridis[3,4], Gregory Faluvegi[3,4], Peter L. Langen[1,2], Joshua P. French[5], Rashed Mahmood[6], Manu A. Thomas[7], Knut von Salzen[8], Daniel C. Thomas[1,2], Cynthia H. Whaley[8], Zbigniew Klimont[9], Henrik Skov[1,2], Jørgen Brandt[1,2]

[1]Department of Environmental Science, Aarhus University, Roskilde, Denmark.
[2] Interdisciplinary Centre for Climate Change, Aarhus University, Roskilde, Denmark.
[3] Center for Climate Systems Research, Columbia University, New York, NY, USA.
[4] NASA Goddard Institute for Space Studies, New York, NY, USA.
[5] Department of Mathematical and Statistical Sciences, University of Colorado Denver, USA.
[6] Barcelona Supercomputing Center, Barcelona, Spain.
[7] Swedish Meteorological and Hydrological Institute, Norrköping, Sweden.
[8] Canadian Centre for Climate Modelling and Analysis, Environment and Climate Change Canada, Victoria, British Columbia, Canada.
[9] International Institute for Applied Systems Analysis (IIASA), Laxenburg, Austria.
[*] Corresponding author

Abstract

The Arctic is warming two to three times faster than the global average, partly due to changes in short-lived climate forcers (SLCFs) including aerosols. In order to study the effects of atmospheric aerosols in this warming, recent past (1990-2014) and future (2015-2050) simulations have been carried out using the GISS-E2.1 Earth system model to study the aerosol burdens and their radiative and climate impacts over the Arctic (>60 °N), using anthropogenic emissions from the Eclipse V6b and the Coupled Model Intercomparison Project Phase 6 (CMIP6) databases, while global annual mean greenhouse gas concentrations were prescribed and kept fixed in all simulations.

Results showed that the simulations have underestimated observed surface aerosol levels, in particular black carbon (BC) and sulfate (SO_4^{2-}), by more than 50%, with the smallest biases calculated for the atmosphere-only simulations, where winds are nudged to reanalysis data. CMIP6 simulations performed slightly better in reproducing the observed surface aerosol concentrations and climate parameters, compared to the Eclipse simulations. In addition, simulations, where atmosphere and ocean are fully-coupled, had slightly smaller biases in aerosol levels compared to atmosphere only simulations without nudging.

Arctic BC, organic aerosol (OA) and SO_4^{2-} burdens decrease significantly in all simulations by 10-60% following the reductions of 7-78% in emission projections, with the CMIP6 ensemble showing larger reductions in Arctic aerosol burdens compared to the Eclipse ensemble. For the 2030-2050 period, the Eclipse ensemble simulated a radiative forcing due to aerosol-radiation interactions (RF_{ARI}) of -0.39±0.01 W m^{-2}, that is -0.08 W m^{-2} larger than the 1990-2010 mean forcing (-0.32 W m^{-2}). of which -0.24±0.01 W m^{-2} were attributed to the anthropogenic aerosols. The CMIP6 ensemble simulated a RF_{ARI} of -0.35 to -0. 40 W m^{-2}

Deleted: Thomas

Deleted: Candian
Formatted: Highlight
Formatted: Highlight
Deleted: S
Deleted: have been significantly underestimated
Deleted: nudged
Formatted: Highlight
Formatted: Highlight
Deleted: simulating both
Deleted: s
Deleted: of aerosols
Deleted: fully-coupled
Formatted: Highlight
Deleted: carbon
Deleted: C
Formatted: Highlight
Formatted: Highlight
Formatted: Highlight
Deleted: both
Deleted: Current Legislation (CLE) and the Maximum Feasible Reduction (MFR) …
Deleted: s
Formatted: Highlight
Formatted: Subscript, Highlight
Formatted: Highlight
Deleted: n aerosol top of the atmosphere (TOA) forcing
Formatted: Highlight
Formatted: Highlight
Deleted: SSP3-7.0 scenario
Deleted: TOA aerosol forcing
Formatted: Subscript, Highlight
Formatted: Highlight

for the same period, which is -0.01 to -0.06 W m^{-2} larger than the 1990-2010 mean forcing of -0.35 W m^{-2}. The scenarios with little to no mitigation (worst-case scenarios) led to very small changes in the RF_{ARI}, while scenarios with medium to large emission mitigations led to increases in the negative RF_{ARI}, mainly due to the decrease of the positive BC forcing and the decrease in the negative SO_4^{2-} forcing. The anthropogenic aerosols accounted for -0.24 to -0.26 W m^{-2} of the net RF_{ARI} in 2030-2050 period, in Eclipse and CMIP6 ensembles, respectively. Finally, all simulations showed an increase in the Arctic surface air temperatures throughout the simulation period. By 2050, surface air temperatures are projected to increase by 2.4 °C to 2.6 °C in the Eclipse ensemble and 1.9 °C to 2.6 °C in the CMIP6 ensemble, compared to the 1990-2010 mean.

Overall, results show that even the scenarios with largest emission reductions leads to similar impact on the future Arctic surface air temperatures and sea-ice extent compared to scenarios with smaller emission reductions, implying reductions of greenhouse emissions are still necessary to mitigate climate change.

1. Introduction

The Arctic is warming two to three times faster than the global average (IPCC, 2013; Lenssen et al., 2019). This is partly due to internal Arctic feedback mechanisms, such as the snow and sea-ice-albedo feedback, where melting ice leads to increased absorption of solar radiation, which further enhances warming in the Arctic (Serreze and Francis, 2006). However, Arctic temperatures are also affected by interactions with warming at lower latitudes (e.g., Stuecker et al., 2018; Graversen and Langen, 2019; Semmler et al., 2020) and by local in situ response to radiative forcing due to changes in greenhouse gases and aerosols in the area (Shindell, 2007; Stuecker et al., 2018). In addition to warming induced by increases in global atmospheric carbon dioxide (CO_2) concentrations, changes in short-lived climate forcers (SLCFs) such as tropospheric ozone (O_3), methane (CH_4) and aerosols (e.g. black carbon (BC) and sulfate (SO_4^{2-})) in the Northern Hemisphere (NH), have contributed substantially to the Arctic warming since 1890 (Shindell and Faluvegi, 2009; Ren et al., 2020). This contribution from SLCFs to Arctic heating together with efficient local amplification mechanisms puts a high priority on understanding the sources and sinks of SLCFs at high latitudes and their corresponding climatic effects.

SLCFs include all atmospheric species, which have short residence times in the atmosphere relative to long-lived greenhouse gases and have the potential to affect Earth's radiative energy budget. Aerosols are important SLCFs and are a predominant component of air quality that affects human health (Burnett et al., 2018, Lelieveld et al., 2019). They mostly affect climate by altering the amount of solar energy absorbed by Earth, as well as changing the cloud properties and indirectly affecting the scattering of radiation, and are efficiently removed from the troposphere within several days to weeks. BC, which is a product of incomplete combustion and open biomass/biofuel burning (Bond et al., 2004: 2013), absorbs a high proportion of incident solar radiation and therefore warms the climate system (Jacobson, 2001). SO_4^{2-}, which is formed primarily through oxidation of sulphur dioxide

Formatted: Subscript, Highlight
Formatted: Highlight
Formatted: Subscript, Highlight
Formatted: Highlight
Deleted: while SSP1-2.6 and SSP2-4.5 scenarios simulated a slightly more negative TOA forcing (-0.40 W m^{-2}), of which t
Formatted: Subscript, Highlight
Formatted: Superscript, Highlight
Formatted: Highlight
Formatted: Subscript, Highlight
Formatted: Highlight
Deleted: .
Deleted: both
Deleted: In
Formatted: Highlight
Formatted: Highlight
Formatted: Highlight
Deleted: while scenarios no or little mitigation leads to much larger sea-ice loss, implying that even though the magnitude of aerosol reductions lead to similar responses in surface air temperatures, high mitigation
Deleted: aerosols
Deleted: limit sea-ice loss
Deleted: ¶
Formatted: Highlight
Formatted: Highlight
Deleted: Black carbon (
Deleted:)
Deleted: Sulphate (
Deleted:)

(SO_2), absorbs negligible solar radiation and cools climate by scattering solar radiation back to space. Organic carbon (OC), which is co-emitted with BC during combustion, both scatters and absorbs solar radiation and therefore causes cooling in some environments and warming in others. Highly reflective regions such as the Arctic are more likely to experience warming effects from these organic aerosols (e.g., Myhre et al, 2013).

Aerosols also influence climate via indirect mechanisms. After being deposited on snow and ice surfaces, BC can amplify ice melt by lowering the albedo and increasing solar heating of the surface (AMAP, 2015). Aerosols also affect cloud properties, including their droplet size, lifetime, and vertical extent, thereby influencing both the shortwave cooling and longwave warming effects of clouds. Globally, this indirect cloud forcing from aerosols is likely larger than their direct forcing, although the indirect effects are more uncertain and difficult to accurately quantify (IPCC, 2013). Moreover, Arctic cloud impacts are distinct from global impacts, owing to the extreme seasonality of solar radiation in the Arctic, unique characteristics of Arctic clouds (e.g., high frequency of mixed-phase occurrence), and rapidly evolving sea-ice distributions. Together, they lead to complicated and unique phenomena that govern Arctic aerosol abundances and climate impacts (e.g., Willis et al., 2018; Abbatt et al., 2019). The changes taking place in the Arctic have consequences for how SLCFs affect the region. For example, reductions in sea-ice extent, thawing of permafrost, and humidification of the Arctic troposphere can affect the emissions, lifetime and radiative forcing of SLCFs within the Arctic (Thomas et al., 2019).

The effect of aerosols on the Arctic climate through the effects of scattering and absorption of radiation, clouds, and surface ice/snow albedo has been investigated in previous studies (i.e. Clarke and Noone, 1985; Flanner et al., 2007; Shindell et al., 2012; Bond et al., 2013; Dumont et al., 2014). The impact of aerosols on the Arctic climate change is mainly driven by a response to remote forcings (Gagné et al., 2015; Sand et al., 2015; Westervelt et al., 2015). Long-range transport is known to play an important role in the Arctic air pollution levels and much of the attention on aerosol climatic effects in the Arctic was focused on long-range transported anthropogenic pollution (Arctic haze) in the past (Quinn et al., 2017; AMAP, 2015; Abbatt et al., 2019). Long-range transport of BC and SO_4^{2-}, in particular from Asia, travelling at a relatively high altitude to the Arctic, can be deposited on the snow and ice, contributing to surface albedo reduction. On the other hand, there has been increasing attention on the local Arctic aerosol sources, in particular natural aerosol sources (Schmale et al., 2021). Lewinschal et al. (2019) estimated an Arctic surface temperature change per unit global sulfur emission of -0.020 to -0.025 K per TgS yr^{-1}. Sand et al. (2020) calculated an Arctic surface air temperature response of 0.06 - 0.1 K per Tg BC yr^{-1} to BC emissions in Europe and North America, and slightly lower response (0.05-0.08 K per Tg BC yr^{-1}) to Asian emissions. Breider et al. (2017) reported a short-wave (SW) aerosol radiative forcing (ARF) of -0.19 ± 0.05 W m^{-2} at the top of the atmosphere (TOA) over the Arctic, which reflects the balance between sulphate cooling (-0.60 W m^{-2}) and black carbon (BC) warming ($+0.44$ W m^{-2}). Schacht et al. (2019) calculated a direct radiative forcing of up to 0.4 W m^{-2} over the Arctic using the ECHAM6.3-HAM2.3 global aerosol-climate model. Markowicz et al. (2021), using the NAAPS radiative transfer model, calculated the total aerosol forcing

Formatted: Highlight

Deleted: to

Formatted: Highlight

Deleted: ing

Formatted: Danish

Formatted: Danish

Formatted: Danish

Formatted: Danish

Formatted: Danish

Formatted: Danish

Formatted: English (US), Highlight

Formatted: Highlight

Deleted: through aerosols

Formatted: Highlight

Formatted: Subscript, Highlight

Formatted: Superscript, Highlight

Formatted: Highlight

Formatted: Highlight

Formatted: Highlight

over the Arctic (>70.5 °N) of -0.4 W m^{-2}. Ren et al. (2020) simulated 0.11 and 0.25 W m^{-2} direct and indirect warning in 2014-2018 compared to 1980-1984 due to reductions in sulfate, using the CAM5-EAST global aerosol-climate model. They also reported that the aerosols produced an Arctic surface warming of +0.30 °C during 1980–2018, explaining about 20% of the observed Arctic warming observed during the last four decades, while according to Shindell and Faluvegi (2009), aerosols contributed 1.09 ± 0.81 °C to the observed Arctic surface air temperature increase of 1.48 ± 0.28 °C observed in 1976-2007. AMAP (2015), based on four ESMs, estimated a total Arctic surface air temperature response due to the direct effect of current global combustion derived BC, OC and sulfur emissions to be +0.35 °C, of which +0.40 °C was attributed to BC in the atmosphere, +0.22 °C to BC in snow, -0.04 °C to OC and -0.23 °C to SO_4^{2-}. On the other hand, Stjern et al. (20117) and Takemura and Suzuki (2019) showed that due to the rapid adjustments from BC, mitigation of BC emissions can lead to weak responses in the surface temperatures. Samset et al. (2018), using a multi-model ensemble of ocean coupled Earth system models (ESMs), where aerosol emissions were either kept at present-day conditions, or anthropogenic emissions of SO_2, and fossil fuel BC and OC were set to zero, showed that Arctic surface warming due to aerosol reductions can reach up to 4°C in some locations, with a multi-model increase for the 60°N–90°N region being 2.8°C. In addition, recent studies also suggest that as global emissions of anthropogenic aerosols decrease, natural aerosol feedbacks may become increasingly important for Arctic climate (Boy et al., 2019; Mahmood et al., 2019).

In this study, we carry out several simulations with the fully coupled NASA Goddard Institute of Space Sciences (GISS) earth system model, GISS-E2.1 (Kelley et al., 2020) to study the recent past and future burdens of aerosols as well as their impacts on TOA radiative forcing and climate-relevant parameters such as surface air temperatures, sea-ice, and snow over the Arctic (>60 °N). In addition, we investigate the impacts from two different emission inventories; Eclipse V6b (Höglund-Isaksson et al.,2020; Klimont et al., 2021) vs. CMIP6 (Hoesly et al., 2018; van Marle et al., 2017: Feng et al.,2020), as well as differences between atmosphere-only vs. fully-coupled simulations, on the evaluation of the model and the climate impact. Section 2 introduces the GISS-E2.1 model, the anthropogenic emissions, and the observation datasets used in model evaluation. Section 3 presents results from the model evaluation as well as recent past and future trends in simulated aerosol burdens, radiative forcing, and climate change over the Arctic. Section 4 summarizes the overall findings and the conclusions.

2. Materials and methods

2.1. Model description

GISS-E2.1 is the CMIP6 version of the GISS modelE Earth system model, which has been validated extensively over the globe (Kelly et al., 2020; Bauer et al., 2020) as well as regionally for air pollutants (Turnock et al., 2020). A full description of GISS-E2.1 and evaluation of its coupled climatology during the satellite era (1979–2014) and the recent past ensemble simulation of the atmosphere and ocean component models (1850-2014) are

Formatted: Highlight
Formatted: English (US), Highlight
Formatted: Highlight
Formatted: English (US), Highlight
Formatted: Highlight
Formatted: English (US), Highlight
Formatted: Highlight
Formatted: English (US), Highlight
Formatted: Highlight
Formatted: English (US)
Formatted: Highlight
Formatted: Subscript, Highlight
Formatted: Highlight
Deleted:
Deleted:

described in Kelly et al. (2020) and Miller et al. (2020), respectively. GISS-E2.1 has a horizontal resolution of 2° in latitude by 2.5° in longitude and 40 vertical layers extending from the surface to 0.1 hPa in the lower mesosphere. The tropospheric chemistry scheme used in GISS-E2.1 (Shindell et al., 2013) includes inorganic chemistry of O_x, NO_x, HO_x, CO, and organic chemistry of CH_4 and higher hydrocarbons using the CBM4 scheme (Gery et al., 1989), and the stratospheric chemistry scheme (Shindell et al., 2013), which includes chlorine and bromine chemistry together with polar stratospheric clouds.

In the present work, we used the One-Moment Aerosol scheme (OMA: Bauer et al., 2020 and references therein), which is a mass-based scheme in which aerosols are assumed to remain externally mixed. All aerosols have a prescribed and constant size distribution, with the exception of sea salt that has two distinct size classes, and dust that is described by a sectional model with an option from 4 to 6 bins. The default dust configuration that is used in this work includes 5 bins, a clay and 4 silt ones, from submicron to 16 μm in size. The first three dust size bins can be coated by sulfate and nitrate aerosols (Bauer & Koch, 2005). The scheme treats sulfate, nitrate, ammonium, carbonaceous aerosols (black carbon and organic carbon, including the NO_x-dependent formation of secondary organic aerosol (SOA) and methanesulfonic acid formation), dust and sea-salt. The model includes secondary organic aerosol production, as described by Tsigaridis and Kanakidou, (2007). SOA is calculated from terpenes and other reactive volatile organic compounds (VOCs) using NOx-dependent calculations of the 2-product model, as described in Tsigaridis and Kanakidou (2007). Isoprene is explicitly used as a source, while terpenes and other reactive VOCs are lumped on a-pinene, taking into account their different reactivity against oxidation. The semi-volatile compounds formed can condense on all submicron particles except sea salt and dust. In the model, an OA to OC ratio of 1.4 used. OMA only includes the first indirect effect, in which the aerosol number concentration that impacts clouds is obtained from the aerosol mass as described in (Menon & Rotstayn, 2006). The parameterization described by Menon and Rotstayn (2006) that we use only affects the cloud droplet number concentration (CDNC), not cloud droplet size, which is not explicitly calculated in GISS-E2.1. Following the change in CDNC, we do not stop the model from changing either liquied water path (LWP) or precipitation rates, since the clouds code sees the different CDNC and responds accordingly. What we do not include is the 2nd indirect effect (autoconversion). In addition to OMA, we have also conducted a non-interactive tracers (NINT: Kelley et al., 2020) simulation from 1850 to 2014, with noninteractive (through monthly varying) fields of radiatively active components (ozone and multiple aerosol species) read in from previously calculated offline fields from the OMA version of the model, ran using the Atmospheric Model Intercomparison Project (AMIP) configuration in Bauer et al. (2020) as described in Kelley et al. (2020). The NINT model includes a tuned aerosol first indirect effect following Hansen et al. (2005).

The natural emissions of sea salt, dimethylsulfide (DMS), isoprene and dust are calculated interactively. Anthropogenic dust sources are not represented in GISS-E2.1. Dust emissions vary spatially and temporally only with the evolution of climate variables like wind speed and soil moisture (Miller et al., 2006). The AMIP type simulations (see section 2.3) uses

Formatted: Highlight
Deleted: and
Formatted: Highlight
Formatted: Highlight
Formatted: Highlight
Formatted: Highlight
Deleted: I
Formatted: English (US)
Formatted: Highlight

prescribed sea surface temperature (SST) and sea ice fraction during the recent past (Rayner et al., 2003). The prescribed SST dataset in GISS-E2.1 is merged product based on the HadISST and NOAA Optimum Interpolation (OI) Sea Surface Temperature (SST) V2 (Reynolds et al., 2002).

2.2. Emissions

In this study, we have used two different emission datasets; the ECLIPSE V6b (Höglund-Isaksson et al.,2020; Klimont et al., 2021), which has been developed with support of the EU-funded Action on Black Carbon in the Arctic (EUA-BCA) and used in the framework of the ongoing AMAP Assessment (AMAP, 2021), referred to as *Eclipse* in this paper, and the CEDS emissions (Hoesly et al., 2018; Feng et al.,2020) combined with selected Shared Socio-economic Pathways (SSP) scenarios used in the CMIP6 future projections (Eyring et al., 2016), collectively referred to as *CMIP6* in this paper.

2.2.1. EclipseV6b emissions

The ECLIPSE V6b emissions dataset is a further evolution of the scenarios established in the EU funded ECLIPSE project (Stohl et al., 2015; Klimont et al., 2017). It has been developed with the global implementation of the GAINS (Greenhouse gas – Air pollution Interactions and Synergies) model (Amann et al., 2011). The GAINS model includes all key air pollutants and Kyoto greenhouse gases, where emissions are estimated for nearly 200 country-regions and several hundred source-sectors representing anthropogenic emissions. For this work, annual emissions were spatially distributed on 0.5°x0.5° lon-lat grids for nine sectors: energy, industry, solvent use, transport, residential combustion, agriculture, open burning of agricultural waste, waste treatment, gas flaring and venting, and international shipping. A monthly pattern for each gridded layer was provided at a 0.5°x0.5° grid level. The ECLIPSE V6b dataset, used in this study, includes an estimate for 1990 to 2015 using statistical data and two scenarios extending to 2050 that rely on the same energy projections from the World Energy Outlook 2018 (IEA, 2018) but have different assumptions about the implementation of air pollution reduction technologies, as described below.

The Current Legislation (CLE) scenario assumes efficient implementation of the current air pollution legislation committed before 2018, while the Maximum Feasible Reduction (MFR) scenario assumes implementation of best available emission reduction technologies included in the GAINS model. The MFR scenario demonstrates the additional reduction potential of SO_2 emissions by up to 60% and 40%, by 2030 for Arctic Council member and observer countries respectively, with implementation of best available technologies mostly in the energy and industrial sectors and to a smaller extent via measures in the residential sector. The Arctic Council member countries' maximum reduction potential could be fully realized by 2030 whereas in the observer countries additional reductions of 15% to 20% would remain to be achieved between 2030 and 2050. The assumptions and the details for the CLE

Formatted: Highlight

Formatted: Space Before: 12 pt, After: 12 pt

Moved (insertion) [1]

Formatted: Highlight

Deleted: ¶
The technology implementation pace in the MFR scenario includes constraints resulting from age structure and typical lifetime of technologies but no constraints resulting from possible economic implications of required large investment in emission reduction technology.

and MFR scenarios (as well as other scenarios developed within the ECLIPSE V6b family) can be found in Höglund-Isaksson et al. (2020) and Klimont et al. (in preparation).

2.2.2. CMIP6 emissions

The CMIP6 emission datasets include a historical time series generated by the Community Emissions Data System (CEDS) for anthropogenic emissions (Hoesly et al., 2018; Feng et al., 2020), open biomass burning emissions (van Marle et al., 2010), and the future emission scenarios driven by the assumptions embedded in the Shared Socioeconomic Pathways (SSPs) and Representative Concentration Pathways (RCPs) (Riahi et al., 2017) that include specific air pollution storylines (Rao et al., 2017). Gridded CMIP6 emissions are aggregated to nine sectors: agriculture, energy, industrial, transportation, residential–commercial–other, solvents, waste, international shipping, and aircraft. SSP data for future emissions from integrated assessment models (IAMs) are first harmonized to a common 2015 base-year value by the native model per region and sector. This harmonization process adjusts the native model data to match the 2015 starting year values with a smooth transition forward in time, generally converging to native model results (Gidden et al., 2018). The production of the harmonized future emissions data is described in Gidden et al. (2019).

2.2.3. Implementation of the emissions in the GISS-E2.1

The Eclipse V6b and CEDS emissions on 0.5° × 0.5° spatial resolution are regridded to 2° × 2.5° resolution in order to be used in the various GISS-E2.1 simulations. In the GISS-E2.1 Eclipse simulations, the non-methane volatile organic carbons (NMVOC) emissions are chemically speciated assuming the SSP2-4.5 VOC composition profiles. In the Eclipse simulations, biomass burning emissions are taken from the CMIP6 emissions, which have been pre-processed to include the agricultural waste burning emissions from the EclipseV6b dataset, while the rest of the biomass burning emissions are taken as the original CMIP6 biomass burning emissions. In addition to the biomass burning emissions, the aircraft emissions are also taken from the CMIP6 database to be used in the Eclipse simulations. As seen in Figure 1, the emissions are consistently higher in the CMIP6 compared to the Eclipse emissions. The main differences in the two datasets are mainly over south-east Asia (not shown) . The CMIP6 emissions are also consistently higher on a sectoral basis compared to the Eclipse emissions. The figure shows that for air pollutant emissions, the CMIP6 SSP1-2.6 scenario and the Eclipse MFR scenario follow each other closely, while the Eclipse CLE scenario is comparable with the CMIP6 SSP2-4.5 scenario for most pollutants; that is to some extent owing to the fact that the CO_2 trajectory of the Eclipse CLE and the SSP2-4.5 are very similar (not shown). A more detailed discussion of differences between historical Eclipse and CMIP6 as well as CMIP6 scenarios are provided in Klimont et al. (in preparation).

2.3. Simulations

In order to contribute to the AMAP Assessment report (AMAP, 2021), the GISS-E2.1 model participated with AMIP-type simulations, which aim to assess the trends of Arctic air

Moved up [1]: The MFR scenario demonstrates the additional reduction potential of SO_2 emissions by up to 60% and 40%, by 2030 for Arctic Council member and observer countries respectively, with implementation of best available technologies mostly in the energy and industrial sectors and to a smaller extent via measures in the residential sector. The Arctic Council member countries' maximum reduction potential could be fully realized by 2030 whereas in the observer countries additional reductions of 15% to 20% would remain to be achieved between 2030 and 2050. ¶

Formatted: Highlight
Formatted: Highlight
Formatted: Highlight
Formatted: Highlight
Formatted: Highlight
Formatted: Highlight
Formatted: Highlight
Formatted: Highlight
Formatted: Highlight
Formatted: Highlight
Formatted: Highlight
Formatted: Highlight
Formatted: Highlight
Deleted: T
Deleted: from the

pollution and climate change in the recent past, as well as with fully-coupled climate simulations. Five fully-coupled Earth system models (ESMs) simulated the future (2015-2050) changes of atmospheric composition and climate in the Arctic (>60°N), as well as over the globe. We have carried out two AMIP-type simulations, one with winds nudged to NCEP (standard AMIP-type simulation in AMAP) and one with freely varying winds, where both simulations used prescribed SSTs and sea-ice (Table 1). In the fully-coupled simulations, we carried out two sets of simulations, each with three ensemble members, that used the CLE and MFR emission scenarios. Each simulation in these two sets of scenarios were initialized from a set of three fully-coupled ensemble recent past simulations (1990-2014) to ensure a smooth continuation from CMIP6 to Eclipse emissions.

In addition to the AMAP simulations, we have also conducted CMIP6-type simulations in order to compare the climate aerosol burdens and their impacts on radiative forcing and climate impacts with those from the AMAP simulations. We have used the SSP1-2.6, 2-4.5, 3-7.0, and 3-7.0-lowNTCF scenarios representing different levels of emission mitigations in the CMIP6 simulations. SSP1 and SSP3 define various combinations of high or low socio-economic challenges to climate change adaptation and mitigation, while SSP2 describes medium challenges of both kinds and is intended to represent a future in which development trends are not extreme in any of the dimensions, but rather follow middle-of-the-road pathways (Rao et al., 2017). SSP1-2.6 scenario aims to achieve a 2100 radiative forcing level of 2.6 W m^{-2}, keeping the temperature increase below 2 °C compared to the preindustrial levels. The SSP2-4.5 describes a "middle of the road" socio-economic family with a 4.5 W m^{-2} radiative forcing level by 2100. The SSP3- 7.0 scenario is a medium-high reference scenario. SSP3-7.0-lowNTCF is a variant of the SSP3-7.0 scenario with reduced near-term climate forcer (NTCF) emissions. The SSP3-7.0 scenario has the highest methane and air pollution precursor emissions, while SSP3-7.0-lowNTCF investigates an alternative pathway for the Aerosols and Chemistry Model Intercomparison Project (AerChemMIP: Collins et al., 2017), exhibiting very low methane, aerosol, and tropospheric-ozone precursor emissions – approximately in line with SSP1-2.6. As seen in Table 1, we have conducted one transient fully-coupled simulation from 1850 to 2014, and a number of future scenarios.

We have employed prescribed global and annual mean greenhouse (CO_2 and CH_4) concentrations, where a linear increase in global mean temperature of 0.2 °C/decade from 2019 to 2050 was assumed, which are approximately in line with the simulated warming rates for the SSP2-4.5 scenario (AMAP, 2021).

2.4. Observations

The GISS-E2.1 ensemble has been evaluated against surface observations of BC, organic aerosols (sum of OC and secondary organic aerosols (SOA), referred as OA in the rest of the paper) and SO_4^{2-}, ground-based and satellite-derived AOD 550 nm, as well as surface and satellite observations of surface air temperature, precipitation, sea surface temperature, sea-ice extent, cloud fraction, and liquid and ice water content in 1995-2014 period. The surface

Formatted: Highlight
Formatted: Superscript, Highlight
Formatted: Highlight
Formatted: Highlight
Formatted: Highlight
Formatted: Superscript, Highlight
Formatted: Highlight
Formatted: Highlight
Formatted: Subscript, Highlight
Formatted: Highlight
Formatted: Subscript, Highlight
Formatted: Highlight
Formatted: Highlight
Formatted: Highlight
Deleted: O

monitoring stations used to evaluate the simulated aerosol levels have been listed in Table S1 and S2 in the supplementary materials.

2.4.1. Aerosols

Measurements of speciated particulate matter (PM), BC, SO_4^{2-}, and (OA) come from three major networks: the Interagency Monitoring of Protected Visual Environments (IMPROVE) for Alaska (The IMPROVE measurements that are in the Arctic (>60°N) are all in Alaska); the European Monitoring and Evaluation Programme (EMEP) for Europe; and the Canadian Air Baseline Measurements (CABM) for Canada (Table S1 and S2). In addition to these monitoring networks, BC, OA, and SO_4^{2-} measurements from individual Arctic stations were used in this study. The individual Arctic stations are Fairbanks and Utqiagvik, Alaska (part of IMPROVE, though their measurements were obtained from their PIs); Gruvebadet and Zeppelin mountain (Ny Alesund), Norway; Villum Research Station, Greenland; and Alert, Nunavut (the latter being an observatory in Global Atmospheric Watch-WMO, and a part of CABM). The measurement techniques are briefly described in the supplement.

AOD at 500 nm from the AErosol RObotic NETwork (AERONET, Holben et al., 1998) was interpolated to 550 nm AOD using the Ångström formula (Ångström, 1929). We also used a new merged AOD product developed by Sogacheva et al. (2020) using AOD from 10 different satellite-based products. According to Sogacheva et al. (2020), this merged product could provide a better representation of temporal and spatial distribution of AOD. However, it is important to note that the monthly aggregates of observations for both AERONET and the satellite products depend on availability of data and are not likely to be the true aggregate of observations for a whole month when only few data points exist during the course of a month. In addition, many polar orbiting satellites take one observation during any given day, and typically at the same local time. Nevertheless, these data sets are key observations currently available for evaluating model performances. Information about the uncertain nature of AOD observations can be found in previous studies (e.g. Sayer et al., 2018; Sayer and Knobelspiesse, 2019; Wei et al., 2019; Schutgens et al., 2020, Schutgens, 2020; Sogacheva et al., 2020).

2.4.2. Surface air temperature, precipitation, and sea-ice

Surface air temperature and precipitation observations used in this study are from University of Delaware gridded monthly mean data sets (UDel; Willmott and Matsuura, 2001). UDel's 0.5° resolution gridded data sets are based on interpolations from station-based measurements obtained from various sources including the Global Historical Climate Network, the archive of Legates and Willmott and others. The Met Office Hadley Center's sea ice and sea surface temperature (HadISST; Rayner et al., 2003) was used for evaluating model simulations of sea ice and SSTs. HadISST data is an improved version of its predecessor known as global sea ice and sea surface temperature (GISST). HadISST data is constructed using information from a variety of data sources such as the Met Office Marine Database, Comprehensive Ocean-Atmosphere Data Set, passive microwave remote sensing retrieval and sea ice charts.

Deleted: black carbon (
Deleted:)
Deleted: sulfate (
Deleted:)
Deleted: organic carbon
Deleted: C
Deleted: the United States
Formatted: Highlight
Formatted: Font: Not Italic, Highlight
Formatted: Highlight
Formatted: Font: Not Italic, Highlight
Formatted: Highlight
Deleted: C

2.4.3. Satellite observations used for cloud fraction and cloud liquid water and ice water

The Advanced Very High Resolution Radiometer (AVHRR-2) sensors onboard the NOAA and EUMETSAT polar orbiting satellites have been flying since the early 1980s. These data have been instrumental in providing the scientific community with climate data records spanning nearly four decades. Tremendous progress has been made in recent decades in improving, training and evaluating the cloud property retrievals from these AVHRR sensors. In this study, we use the retrievals of total cloud fraction from the second edition of EUMETSATs Climate Monitoring Satellite Application Facility (CM SAF) Cloud, Albedo and surface Radiation data set from AVHRR data (CLARA-A2, Karlsson et al., 2017). This cloud property climate data record is available for the period 1982-2018. Its strengths and weaknesses and inter-comparison with the other similar climate data records are documented in Karlsson and Devasthale (2018). Further data set documentation including Algorithm Theoretical Basis and Validation reports can be found in Karlsson et al. (2017).

Cloud liquid and ice water path estimates derived from the cloud profiling radar on board CloudSat (Stephens et al., 2002) and constrained with another sensor onboard NASA's A-Train constellation, MODIS-Aqua (Platnick et al., 2015), are used for the model evaluation. These Level 2b retrievals, available through 2B-CWC-RVOD product (Version 5), for the period 2007-2016 are analysed. This constrained version is used instead of its radar-only counterpart, as it uses additional information about visible cloud optical depths from MODIS, leading to better estimates of cloud liquid water paths. Because of this constraint the data are available only for the day-lit conditions, and hence, are missing over the polar regions during the respective winter seasons. The theoretical basis for these retrievals can be found in http://www.cloudsat.cira.colostate.edu/sites/default/files/products/files/2B-CWC-RVOD_PDICD.P1_R05.rev0_.pdf (last access: October 26th 2020). Being an active cloud radar, CloudSat provides orbital curtains with a swath width of just about 1.4 km. Therefore, the data are gridded at 5°x5° to avoid too many gaps or patchiness and to provide robust statistics.

3. Results

3.1. Evaluation

The simulations are compared against surface measurements of BC, OA, SO_4^{2-} and AOD, as well as surface and satellite measurements of surface air temperature, precipitation, sea surface temperature, sea-ice extent, total cloud fraction, liquid water path, and ice water path described in section 2.4, by calculating the correlation coefficient (*r*) and normalized mean bias (*NMB*). OA refers to the sum of primary organic carbon (OC) and secondary organic aerosols (SOA).

3.1.1. Aerosols

Deleted: C

Formatted: Highlight

Formatted: Highlight

Formatted: Highlight

The recent past simulations are for BC, OA, SO_4 and AOD (Table 2) against available surface measurements. The monthly observed and simulated time series for each station are accumulated per species in order to get a full Arctic timeseries data, which also includes spatial variation, to be used for the evaluation of the model. In addition to Table 2, the climatological mean (1995-2014) of the observed and simulated monthly surface concentrations of BC, OA, SO_4^{2-} and AOD at 550 nm (note that AOD is averaged over 2008, 2009 and 2014) are shown in Figure 2. The AOD observation data for years 2008, 2009, and 2014 are used in order to keep the comparisons in line with the multi-model evaluations being carried out in the AMAP assessment report (AMAP, 2021). We also provide spatial distributions of the NMB, calculated as the mean of all simulations for BC, OA, SO_4 and AOD in Figure 3. The statistics for the individual stations are provided in the Supplementary Material, Tables S3-S6.

Results showed overall an underestimation of aerosol species over the Arctic, as discussed below. Surface BC levels are underestimated at all Arctic stations from 15% to 90%. Surface OA levels are also underestimated from -5% to -70%, except for a slight overestimation of <1% over Karvatn (B5) and a large overestimation of 90% over Trapper Creek (B6). Surface SO_4^{2-} concentrations are also consistently underestimated from -10% to -70%, except for Villum Research Station (S11) over northeastern Greenland where there is an overestimation of 45%. Finally, AODs are also underestimated over all stations from 20% to 60%. Such underestimations at high latitudes have also been reported by many previous studies (e.g. Skeike et al., 2011; Eckhardt et al., 2015; Lund et al., 2017, 2018; Schacht et al., 2019; Turnock et al., 2020), pointing to a variety of reasons including uncertainties in emission inventories, errors in the wet and dry deposition schemes, the absence or underrepresentation of new aerosol formation processes, and the coarse resolution of global models leading to errors in emissions and simulated meteorology, as well as in representation of point observations in coarse model grid cells. Turnock et al. (2020) evaluated the air pollutant concentrations in the CMIP6 models, including the GISS-E2.1 ESM, and found that observed surface $PM_{2.5}$ concentrations are consistently underestimated in CMIP6 models by up to 10 μg m^{-3}, particularly for the Northern Hemisphere winter months, with the largest model diversity near natural emission source regions and the Polar regions.

The BC levels are largely underestimated in simulations by 50% (CMIP6_Cpl_Hist) to 67% (Eclipse_AMIP). The CMIP6 simulations have lower bias compared to EclipseV6b simulations due to higher emissions in the CMIP6 emission inventory (Figure 1). Within the EclipseV6b simulations, the lowest bias (-57%) is calculated for the Eclipse_AMIP_NCEP simulation, while the free climate and coupled simulations showed a larger underestimation (>62%), which can be attributed to a better simulation of transport to the Arctic when nudged winds are used. The Eclipse simulations also show that the coupled simulations had slightly smaller biases (*NMB*=-63%) compared to the AMIP-type free climate simulation (AMIP-OnlyAtm: *NMB*=-67%). The climatological monthly variation of the observed levels is poorly reproduced by the model with *r* values around 0.3. BC levels are mainly underestimated in winter and spring, which can be attributed to the underestimation of the

Deleted: C
Deleted: different
Formatted: Highlight
Deleted: , where individual
Deleted: s
Deleted: n
Deleted: C
Deleted: OC
Deleted: OC
Formatted: Highlight
Deleted: <1%
Deleted: Finally
Formatted: Highlight
Formatted: Highlight

anthropogenic emissions of BC, while the summer levels are well captured by the majority of the simulations (Figure 2).

Surface OA concentrations are underestimated from 8% (Eclipse_AMIP_NCEP) to 35% (Eclipse_AMIP) by the Eclipse ensemble, while the CMIP6_Cpl_Hist simulation overestimated surface OA by 13%. The Eclipse simulations suggest that the nudged winds lead to a better representation of transport to the Arctic, while the coupled simulations had smaller biases compared to the AMIP-type free climate simulation (AMIP-OnlyAtm), similar to BC. The climatological monthly variation of the observed concentrations are reasonably simulated, with *r* values between 0.51 and 0.69 (Table 2 and Figure 2). As can be seen in Figure S1, the OA levels are dominated by the biogenic SOA, in particular via α-pinene (monoterpenes) oxidation, compared to anthropogenic (by a factor of 4-9) and biomass burning (by a factor of 2-3) OA. While OC and BC are emitted almost from similar sources, this biogenic-dominated OA seasonality also explains why simulated BC seasonality is not as well captured, suggesting the underestimations in the anthropogenic emissions of these species, in particular during the winter.

Surface SO_4^{2-} levels are simulated with a smaller bias compared to the BC levels, however still underestimated by 40% (CMIP6_Cpl_Hist) to 53% (Eclipse_AMIP_NCEP). The Eclipse_AMIP_NCEP simulation is biased higher (NMB=-53%) compared to the Eclipse_AMIP (NMB=-50%), probably due to higher cloud fraction simulated by the nudged version (see section 3.1.6), leading to higher in-cloud SO_4^{2-} production. The climatological monthly variation of observed SO_4^{2-} concentrations are reasonably simulated in all simulations (r=0.65-0.74). The observed springtime maximum is well captured by the GISS-E2.1 ensemble, with underestimations in all seasons, mainly suggesting underestimations in anthropogenic SO_2 emissions (Figure 2), as well as simulated cloud fractions, which have high positive bias in winter and transition seasons, while in summer, the cloud fraction is well captured with a slight underestimation. The clear sky AOD over the Aeronet stations in the Arctic region is underestimated by 33% (Eclipse_AMIP) to 47% (Eclipse_CplHist1). Similar negative biases are found with comparison to the satellite based AOD product (Table 2). The climatological monthly variation is poorly captured with *r* values between -0.07 to 0.07 compared to AERONET AOD and 0 to 0.13 compared to satellite AOD. The simulations could not represent the climatological monthly variation of the observed AERONET AODs (Figure 2).

3.1.2. Climate

The different simulations are evaluated against a set of climate variables and the statistics are presented in Table 3a and 3b, and in Figures 4 and 5. The climatological mean (1995-2014) monthly Arctic surface air temperatures are slightly overestimated by up to 0.55 °C in the AMIP simulations, while the coupled ocean simulations underestimate the surface air temperatures by up to -0.17 °C. All simulations were able to reproduce the monthly climatological variation with *r* values of 0.99 and higher (Figure 4). Results show that both absorbing (BC) and scattering aerosols (OC and SO_4^{2-}) are underestimated by the GISS-E2.1 model, implying that these biases can partly cancel out their impacts on radiative forcing due

Deleted: OC

Deleted: OC

Deleted:). The climatological monthly variation of the OC levels are also well simulated in all seasons (

Formatted: Highlight

Formatted: Highlight

Formatted: Highlight

Formatted: Highlight

Formatted: Subscript, Highlight

Formatted: Superscript, Highlight

Formatted: Highlight

Formatted: Highlight

Formatted: Subscript, Highlight

Formatted: Highlight

Deleted: ¶

Formatted: Highlight

to aerosol-radiation interactions. This, together with the very low biases in surface temperatures suggests that aerosols over the Arctic do not affect the Arctic climate and that the changes in Arctic climate are mainly driven by changes due to greenhouse gas concentrations. The monthly mean precipitation has been underestimated by around 50% by all simulations (Table 3a), with largest biases during the summer and autumn (Figure 4). The observed monthly climatological mean variation was very well simulated by all simulations, with *r* values between 0.80 and 0.90.

Arctic SSTs are underestimated by the ocean-coupled simulation up to -1.96 °C, while the atmosphere-only runs underestimated SSTs by -1.5 °C (Table 3a). This difference is attributed to the differences in the SST data used as model input (Reynolds et al., 2002) and data used to evaluate the model (Rayner et al., 2003). The monthly climatological mean variation is well captured with *r* values above 0.99 (Table 3a, Figure 4), with a similar cold bias in almost all seasons. The sea-ice extent was overestimated by all coupled simulations by about 12%, while the AMIP-type Eclipse simulations slightly underestimated the extent by 3% (Table 3a). The observed variation was also very well captured with very high *r* values. The winter and spring biases were slightly higher compared to the summer and autumn biases (Figure 4).

All simulations overestimate the climatological (1995-2014) mean total cloud fraction by 21% to 25% during the extended winter months (October through February), where the simulated seasonality is anti-correlated in comparison to AVHRR CLARA-A2 observations, whereas, a good correlation is seen during the summer months irrespective of the observational data reference. The largest biases were simulated by the atmosphere-only simulations, with the nudged simulation having the largest bias (*NMB*=25%). The coupled model simulations are closer to the observations during the recent past. On the other hand, the climatology of the annual-mean cloud fraction was best simulated by the nudged atmosphere-only simulation (Eclipse_AMIP_NCEP) with a *r* value of 0.40, while other simulations showed a poor performance (*r*=-0.17 to +0.10), except for the summer where the bias is lowest (Figure 5). The evaluation against CALIPSO data however shows much smaller biases (*NMB* = +3% to +6%). This is because in comparison to CALIPSO satellite that carries an active lidar instrument (CALIOP), the CLARA-A2 dataset has difficulties in separating cold and bright ice/snow surfaces from clouds thereby underestimating the cloudiness during Arctic winters. Here both datasets are used for the evaluation as they provide different observational perspectives and cover the typical range of uncertainty expected from the satellite observations. Furthermore, while the CLARA-A2 covers the entire evaluation period in current climate scenario, CALIPSO observations are based on 10-year data covering the 2007-2016 period.

Figure 5 shows the evaluation of the simulations with respect to LWP and IWP. It has to be noted here that to obtain a better estimate of the cloud water content, the CloudSat observations were constrained with MODIS observations which resulted in a lack of data during the months with darkness (Oct-Mar) over the Arctic (see Section 2.4.3). Hence, we present the results for the polar summer months only. As seen in Figure 5, all simulations

Deleted: largely

Formatted: Highlight

Formatted: Highlight

Deleted: All simulations overestimated the climatological (1995-2014) mean total cloud fraction by 21% to 25% during the extended winter months (October through February).

Formatted: Highlight

Deleted: (

Formatted: Highlight

Formatted: Font: Italic, Highlight

Formatted: Highlight

Deleted: The evaluation against CALIPSO data however shows much smaller biases (*NMB* = +3% to +6%). This decrease in overestimation is due to the strong underestimation of Arctic wintertime cloud formation by AVHRR CLARA-A2 observations due to difficulties in separating cold and bright ice/snow surfaces from clouds (Karlsson et al., 2017), leading to larger positive bias calculated for the model.

overestimated the climatological (2007-2014) mean Polar summer LWP by up to almost 75%. The smallest bias (14%) is calculated for the nudged atmosphere-only (Eclipse_OnlyAtm_NCEP), while the coupled simulations had biases of 70% or more. Observations show a gradual increase in the LWP, peaking in July, whereas the model simulates a more constant amount for the nudged simulation and a slightly decreasing tendency for the other configurations. All model simulations overestimate LWP during the spring months. The atmosphere-only nudged simulations tend to better simulate the observed LWP during the summer months (June through September). The coupled simulations, irrespective of the emission dataset used, are closer to observations only during the months of July and August.

The climatological (2007-2014) mean Polar summer IWP is slightly better simulated compared to the LWP, with biases within -60% with the exception of the nudged Eclipse (Eclipse_AMIP_NCEP) simulation (*NMB*=-74%). All simulations simulated the monthly variation well, with *r* values of 0.95 and more.

In the Arctic, the net cloud forcing at the surface changes sign from positive to negative during the polar summer (Kay and L'Ecuyer, 2013). This change typically occurs in May driven mainly by shortwave cooling at the surface. Since the model simulates the magnitude of the LWP reasonably, particularly in summer, the negative cloud forcing can also be expected to be realistic in the model (e.g. Gryspeerdt et al. 2019). Furthermore, the aerosol and pollution transport into the Arctic typically occurs in the lowermost troposphere where liquid water clouds are prevalent during late spring and summer seasons. The interaction of ice clouds with aerosols is, however, more complex, as ice clouds could have varying optical thicknesses, with mainly thin cirrus in the upper troposphere and relatively thicker clouds in the layers below. Without the knowledge on the vertical distribution of optical thickness, it is difficult to infer the potential impact of the underestimation of IWP on total cloud forcing and their implications.

3.2. Arctic burdens and radiative forcing due to aerosol-radiation interactions (RF_{ARI})

The recent past and future Arctic column burdens for BC, OA and SO_4^{2-} for the different scenarios and emissions are provided in Figure 6. In addition, Table 4 shows the calculated trends in the burdens for BC, OA and SO_4^{2-} for the different scenarios, while Table 5 provides the 1990-2010 and 2030-2050 mean burdens of the aerosol components. The BC and SO_4^{2-} burdens started decreasing from the 1990s, while OA burden remains relatively constant, although there is large year-to-year variability in all simulations. All figures show a decrease in burdens after 2015, except for the SSP3-7.0 scenario, where the burdens remain close to the 2015 levels. The high variability in BC and OA burdens over the 2000's is due to the biomass burning emissions from GFED, which have not been harmonized with the no-satellite era. It should also be noted that these burdens can be underestimated considering the negative biases calculated for the surface concentrations and in particular for the AODs reported in Table 2 and Tables S2-6.

Deleted:
Formatted: Highlight
Deleted: B
Formatted: Highlight
Formatted: Subscript, Highlight
Formatted: Highlight
Deleted: OC
Formatted: Highlight
Deleted: OC
Deleted: OC
Deleted: are
Deleted: harmonised

In addition to the burdens of these aerosol species, the TOA radiative forcing due to aerosol-radiation interaction (RF_{ARI}) over the Arctic are simulated by the GISS-E2.1 ensemble. RF_{ARI} is calculated as the sum of shortwave and longwave forcing from the individual aerosol species between 1850 and 2050 are presented in Figure 7. The instantaneous forcings are calculated with a double call to the model's radiation code, with and without aerosols. The model outputs separate forcing diagnostics for anthropogenic and biomass burning BC and OC, as well as biogenic SOA, making it possible to attribute the forcing to individual aerosol species. The negative RF_{ARI} has increased significantly since 1850 until the 1970's due to an increase in aerosol concentrations. Due to the efforts of mitigating air pollution and thus a decrease in emissions, the forcing became less negative after the 1970's until 2015. Figure 7 also shows a visible difference in the anthropogenic RF_{ARI} simulated by the NINT (prescribed aerosols) and OMA (interactive aerosols) simulations in the CMIP6 ensemble, where the anthropogenic RF_{ARI} by NINT simulation is less negative (by almost 30%) compared to the OMA simulation (Figure 7b). On the other hand, no such difference is seen in the net RF_{ARI} time series (Figure 7a). This compensation is largely driven by the 50% more positive dust and 10% less negative sea-salt RF_{ARI} in the OMA simulation.

3.2.1. Black carbon

All simulations show a statistically significant (as calculated by Mann-Kendall trend analyses) decrease in the Arctic BC burdens (Table 4) between 1990-2014, except for the CMIP6_Cpl_Hist, which shows a slight non-significant increase that can be attributed to the large increase in global anthropogenic BC emissions in CMIP6 after year 2000 (Figure 1). From 2015 onwards, all future simulations show a statistically significant decrease in the Arctic BC burden (Table 4). The Eclipse CLE ensemble shows a 1.1 kTon (31%) decrease in the 2030-2050 mean Arctic BC burden compared to the 1990-2010 mean, while the decrease in 2030-2050 mean Arctic BC burden is larger in the MFR ensemble (2.3 kTon: 62%). In the CMIP6 simulations, the 2030-2050 mean Arctic BC burdens decrease by 0.70 to 1.59 kTon, being largest in SSP1-2.6 and lowest in SSP3-7.0-lowNTCF, while the SSP3-7.0 simulation leads to an increase of 0.43 kTon (12%) in 2030-2050 mean Arctic BC burdens. It is important to note that the changes in burden simulated by the Eclipse CLE ensemble (-1.1 kTon) is comparable with the change of -1 kTon in the SSP2-4.5 scenario, consistent with the projected emission changes in the two scenarios (Figure 1).

As seen in Table 6, the GISS-E2.1 ensemble calculated a BC RF_{ARI} of up to 0.23 W m^{-2} over the Arctic, with both CMIP6 and Eclipse coupled simulations estimating the highest forcing of 0.23 W m^{-2} for the 1990-2010 mean (Table 6a). This agrees with previous estimates of the BC RF_{ARI} over the Arctic (e.g. Schacht et al., 2019). In the future, the positive BC RF_{ARI} is generally decreasing (Figure 6) due to lower BC emissions, except for the SSP3-7.0 scenario, where the BC forcing becomes more positive by 0.05 W m^{-2}. The changes in the Arctic RF_{ARI} in Table 6a follows the Arctic burdens presented in Table 5, and emission projections presented in Figure 1, leading to largest reductions in BC RF_{ARI} simulated in SSP1-2.6 (-0.10 Wm^{-2}). Similar to the burdens, the Eclipse CLE and CMIP6 SSP2-4.5 scenarios simulate a very close decrease in the 2030-2050 mean BC RF_{ARI} of -0.06 Wm^{-2} and -0.06 Wm^{-2}, respectively.

Formatted ... [1]
Formatted ... [2]
Formatted ... [3]
Formatted ... [4]
Formatted ... [5]
Formatted ... [6]
Formatted ... [7]
Formatted ... [8]
Formatted ... [9]
Formatted ... [10]
Formatted ... [11]
Formatted ... [12]
Deleted: ¶ ... [13]
Formatted ... [14]
Deleted: negative
Deleted: trend
Deleted: slope = -0.025±0.003 kTon yr^{-1})
Deleted: over the Arctic
Deleted: asing
Deleted: trend of 0.007 kTon yr^{-1}, which
Deleted: The Eclipse ensemble also shows that the 1990- ... [15]
Deleted: negative trend
Deleted: The Eclipse simulations show a smaller negative in ... [16]
Deleted: simulations
Deleted: calculate a negative trend by -0.02±0.00 kTon yr^{-1} ... [17]
Deleted: 1
Deleted: scenario (-0.04±0.00 kTon yr^{-1}), leading to decrease ... [18]
Deleted: in of 2030-2050 mean
Deleted: gives the largest reduction by -0.07 kTon yr^{-1} (1.6 ... [19]
Deleted: (-0.004 kTon yr^{-1}) with the 2030-2050 mean being ... [20]
Deleted: T
Deleted: change
Deleted: in
Deleted: scenario
Formatted ... [21]
Formatted ... [22]
Formatted ... [23]
Formatted ... [24]
Formatted ... [25]
Formatted ... [26]
Formatted ... [27]
Formatted ... [28]
Formatted ... [29]
Formatted ... [30]
Formatted ... [31]
Formatted ... [32]

3.2.2. Organic aerosols

The Eclipse historical ensemble simulate a positive OA burden trend between 1990 and 2014, however this trend is not significant at the 95% confidence level (Table 4). The CMIP6_Cpl_Hist simulation gives a larger trend, due to a large increase in global anthropogenic OC emissions in CMIP6 (Figure 1). The nudged AMIP Eclipse simulation calculates the largest 1990-2010 mean OA burden (57 kTon), while the coupled simulation shows a slightly lower 1990-2010 mean burden (55 kTon). This largest OA burden in the Eclipse_AMIP_NCEP simulation is attributed to the largest biogenic SOA burden calculated in this scenario, as well as a better-simulated transport from source regions due to the nudged winds (Figure S1). The anthropogenic and biogenic contributions to SOA burdens in the coupled Eclipse and CMIP6 recent past simulations imply that the differences in the burdens between the two ensembles can be attributed to the different anthropogenic emissions datasets used in the Eclipse and CMIP6 simulations (Figure S1), as well as the differences in SOA contributions due to simulated increases in the biogenic emissions (Figure S5) . The AMIP-type Eclipse run simulates a lower 1990-2010 mean OA burden (50 kTon), attributed to the smallest biogenic SOA burden in this scenario. The Eclipse CLE ensemble shows a decrease of 6.6 kTon (12%) in 2030-2050 mean OA burden compared to the 1990-2010 mean, while the MFR ensemble shows a larger decrease in the same period (15.2 kTon: 27%). The CMIP6 simulations show a much larger decrease of 2030-2050 mean Arctic OA burdens, with a decrease of 8.1 kTon (SSP2-4.5) to 17 kTon (SSP1-2.6), while the SSP3-7.0 simulation shows an increase in OA burdens in the same period by 1.3 kTon (2%). Similar to BC burdens, Eclipse CLE and CMIP6 SSP2-4.5 scenarios project similar changes in 2030-2050 mean OA burden (6.6 kTon and 8.1 kTon, respectively).

As shown in Table 6a, the Eclipse ensemble calculated an OA RF_{ARI} of -0.05 to -0.08 Wm^{-2} for the 1990-2010 mean, where the nudged AMIP-type simulation shows the largest RF_{ARI}, due to the largest Arctic OA burden calculated for this period (Table 5). For the future, both Eclipse CLE and MFR ensembles show an increase in the negative 2030-2050 mean RF_{ARI} by -0.02 Wm^{-2}, which is very close to the increase in the negative forcing calculated for the various CMIP6 simulations (-0.01 to -0.03 Wm^{-2}). Following the burdens, the largest increase in the 2030-2050 mean OA RF_{ARI} is calculated for the SSP3-7.0 (-0.03 Wm^{-2}), and the lowest for SSP1-2.6 and 3-7.0-lowNTCF (-0.01 Wm^{-2}).

3.2.3. Sulfate

Regarding SO_4^{2-} burdens, all simulations show a statistically significant negative trend both in 1990-2014 and in 2015-2050, as seen in Figure 6 and Table 5. Both the nudged AMIP-type and coupled Eclipse simulations showed a 1990-2010 mean SO_4^{2-} burden of 93 kTon, while the AMIP-type simulation showed a slightly larger SO_4^{2-} burden of 95 kTon, attributed to the larger cloud fraction simulated in this model version (Table 2). For the 2015-2050 period, the Eclipse ensemble simulates a mean Arctic SO_4^{2-} burden decrease of 30-40 kTon (32-42%), compared to the 1990-2010 mean, while CMIP6 ensemble simulates a reduction of 16-45 kTon (16-45%). The SSP2-4.5 and Eclipse CLE scenarios simulate a very similar decrease (30 kTon) in 2030-2050 mean Arctic SO_4^{2-} burdens, while the MFR and SSP1-2.6 scenarios

Formatted: Font: Italic

Deleted: ¶

Deleted: simula…imulateions…show overall … positive OA burden trend of OC b…etween 1990 and 2014 (0.03±0.06 kTon yr^{-1})… however this trend is not significant at the 95% confidence level (Table 4) (p=0.5-0.9)… The CMIP6_Cpl_Hist simulation gives a larger trend (0.12 kTon yr^{-1})… similar to the BC burden, …ue to a large increase in global anthropogenic OC…C emissions in CMIP6 (Figure 1). The nudged AMIP Eclipse simulation calculates the largest 1990-2010 mean OC…A burden (57 kTon), while the coupled simulation shows a slightly lower 1990-2010 mean burden (55 kTon). This largest OC ... [33]

Formatted: Highlight

Formatted ... [34]

Deleted: OC

Deleted: simulations …hows a negative trend of -0.20±0.02 kTon yr^{-1} between 2015 and 2050, leading to … decrease of 6.62…kTon (12%) in 2030-2050 mean OA burden compared to the 1990-2010 mean, while the MFR ensemble simulations shows a larger decrease in the same period steeper trend of -0.36±0.02 kTon yr^{-1} …154…29…kTon: 27% decrease in 2030-2050 mean vs 1990-2010 mean…. The CMIP6 simulations show a much larger decrease steeper trend …f 2030-2050 mean Arctic OC…A burdensby -0.45±0.29 kTon yr^{-1} compared to the Eclipse simulations… with a decrease of 81…19…kTon (SSP2-4.53-7.0… to 17 kTon (SSP1-2.6), while the SSP3-7.0 simulation shows an increase in OA burdens in the same period by 1.3 kTon (2%) in the 2030-2050 mean compared to the 1990-2010 mean… Similar to burdens, Eclipse CLE and CMIP6 SSP2-4.5 scenarios project similar changes in 2030-2050 mean OC…A burden (6.69…kTon and 7.… ... [35]

Formatted: Highlight

Formatted ... [36]

Formatted: Font: Italic

Deleted: Eclipse and CMIP6 simulations show a comparable decrease of Arctic sulfate burdens in the recent past period (-1.16±0.23 T yr^{-1} and -1.09 kTon yr^{-1}, respectively). …oth the nudged AMIP-type and coupled Eclipse simulations showed a 1990-2010 mean SO_4^{2-} burden of 932 ... [37]

Formatted: Highlight

Deleted: The Eclipse CLE scenario shows a decrease of -0.14±0.02 kTon/yr in the

Formatted ... [38]

Deleted: leading to a decrease of 28 kTon decrease in 2030-2050 mean …ompared to the 1990-2010 mean, while CMIP6 ensemble simulates a reduction of 16-45 kTon (16-45%), while the MFR shows a very similar trend of -0.15±0.03 kTon yr^{-1}, however with a larger decrease of 2030-2050 mean (-38 kTon) ... [39]

Formatted ... [40]

also simulate comparable reductions in the burdens (Table 5). Following the emission projections, the SSP1-2.6 scenario gives the largest decrease (45 kTon: 45%), and the SSP3-7.0 scenario gives the smallest reduction (16 kTons: 16%) in Arctic 2030-2050 mean SO_4^{2-} burdens.

The SO_4^{2-} RF_{ARI} is decreasing (Figure 6) following the decreasing emissions (Figure 1) and burdens (Figure 5). Both Eclipse and CMIP6 ensembles simulate a decrease in SO_4^{2-} RF_{ARI} by 0.06-0.18 Wm^{-2}. The 2030-2050 mean SO_4^{2-} RF_{ARI} follows the burdens (Table 6), with CLE and SSP2-4.5 giving similar decreases in the negative SO_4^{2-} RF_{ARI} of 0.11 Wm^{-2}, while the Eclipse MFR and SSP1-2.6 simulates a very similar decrease in the 2030-2050 mean SO_4^{2-} RF_{ARI} (0.16 and 0.18 Wm^{-2}, respectively).

3.2.4. Net aerosol radiative forcing

The coupled simulations in both Eclipse and CMIP6 ensemble show an Arctic RF_{ARI} of -0.32 to -0.35 Wm^{-2} for the 1990-2010 mean, slightly lower than recent estimates (e.g. -0.4 W m^{-2} by Markowicz et al., 2021). In the Eclipse ensemble, -0.22±0.01 Wm^{-2} is calculated to be originated by the anthropogenic aerosols, while in the CMIP6 near-past simulations show a contribution of -019 to -0.26 Wm^{-2} from anthropogenic aerosols (Table 6b). The AMIP-type Eclipse simulations calculated a much larger RF_{ARI} of -0.47 W m^{-2} for the same period, which can be mainly due to the increase in the positive forcing of the BC aerosols in the coupled simulations due to larger burdens. This effect is amplified due to the larger sea-ice concentration simulated with the coupled model, leading to brighter surfaces compared to the AMIP simulations. For the 2030-2050 period, the Eclipse ensemble simulated an increase in the negative in RF_{ARI} by -0.07 W m^{-2}, while the negative anthropogenic in RF_{ARI} increased by only -0.02 W m^{-2}, suggesting that the contribution from natural aerosols become more important in the future. The results show that the positive dust forcing is decreased by 0.03 Wm^{-2} (from 0.12 Wm^{-2} to 0.09 Wm^{-2}), while the negative sea-salt forcing becomes more negative by -0.03 Wm^{-2} due to the increase of ice-free ocean fraction due to melting of sea-ice (see Section 3.3). For the same period, the CMIP6 future ensemble simulated an increase of the negative RF_{ARI} by -0.01 Wm^{-2} to -0.06 Wm^{-2}, the largest change being in SSP1-2.6 and SSP2-4.5, mainly driven by the change in BC forcing (Table 6a). Table 6 also shows that the SSP1-1.6 simulates no change in the anthropogenic forcing, while SSP2-4.5 shows a similar increase of -0.01 Wm^{-2} in the Eclipse ensemble. In contrary, the SSP3-7.0 and SSP3-7.0-lowNTCF simulates a large decrease in the anthropogenic negative RF_{ARI} by 0.05 Wm^{-2} and 0.02 Wm^{-2}, respectively.

The different behavior in the two ensembles is further investigated by looking at the aerosol-radiation forcing calculated for the individual aerosol species of BC, OA, SO_4^{2-} and NO_3^- presented in Figure 8 that shows the box-whisker plots using the full range of scenarios. The increase in cooling effect of aerosols calculated by the Eclipse ensemble is attributed mainly to the decrease in BC as opposed to other aerosol species (Figure 8). More negative forcing is calculated for the OA and NO_3^-, while the SO_4^{2-} forcing is becoming less negative due to large reductions in SO_2 emissions (Figure 1). The net aerosol forcing is therefore slightly more negative. In the CMIP6 ensemble, the BC forcing does not change as much compared

Deleted: On the other hand, the CMIP6 simulation predicts a much larger decrease of sulfate burdens by -0.49±0.40 kTon yr^{-1} in the future, largely driven by t…e SSP1-2.6 scenario that …ives the largesta…decrease (of -….50.94…kTon: yr1 ... [41]

Formatted ... [42]

Deleted: leading to a decrease of 45 kTon in 2030-2050 mean compared to the 1990-2010 mean

Formatted ... [43]

Formatted: Font: Italic, Highlight

Deleted: ¶
Arctic radiative forcing¶
¶
The TOA aerosol radiative forcings over the Arctic as calculated by the sum of shortwave and longwave TOA forcings from all aerosol species between 1850 and 2050 are presented in Figure 7. The instantaneous forcings are calculated with a double call to the model's radiation code, with and without aerosols. The negative aerosol forcing has increased significantly since 1850 until the 1970's due to an increase in aerosol concentrations. Due to the efforts of mitigating air pollution and thus a decrease in emissions, the forcing became less negative after the 1970's until 2015. ¶
¶
The coupled …clipse and CMIP6 ensemble show simulations calculated …n Arctic RF_{ARI}n aerosol TOA radiative forcing…of -0.32±0.01…to -0.35 W ... [44]

Formatted: Highlight

Formatted: Don't adjust space between Latin and Asian text, Don't adjust space between Asian text and numbers

Formatted ... [45]

Deleted: while…he AMIP-type Eclipse simulations calculated a much larger RF_{ARI}forcing ... [46]

Formatted ... [47]

Deleted: both …he Eclipse CLE and MFR en…nsembles…simulated an increase in the negative in RF_{ARI} by -0.07 W m^{-2} n aerosol TOA forcing of -0.39±0.01 W m^{-2}. For the anthropogenic aerosols (Figure 7), the Eclipse TOA forcing in 1990-2010 is calculated to be -0.22±0.01 W m^{-2} by the Eclipse ensemble… while the negative anthropogenic in RF_{ARI} increased by only -0.02 while in the 2030-2050 period, the TOA anthropogenic forcing (including biomass burning) became more negative in the Eclipse ensemble (-0.24±0.01 … m^{-2}: -0.24±0.00 W m^{-2} and -0.23±0.00 W m^{-2} for CLE and MFR, respectively… that the contribution from natural aerosols become more important in the future.). ... [48]

Formatted ... [49]

Deleted: ¶
The forcing calculated for the individual aerosol species of BC, OC, SO_4^{2-} and NO_3^- are also investigated separately (Table 4 and Figure 8). The increase in cooling effect of aerosols calculated by the Eclipse ensemble is attributed ... [50]

Deleted: As seen in Table 4, the GISS-E2.1 ensemble calculated a BC TOA direct radiative forcing of up to 0.23 W m^{-2} over the Arctic, with both CMIP6 and Eclipse coupled ... [51]

Formatted: Highlight

Deleted: behaviour…ehavior in the two ensembles is further investigated by looking at the aerosol-radiation forcing calculated for the individual aerosol species of BC, OC… ... [52]

to the Eclipse ensemble to counteract the change in impact from SO_4^{2-}, giving a slightly more positive net aerosol forcing. The CMIP6 ensemble also simulates a larger increase in the negative NO_3^- forcing compared to the Eclipse ensemble (Shindell et al., 2013). Overall, the changes in the different aerosol species leads to a more negative aerosol forcing by mid-century compared to the 1990-2010 period.

The spatial distributions of the statistically significant change in the Arctic RF_{ARI} in 2030-2050 mean with respect to the 1990-2010 mean in the different ensemble members are presented in Figure 9. Results show a decrease of the negative RF_{ARI} over Europe, and partly over North America, and an increase over northern Pacific in all ensemble members. Globally, larger changes are simulated over the East and South Asia (Figure S2), where largest anthropogenic emission reductions take place. The global net RF_{ARI} is dominated by the sea-salt particles, accounting for about 60% of the 1990-2010 mean forcing of -2 to -2.3 Wm^{-2} in and 2030-2050 mean forcing of -19 to 2.1 Wm^{-2}.

3.3. Climate change

3.3.1. Surface air and sea surface temperatures

The surface air temperature and sea-ice extent are calculated in the different simulations for the 1990-2050 period. As seen in Figure 10, the Arctic surface air temperatures increase in all scenarios. Between 1990 and 2014, the surface air temperatures over the Arctic increased statistically significant by 0.5 °C decade^{-1} (Eclipse_CplHist) to 1 °C decade^{-1} (CMIP6_Cpl_Hist), with CMIP6 showing larger increases compared to the Eclipse ensemble (Table 7). On the other hand, the observed surface air temperature during 1990-2014 shows a smaller and statistically non-significant increase of 0.2 °C decade^{-1}. From 2015 onwards, surface air temperatures continue to increase significantly by 0.3 to 0.6 °C decade^{-1}, with larger increases in the Eclipse ensemble, due to larger reductions in the emissions and therefore in the burdens and associated RF_{ARI}.

The 2030-2050 mean surface air temperatures are projected to increase by 2.1 °C and 2.3 °C compared to the 1990-2010 mean temperature (Table 8, Figure 10) according to the Eclipse CLE and MFR ensembles, respectively, while the CMIP6 simulation calculated an increase of 1.9 °C (SSP1-2.6) to 2.2 °C (SSP3-7.0). Changes in both ensembles are statistically significant on a 95% level. These warmings are smaller compared to the 4.5 - 5 °C warmer 2040 temperatures compared to the 1950-1980 average in the CMIP6 SSP1-2.6, SSP2-4.5 and SSP3-7.0 scenarios, reported by Davy and Outen (2020). It should however be noted that due to the different baselines used in the present study (1990-2010) and the 1950-1980 baseline used in Davy and Outen (2020), it is not possible to directly compare these datasets. Figure 11 shows the spatial distributions of the statistically significant (as calculated by student t-test) Arctic surface air temperature change between the 1990-2010 mean and the 2030-2050 mean for the individual Eclipse and CMIP6 future scenarios. All scenarios calculate a warming in the surface air temperatures over the central Arctic, while there are differences over the land areas. The Eclipse CLE and MFR ensembles show similar warming mainly over the Arctic ocean as well as North America and North East Asia and cooling over

Deleted: higher
Deleted: .
Deleted: ¶
Formatted: Highlight
Formatted: Subscript, Highlight
Formatted: Highlight
Formatted: Subscript, Highlight
Formatted: Highlight
Formatted: Subscript, Highlight
Formatted: Highlight
Deleted: Overall, the Eclipse ensemble simulates slightly larger change in the aerosol forcings over the 2015-2050 period, based on the 1990-2010 mean, compared to the CMIP6 ensemble. These changes are consistent with the changes in the aerosol burdens, where Eclipse simulations calculated slightly larger changes in burdens compared to CMIP6 sinnulations. The Eclipse ensemble simulation shows that the aerosol forcing (anthropogenic+natural) anomaly becomes negative (-0.09±0.03 W m^{-2}) in 2050 compared to the 2015 anomaly (0.05±0.02 W m^{-2}). The CMIP6 ensemble on the other hand shows that the 2050 anomaly becomes -0.05±0.04 W m^{-2}. ¶
Formatted: Subscript, Highlight
Formatted: Highlight
Deleted: *4*
Deleted: , precipitation, sea surface temperature
Deleted: 9
Formatted: Highlight
Deleted: 0
Deleted: , with a statistically significant ensemble mean trend of 7±2 °C decade^{-1}
Deleted: 5
Deleted: 5±1
Formatted: Highlight
Formatted: Subscript, Highlight
Formatted: Highlight
Deleted: in the Eclipse simulations and by 4±1 °C decade^{-1} in the CMIP6 simulations.
Deleted: The Eclipse ensemble simulated an annual average surface temperature in the Arctic of -7.44±0.94 °C in 1990 while the NINT-Cpl and CMIP6_Cpl_Hist simulated -8.32 °C and -9.21 °C, respectively. The full ensemble simulated an
Deleted: 4
Deleted: 9
Formatted: Highlight
Deleted:
Deleted: 0
Formatted: Highlight
Formatted: Highlight

the Greenland Sea. The latter is a well-known feature of observations and future projections, linked, i.e., to the deep mixed layer in the area and declines in the Atlantic Meridional Circulation (e.g. IPCC, 2014; Menary and Wood, 2018; Keil et al., 2020). There are also differences between the Eclipse and the CMIP6 ensembles as seen in Figure 11. All CMIP6 scenarios show a warming over the central Arctic and a limited cooling over northern Scandinavia, following the changes in RF_{ARI} shown in Figure 9, except for the SSP3-7.0 scenario that shows no cooling in the region. The SSP3-7.0-lowNTCF scenario shows an additional cooling over Siberia. These warmings are comparable with earlier studies, such as Samset et al. (2017) estimating a warming of 2.8 °C, attributed to aerosols.

3.3.2. Sea-ice

The Arctic sea-ice extent is found to decrease significantly in all simulations (Figure 10 and Table 7). Similar to the near-surface temperatures, during the 1990-2014 period, the CMIP6 ensemble simulated a large decrease of sea-ice extent compared to the Eclipse ensemble. On the other hand, the CMIP6_Cpl_Hist largely overestimated the observed decrease of 30 000 $km^2\ yr^{-1}$. This overestimation has also been reported for some of the CMIP5 and CMIP6 models (Davy and Outten, 2020). After 2015, the Eclipse CLE ensemble projected larger decreases in the sea-ice extent compared to the CMIP6 ensemble (Table 7), in agreement with the changes in the near-surface temperatures. The evolutions of March and September sea-ice extents, representing the Arctic annual maximum and minimum extents, respectively, are also analyzed. The Eclipse ensemble projects a decrease of 23 000 ± 11 000 $km^2\ yr^{-1}$ in March sea-ice extent during the 2015-2050 period, while the CMIP6 ensemble projects a decrease of 10 000 ± 6000 $km^2\ yr^{-1}$ for the same period, both statistically significant. In September, much larger decreases are projected by both ensembles. The Eclipse ensemble simulates a decrease of 64 000 ± 10 000 $km^2\ yr^{-1}$ in the 2015-2050 period while the CMIP6 ensemble predicts a decrease of 50 000 ± 20 000 $km^2\ yr^{-1}$.

The 2030-2050 annual mean sea-ice extent (Table 8) is projected to be 1.5 and 1.7 million km^2 lower compared to the 1990-2010 mean in the Eclipse CLE and MFR scenarios, respectively, both statistically significant on a 95% level. The CMIP6 simulations predict a lower decrease of sea-ice extent by 1.2 - 1.5 million km^2, however these changes are not statistically significant. These results are comparable with the results from the CMIP6 models (Davy and Outten, 2020). In the 2030-2050 March mean the sea-ice extent is projected to be 925 000 km^2 lower in the Eclipse ensemble (statistically significant), while the CMIP6 ensemble projects a decrease of 991 000 km^2 (not statistically significant). A much larger decrease is projected for the 2030-2050 September mean, being 2.6 million km^2 and 2.3 million km^2 in Eclipse and CMIP6 ensembles, respectively. As seen in Figure 12, the Eclipse ensemble predicts an up to 90% lower September sea-ice fraction in a band marking the maximum retreat of the sea ice line at the end of the summer, while the changes simulated by the CMIP6 ensemble are not statistically significant on 95% level (therefore not shown in Figure 11), which can be attributed to the single ensemble member per scenario in the CMIP6 ensemble, as well as the not significant changes in the near-surface temperatures (not shown). In March (Figure S3), the Eclipse ensemble simulated a decrease in maximum sea-ice extent at the end of winter over the northern Pacific, while the CMIP6 ensemble did not show any

Deleted: south of Greenland

Deleted: a

Deleted: 0

Formatted: Subscript

Deleted: n

Deleted: ¶
Following surface air temperatures, sea surface temperatures significantly increase ($p<0.05$) in all simulations (Figure 9). Between 1990-2014, the Eclipse simulations show a warming trend of SSTs by 0.006±0.003 °C yr^{-1}, while the CMIP6 simulations show a much larger increase of 0.012 °C yr^{-1}. Both ensembles underestimated the observed SST trend of 0.017 °C yr^{-1}. The Eclipse CLE and MFR scenarios predict a similar increase of 0.005 °C yr^{-1}, leading to a slight increase of 0.25 °C in 2030-2050 mean surface air temperature compared to the 1990-2010 mean, while the CMIP6 simulations show an increase of 0.003±0.001 °C yr^{-1} , leading to an increase of 0.22 °C to 0.25 °C. Figure S2 shows the spatial distribution of the sea surface temperature change between the 1990-2010 mean and the 2030-2050 mean for the individual Eclipse and CMIP6 future scenarios. All simulations show a cooling of the sea surface over the southern Greenland and north western Atlantic and a ... [54]

Deleted: *4*

Deleted: 9

Formatted: Highlight

Deleted: D

Deleted: Eclipse

Deleted: 34 000±5 800 $km^2\ yr^{-1}$, in agreement with the

Deleted: 4

Deleted: , while CMIP6_Cpl_Hist simulated a decrease of 59 ... [55]

Formatted: Highlight

Deleted: a 37 000 ± 12 000 $km^2\ yr^{-1}$ decrease while the MFR ... [56]

Deleted: analysed

Deleted: , representing the Arctic annual maximum and ... [57]

Formatted: Highlight

Deleted: decrease by

Deleted: .

Deleted:

Deleted: decrease by

Deleted: .

Deleted: 1

Deleted: decrease of

Deleted: by up to 90%

Deleted: .

Deleted: The CMIP6 SSP1-2.6 simulation shows a similar ... [58]

Deleted: 1

Deleted: all

Deleted: mode

Deleted: ls agree on

statistically significant changes in sea-ice. In addition, the Eclipse ensemble shows a decrease over the north Atlantic close to Greenland. All simulations show a similar and statistically significant decrease in annual mean sea-ice extent (Figure S4 over the central Arctic, with the CMIP6 ensemble showing also some increase in the sea-ice extent over the Canadian Arctic, that is largest in SSP3-7.0.

The retreat in sea-ice extent also led to an increase of oceanic emissions of DMS and sea-salt (Figure S5); however, the increases are not significant on a 95% significance level. The simulated increase, in particular for the DMS emissions, is slightly larger in the Eclipse ensemble compared to the CMIP6 ensemble, due to a larger decrease of sea-ice extent in the Eclipse ensemble. Also note that GISS-E2.1 is using prescribed and fixed maps of DMS concentration in the ocean. When ocean locations that are year-round under sea-ice at present get exposed, the DMS that would exist in that sea water is not included in the simulations, likely underestimating the increased flux of DMS into the atmosphere as the sea ice retreats.

4. Summary and Conclusions

The GISS-E2.1 earth system model has been used to simulate the recent past (1990-2014) and future (2015-2050) aerosol burdens and their climate impacts over the Arctic. An ensemble of seventeen simulations has been conducted, using historical and future anthropogenic emissions and projections from CMIP6 and ECLIPSE V6b, the latter supporting the ongoing Arctic Monitoring and Assessment Programme.

The evaluation of the recent past simulations shows underestimates of Arctic surface aerosol levels by up to 50%, with the smallest biases calculated for the simulations where winds are nudged, and sea-surface temperature and sea-ice are prescribed (AMIP-type: atmosphere-only). An exception is SO_4^{2-}, where the nudged Eclipse AMIP simulation had the highest bias, due to the high cloud bias that leads to more in-cloud sulfate production from SO_2. The model skill analyses indicate slightly better performance of the CMIP6 version of the GISS-E2.1 model in simulating both the aerosol levels and climate parameters compared to the Eclipse version. In addition, the underestimations in the cloud properties, such as the cloud fraction and liquid water path, suggest missing sources of aerosols, in particular the marine sources, which can be important sources of CCN in the Arctic. Results also suggest that the underestimation of both absorbing and scattering aerosol levels can partly cancel out their impacts on RF_{ARI} and near-surface temperatures as the temperatures are very well reproduced by the model.

From 2015 onwards, all simulations, except for the worst case CMIP6 scenario SSP3-7.0, show a statistically significant decrease in the Arctic BC, OA and SO_4^{2-} burdens, with the CMIP6 ensemble simulating larger aerosol burdens Eclipse, while the Eclipse ensemble shows larger reductions (10-60%) in Arctic aerosol burdens compared to the reduction simulated by the CMIP6 ensemble (10-45%). The largest burden reductions are calculated by the highly ambitious emission reductions in the two ensembles; i.e. the Eclipse MFR (25-60%) and the CMIP6 SSP1-2.6 (25-45%).

Formatted: Highlight
Deleted: 2)
Deleted: s
Deleted: 3-S7
Deleted: (Figure S8)
Formatted: Highlight
Deleted: Eclipse simulations
Deleted: _A
Deleted: _NCEP
Formatted: Highlight
Formatted: Subscript, Highlight
Formatted: Highlight
Deleted: In addition, fully-coupled simulations had slightly smaller biases in aerosol levels compared to atmosphere-only simulations (winds not nudged). Results from the various Eclipse ensemble simulations showed that lowest biases in surface aerosols concentrations are calculated for atmosphere only (prescribed sea-ice and sea-surface temperature) simulations with nudged winds.
Formatted: Highlight
Deleted: OC
Deleted: CMIP6
Deleted: ing
Deleted: Eclipse
Deleted: T
Deleted: CLE
Deleted: show the largest reductions
Deleted: Results indicated that the differences in burdens between the two ensembles can be attributed to the different anthropogenic emissions datasets used. Results from the various Eclipse simulations showed that the biogenic SOA contribution to the OC burdens was higher in the nudged atmosphere only simulation, compared to the non-nudged and coupled simulations.

The present-day (1990-2010 mean) CMIP6 and Eclipse simulations calculated an aerosol radiative forcing due to aerosol-radiation interactions (RF_{ARI}) of -0.32 to -0.35 W m^{-2}. For the same period, the atmosphere only (AMIP) Eclipse simulations calculated a much larger negative RF_{ARI} of -0.47 W m^{-2}. This smaller RF_{ARI} by the coupled simulations is mainly due to larger BC burdens in the coupled simulations, leading to more positive forcing, which is amplified by the larger albedo effect due to larger sea-ice extent simulated in the coupled simulations. In the 2030-2050 period, the Eclipse ensemble simulated a RF_{ARI} -0.39±0.01 W m^{-2}, of which -0.24±0.01 W m^{-2} are attributed to the anthropogenic aerosols (BC, OA, SO_4^{2-} and NO_3^-). For the same period, the worst case CMIP6 scenario (SSP3-7.0) simulated a similar RF_{ARI} (-0.35 W m^{-2}) compared to the 1990-2010 mean , while large emission reductions led to a more negative RF_{ARI} (-0.40 W m^{-2}), mainly due to decrease in the positive forcing of the BC aerosols. Overall, the Eclipse ensemble simulated slightly larger changes in the RF_{ARI} over the 2015-2050 period, relative to the 1990-2010 mean, compared to the CMIP6 ensemble, which can be attributed to the larger reductions in burdens in the Eclipse ensemble. The differences between the two ensembles are further attributed to differences in the BC and SO_4^{2-} forcings. The results suggest that the different anthropogenic emission projections lead to only small differences in how the RF_{ARI} will evolve in the future over the Arctic.

The future scenarios with the largest aerosol reductions, i.e. MFR in the Eclipse and SSP1-2.6 in the CMIP6 ensemble projects a largest warming and sea-ice retreat. The Eclipse ensemble shows a slightly larger warming of 2030-2050 mean surface air temperatures compared to the 1990-2010 mean warming (2.1 to 2.5 °C) compared to that from the CMIP6 ensemble (1.9 °C to 2-2 °C). Larger warming in the Eclipse ensemble also resulted in a slightly larger reduction in sea-ice extent (-1.5 to -1.7 million km^{-2} in CLE and MFR, respectively) in 2030-2050 mean compared to the reduction in the CMIP6 scenario (-1.3 to -1.6 million km^{-2} in SSP1.2-6 and SSP3-7.0, respectively). However, the changes simulated by the two ensembles are within one standard deviation of each other.

The overall results showed that the aerosol burdens will substantially decrease in the short- to mid-term future, implying improvements in impacts on human health and ecosystems., Results also show that even the scenarios with largest emission reductions, i.e. Eclipse MFR and CMIP6 SSP1-2.6, lead to similar impact on the future Arctic surface air temperatures and sea-ice loss compared to scenarios with very little mitigation such as the CMIP6 SSP3-7.0, exacerbating the dominant role played by well-mixed greenhouse gases and underlining the importance of continued greenhouse gas reductions.

Author contributions. UI coordinated the study, conducted the model simulations, as well as model evaluation and analyses of the simulations, and wrote the manuscript. KT and GF supported the model simulations and processing of the Eclipse V6b emissions for the GISS-E2.1 model. JPF contributed to the plotting of the spatial distributions by further developing the autoimage R package (French, 2017). RM prepared and provided the AOD measurements, as well as the surface air temperature, sea surface temperature and sea-ice

Formatted: Highlight
Deleted: n aerosol TOA forcing
Formatted: Highlight
Deleted: and -0.32±0.01 W m^{-2}, respectively
Formatted: Subscript, Highlight
Deleted: aerosol TOA forcing
Formatted: Subscript, Highlight
Formatted: Highlight
Formatted: Highlight
Deleted: .
Deleted: For
Deleted: both
Deleted: n aerosol TOA forcing of
Deleted: OC
Formatted: Highlight
Deleted: TOA aerosol forcing
Deleted: SSP1-2.6 and SSP2-4.5 scenarios simulated
Deleted: TOA forcing
Deleted: of which the anthropogenic aerosols were responsible for -0.26 W m^{-2}).
Deleted: aerosol forcings
Deleted: se
Deleted: between the two ensembles and within them
Deleted: aerosol radiative forcing
Deleted: Overall, both Eclipse and CMIP6 ensembles show a similar increasing trend of surface air temperatures over the Arctic between 1990 and 2050, with the CMIP ensemble showing a slightly higher warming trend (6±3 °C $decade^{-1}$) compared to the trend calculated by the Eclipse ensemble (5±1 °C $decade^{-1}$). On the other hand, t
Formatted: Highlight
Deleted: of 2
Deleted: over the Arctic
Deleted: The Eclipse ensemble simulates
Deleted: in the Eclipse ensemble
Formatted: Font colour: Text 1, English (US)
Formatted: Highlight
Formatted: Highlight
Deleted: smaller emission reductions. On the other hand, scenarios with …
Deleted: leads to much larger sea-ice loss, implying that even though impacts are small in temperatures, high mitigation of aerosols are still necessary to limit sea-ice loss

data. MAT prepared the cloud observation data. CHW prepared the Arctic surface aerosol measurement data. KvS coordinated the experimental setup for the Eclipse simulations in the framework of the ongoing AMAP assessment. ZG prepared and provided the Eclipse V6b anthropogenic emissions. HS and DCT prepared the Villum Research Station aerosol data. JB and PL contributed to analyses of aerosols and climate parameters, respectively, and manuscript writing. All authors contributed to the analyses and interpretation of the results, as well as contributing to the writing of the manuscript.

Competing Interests. The authors declare that they have no conflict of interest.

Special issue statement. This article is part of the special issue "Arctic climate, air quality, and health impacts from short-lived climate forcers (SLCFs): contributions from the AMAP Expert Group".

Acknowledgements. This paper was developed as part of the Arctic Monitoring Assessment Programme (AMAP), AMAP 2021Assessment: Arctic climate, air quality, and health impacts from short-lived climate forcers (SLCFs). HadISST data were obtained from https://www.metoffice.gov.uk/hadobs/hadisst/ and are © British Crown Copyright, Met Office, provided under a Non-Commercial Government Licence http://www.nationalarchives.gov.uk/doc/non-commercial-government-licence/version/2/. UDel_AirT_Precip data provided by the NOAA/OAR/ESRL PSL, Boulder, Colorado, USA, from their Web site at https://psl.noaa.gov/. Alert sulfate data are from Sangeeta and EC & OA data from Lin Huang, respectively, as part of Canadian Aerosol Baseline Measurement (CABM) program at ECCC and would like to thank operators & technicians for collection of filters, calibration and analysis and Canadian Forces Services Alert for the operation of the military base. These datasets are also available on Global Atmospheric Watch program, World Data Center for aerosols, EBAS database (http://ebas.nilu.no/default.aspx).Aside from Alert, Canada's surface air quality data are from the National Atmospheric Pollutant Surveillance network (NAPS: https://open.canada.ca/data/en/dataset/1b36a356-defd-4813-acea-47bc3abd859b).
Fairbanks aerosol measurements are from William Simpson and KC Nattinger. Aside from Fairbanks, Alaskan measurements are from the IMPROVE network. IMPROVE is a collaborative association of state, tribal, and federal agencies, and international partners. The US Environmental Protection Agency is the primary funding source, with contracting and research support from the National Park Service. The Air Quality Group at the University of California, Davis is the central analytical laboratory, with ion analysis provided by Research Triangle Institute, and carbon analysis provided by Desert Research Institute.
European measurements are from the EMEP network, and obtained from the EBAS database (http://ebas.nilu.no). Other European data include the Gruvebadet measurements, for which we acknowledge Mauro Mazzola (mauro.mazzola@cnr.it), Stefania Gilardoni (stefania.gilardoni@cnr.it), and Angelo Lupi (angelo.lupi@cnr.it) from the Institute of Polar Sciences fo Gruvabadet eBC measurements; and Rita Traversi (rita.traversi@unifi.it), Mirko Severi (mirko.severi@unifi.it), and Silvia Becagli (silvia.becagli@unifi.it) from University of Florence http://www.isac.cnr.it/~radiclim/CCTower/ ?Data:Aerosol; the Zeppelin datasets, for which we acknowledge Vito Vitale and Angelo Lupi (also available on

Deleted: TM

Deleted: OC

http://ebas.nilu.no); and the Villum Station datasets (www.villumresearchstation.dk) from Henrik Skov (hsk@envs.au.dk; also available in http://ebas.nilo.no). The AERONET AOD measurements were obtained from NASA's Goddard Space Flight Center (https://aeronet.gsfc.nasa.gov/new_web/index.html). The authors acknowledge Dr. L. Sogacheva and AEROSAT team for satellite based merged AOD data.

Financial support. This research has been supported by the Aarhus University Interdisciplinary Centre for Climate Change (iClimate) OH fund (no. 2020-0162731), the FREYA project, funded by the Nordic Council of Ministers (grant agreement no. MST-227-00036 and MFVM-2019-13476), and the EVAM-SLCF funded by the Danish Environmental Agency (grant agreement no. MST-112-00298). KT and GF thank the NASA Modeling, Analysis and Prediction program (MAP) for support. ZK was financially supported by the EU-funded Action on Black Carbon in the Arctic (EUA-BCA) under the EU Partnership Instrument. JPF was partially supported by NSF award 1915277.

References

Abbatt, J. P. D., Leaitch, W. R., Aliabadi, A. A., Bertram, A. K., Blanchet, J.-P., Boivin-Rioux, A., Bozem, H., Burkart, J., Chang, R. Y. W., Charette, J., Chaubey, J. P., Christensen, R. J., Cirisan, A., Collins, D. B., Croft, B., Dionne, J., Evans, G. J., Fletcher, C. G., Galí, M., Ghahremaninezhad, R., Girard, E., Gong, W., Gosselin, M., Gourdal, M., Hanna, S. J., Hayashida, H., Herber, A. B., Hesaraki, S., Hoor, P., Huang, L., Hussherr, R., Irish, V. E., Keita, S. A., Kodros, J. K., Köllner, F., Kolonjari, F., Kunkel, D., Ladino, L. A., Law, K., Levasseur, M., Libois, Q., Liggio, J., Lizotte, M., Macdonald, K. M., Mahmood, R., Martin, R. V., Mason, R. H., Miller, L. A., Moravek, A., Mortenson, E., Mungall, E. L., Murphy, J. G., Namazi, M., Norman, A.-L., O'Neill, N. T., Pierce, J. R., Russell, L. M., Schneider, J., Schulz, H., Sharma, S., Si, M., Staebler, R. M., Steiner, N. S., Thomas, J. L., von Salzen, K., Wentzell, J. J. B., Willis, M. D., Wentworth, G. R., Xu, J.-W., and Yakobi-Hancock, J. D.: Overview paper: New insights into aerosol and climate in the Arctic, Atmos. Chem. Phys., 19, 2527–2560, https://doi.org/10.5194/acp-19-2527-2019, 2019.

AMAP 2021 Assessment: Arctic climate, air quality, and health impacts from short-lived climate forcers (SLCFs).

AMAP, 2015. AMAP Assessment 2015: Black carbon and ozone as Arctic climate forcers. Arctic Monitoring and Assessment Programme (AMAP), Oslo, Norway. vii + 116 pp.

Amann, M., Bertok, I., Borken-Kleefeld, J., Cofala, J., Heyes, C., Höglund-Isaksson, L., Klimont, Z., Nguyen, B., Posch, M., Rafaj, P., Sandler, R., Schöpp, W., Wagner, F., Winiwarter, W.: Cost-effective control of air quality and greenhouse gases in Europe: Modeling and policy applications. Environmental Modelling & Software, 26, (12), 1489-1501, 2011.

Ångström, A.: On the Atmospheric Transmission of Sun Radiation and on Dust in the Air. Geografiska Annaler, 11, 156-166. doi:10.2307/519399, 1929.

1644 Bauer, S. E., Tsigaridis, K., Faluvegi, G.,Kelley, M., Lo, K. K., & Miller, R. L.,et al.:
1645 Historical (1850–2014) aerosol evolution and role on climate forcing using the GISS
1646 ModelE2.1contribution to CMIP6. Journal ofAdvances in Modeling Earth Systems,12,
1647 e2019MS001978, https://doi.org/10.1029/2019MS001978, 2020.

1648 Bauer, S.E., and Koch, D.: Impact of heterogeneous sulfate formation at mineral dust
1649 surfaces on aerosol loads and radiative forcing in the Goddard Institute for Space Studies
1650 general circulation model. J. Geophys. Res., 110, D17202, doi:10.1029/2005JD005870, 2005.

1651 Bond, T.C., Doherty, S.J., Fahey, D.W., Forster, P.M. , Berntsen, T., De Angelo, B.J.,
1652 Flanner, M.G., Ghan, S., Karcher, B., Koch, D., Kinne, S., Kondo, Y., Quiinn, P.K., Sarofim,
1653 M.C., Schultz, M.G., Schulz, M., Venkataraman, C., Zhang, H., Zhang, S., Bellouin, N.,
1654 Guttikunda, S.K., Hopke, P.K., Jacobson, M.Z., Kaiser, J.W., Klimont, Z., Lohmann, U.,
1655 Schwarz, J.P., Shindell, D., Storelvmo, T., Warren, S.G., Zender, C.S.: Bounding the role of
1656 black carbon in the climate system: a scientific assessment, J. Geophys. Res. Atmos., 118
1657 (11), 5380-5552, 10.1002/jgrd.50171, 2013.

1658 Bond, T. C., D. G. Streets, K. F. Yarber, S. M. Nelson, J. H. Woo, and Z. Klimont: A
1659 technology-based global inventory of black and organic carbon emissions from combustion,
1660 J. Geophys. Res., 109, D14203, doi:10.1029/2003JD003697, 2014.

1661 Boy, M., Thomson, E. S., Acosta Navarro, J.-C., Arnalds, O., Batchvarova, E., Bäck, J.,
1662 Berninger, F., Bilde, M., Brasseur, Z., Dagsson-Waldhauserova, P., Castarède, D., Dalirian,
1663 M., de Leeuw, G., Dragosics, M., Duplissy, E.-M., Duplissy, J., Ekman, A. M. L., Fang, K.,
1664 Gallet, J.-C., Glasius, M., Gryning, S.-E., Grythe, H., Hansson, H.-C., Hansson, M., Isaksson,
1665 E., Iversen, T., Jonsdottir, I., Kasurinen, V., Kirkevåg, A., Korhola, A., Krejci, R.,
1666 Kristjansson, J. E., Lappalainen, H. K., Lauri, A., Leppäranta, M., Lihavainen, H.,
1667 Makkonen, R., Massling, A., Meinander, O., Nilsson, E. D., Olafsson, H., Pettersson, J. B.
1668 C., Prisle, N. L., Riipinen, I., Roldin, P., Ruppel, M., Salter, M., Sand, M., Seland, Ø., Seppä,
1669 H., Skov, H., Soares, J., Stohl, A., Ström, J., Svensson, J., Swietlicki, E., Tabakova, K.,
1670 Thorsteinsson, T., Virkkula, A., Weyhenmeyer, G. A., Wu, Y., Zieger, P., and Kulmala, M.:
1671 Interactions between the atmosphere, cryosphere, and ecosystems at northern high latitudes,
1672 Atmos. Chem. Phys., 19, 2015–2061, https://doi.org/10.5194/acp-19-2015-2019, 2019.

1673 Breider, T. J., Mickley, L. J., Jacob, D. J., Ge, C., Wang, J., Payer Sulprizio, M., Croft, B.,
1674 Ridley, D. A., McConnell, J. R., Sharma, S., Husain, L., Dutkiewicz, V. A., Eleftheriadis, K.,
1675 Skov, H. and Hopke, P. K.: Multidecadal trends in aerosol radiative forcing over the Arctic:
1676 Contribution of changes in anthropogenic aerosol to Arctic warming since 1980, J. Geophys.
1677 Res. Atmos., 122(6), 3573–3594, doi:10.1002/2016JD025321, 2017.

1678 Burnett, R., Chena, H., Szyszkowicza, M., Fann, N., Hubbell, B., Pope III, C. A., Apte, J. S.,
1679 Brauer, M., Cohen, A., Weichenthal, S., Coggins, J., Di Q., Brunekreef B., Frostad, J., Lim,
1680 S. S., Kan, H., Walker, K. D., Thurston, G. D., Hayes, R. B., Lim, C. C., Turner, M. C.,
1681 Jerrett, M., Krewski, D., Gapstur, S. M., Diver, W. R., Ostro, B., Goldberg, D., Crouse, D.
1682 L., Martin, R. V., Peters, P., Pinault, L., Tjepkema, M., van Donkelaar, M., Villeneuve, P. J.,
1683 Miller, A. B., Yin, P., Zhou, M., Wang, L., Janssen, N. A. H., Marra, M., Atkinson, R. W.,
1684 Tsang, H., Thach, T. Q., Cannon, J. B., Allen, R. T., Hart, J. E., Laden, F., Cesaroni, G.,

Forastiere, F., Weinmayr, G., Jaensch, A., Nagel, G., Concin, H. and Spadar, J. V., Global estimates of mortality associated with long term exposure to outdoor fine particulate matter. Proceedings of the National Academy of Sciences, 38 (115), pp. 9592–9597. doi: 10.1073/pnas.1803222115. 2018.

Clarke, A.D., and Noone, K.J.: Soot in the Arctic snowpack: A cause for perturbations in radiative transfer, Atmos. Environ., 19, 2045– 2053, 1985.

Collins, W. J., Lamarque, J.-F., Schulz, M., Boucher, O., Eyring, V., Hegglin, M. I., Maycock, A., Myhre, G., Prather, M., Shindell, D., and Smith, S. J.: AerChemMIP: quantifying the effects of chemistry and aerosols in CMIP6, Geosci. Model Dev., 10, 585–607, https://doi.org/10.5194/gmd-10-585-2017, 2017.

Davy, R., and Outten, S.: The Arctic Surface Climate in CMIP6: Status and Developments since CMIP5, *J. Climate*, 33 (18), 8047–8068, https://doi.org/10.1175/JCLI-D-19-0990.1, 2020.

Dumont, M., Brun, E., Picard, G. et al.: Contribution of light-absorbing impurities in snow to Greenland's darkening since 2009. Nature Geosci 7, 509–512, https://doi.org/10.1038/ngeo2180, 2014.

Eck, T.F., B.N.Holben, J.S.Reid, O.Dubovik, A.Smirnov, N.T.O'Neill, I.Slutsker, and S.Kinne: Wavelength dependence of the optical depth of biomass burning, urban and desert dust aerosols, J. Geophys. Res., 104, 31 333-31 350, 1999.

Eckhardt, S., Quennehen, B., Olivié, D. J. L., Berntsen, T. K., Cherian, R., Christensen, J. H., Collins, W., Crepinsek, S., Daskalakis, N., Flanner, M., Herber, A., Heyes, C., Hodnebrog, Ø., Huang, L., Kanakidou, M., Klimont, Z., Langner, J., Law, K. S., Lund, M. T., Mahmood, R., Massling, A., Myriokefalitakis, S., Nielsen, I. E., Nøjgaard, J. K., Quaas, J., Quinn, P. K., Raut, J.-C., Rumbold, S. T., Schulz, M., Sharma, S., Skeie, R. B., Skov, H., Uttal, T., von Salzen, K., and Stohl, A.: Current model capabilities for simulating black carbon and sulfate concentrations in the Arctic atmosphere: a multi-model evaluation using a comprehensive measurement data set, Atmos. Chem. Phys., 15, 9413–9433, https://doi.org/10.5194/acp-15-9413-2015, 2015.

Eyring, V., Bony, S., Meehl, G. A., Senior, C. A., Stevens, B., Stouffer, R. J., and Taylor, K. E.: Overview of the Coupled Model Intercomparison Project Phase 6 (CMIP6) experimental design and organization, Geosci. Model Dev., 9, 1937–1958, https://doi.org/10.5194/gmd-9-1937-2016, 2016.

Feng, L., Smith, S. J., Braun, C., Crippa, M., Gidden, M. J., Hoesly, R., Klimont, Z., van Marle, M., van den Berg, M., and van der Werf, G. R.: The generation of gridded emissions data for CMIP6, Geosci. Model Dev., 13, 461–482, https://doi.org/10.5194/gmd-13-461-2020, 2020.

Flanner, M.G., Zender, C.S., Randerson, J.T., and Rasch, P.J.: Present-day climate forcing and response from blackcarbon in snow, J. Geophys. Res., 112, D11202, doi:10.1029/2006JD008003, 2007.

French, J.P.: autoimage: Multiple Heat Maps for Projected Coordinates, The R Journal, 9 (1), 284-297, 2017.

Gagné, M.-È., Gillett, N.P., and Fyfe, J. C.: Impact of aerosolemission controls on futureArctic sea ice cover, Geo-phys. Res. Lett., 42, 8481–8488,doi:10.1002/2015GL065504, 2015.

Gery, M., Whitten, G.Z., Killus, J.P., and Dodge, M.C.: A photochemical kinetics mechanism for urban and regional scale computer modelling, J.Geophys.Res., 94, 18925-18956, 1989.

Gidden, M. J., Riahi, K., Smith, S. J., Fujimori, S., Luderer, G., Kriegler, E., van Vuuren, D. P., van den Berg, M., Feng, L., Klein, D., Calvin, K., Doelman, J. C., Frank, S., Fricko, O., Harmsen, M., Hasegawa, T., Havlik, P., Hilaire, J., Hoesly, R., Horing, J., Popp, A., Stehfest, E., and Takahashi, K.: Global emissions pathways under different socioeconomic scenarios for use in CMIP6: a dataset of harmonized emissions trajectories through the end of the century, Geosci. Model Dev., 12, 1443–1475, https://doi.org/10.5194/gmd-12-1443-2019, 2019.

Gidden, M. J., Fujimori, S., van den Berg, M., Klein, D., Smith, S. J., van Vuuren, D. P., and Riahi, K.: A methodology and implementation of automated emissions harmonization for use in Integrated Assessment Models, Environ. Modell. Softw., 105, 187–200, 2018.

Graversen R, Langen P.L.: On the Role of the Atmospheric Energy Transport in 2xCO2-Induced Polar Amplification in CESM1. Journal of Climate, 32(13), 3941-3956, 2019.

Gryspeerdt, E., Goren, T., Sourdeval, O., Quaas, J., Mülmenstädt, J., Dipu, S., Unglaub, C., Gettelman, A., and Christensen, M.: Constraining the aerosol influence on cloud liquid water path, Atmos. Chem. Phys., 19, 5331–5347, https://doi.org/10.5194/acp-19-5331-2019, 2019.

Hansen, J., M. Sato, R. Ruedy, L. Nazarenko, A. Lacis, G.A. Schmidt, G. Russell, I. Aleinov, M. Bauer, S. Bauer, N. Bell, B. Cairns, V. Canuto, M. Chandler, Y. Cheng, A. Del Genio, G. Faluvegi, E. Fleming, A. Friend, T. Hall, C. Jackman, M. Kelley, N.Y. Kiang, D. Koch, J. Lean, J. Lerner, K. Lo, S. Menon, R.L. Miller, P. Minnis, T. Novakov, V. Oinas, J.P. Perlwitz, J. Perlwitz, D. Rind, A. Romanou, D. Shindell, P. Stone, S. Sun, N. Tausnev, D. Thresher, B. Wielicki, T. Wong, M. Yao, and S. Zhang: Efficacy of climate forcings. J. Geophys. Res., 110, D18104, doi:10.1029/2005JD005776, 2005.

Hoesly, R. M., Smith, S. J., Feng, L., Klimont, Z., Janssens-Maenhout, G., Pitkanen, T., Seibert, J. J., Vu, L., Andres, R. J., Bolt, R. M., Bond, T. C., Dawidowski, L., Kholod, N., Kurokawa, J.-I., Li, M., Liu, L., Lu, Z., Moura, M. C. P., O'Rourke, P. R., and Zhang, Q.: Historical (1750–2014) anthropogenic emissions of reactive gases and aerosols from the Community Emissions Data System (CEDS), Geosci. Model Dev., 11, 369–408, https://doi.org/10.5194/gmd-11-369-2018, 2018.

Holben B.N., T.F.Eck, I.Slutsker, D.Tanre, J.P.Buis, A.Setzer, E.Vermote, J.A.Reagan, Y.Kaufman, T.Nakajima, F.Lavenu, I.Jankowiak, and A.Smirnov: AERONET - A federated instrument network and data archive for aerosol characterization, Rem. Sens. Environ., 66, 1-16, 1998.

Höglund-Isaksson, L., Gómez-Sanabria, A., Klimont, Z., Rafaj, P., Schöpp, W.: Technical potentials and costs for reducing global anthropogenic methane emissions in the 2050 timeframe –results from the GAINS model. Environmental Research Communications, 2 (2), 2020.

International Energy Agency (IEA): World Energy Outlook 2018, 661 pp., ISBN 978-92-64-30677-6, 2018.

IPCC, 2014: Climate Change 2014: Synthesis Report. Contribution of Working Groups I, II and III to the Fifth Assessment Report of the Intergovernmental Panel on Climate Change [Core Writing Team, R.K. Pachauri and L.A. Meyer (eds.)]. IPCC, Geneva, Switzerland, 151 pp.

IPCC, 2013: Climate Change 2013: The Physical Science Basis. Contribution of Working Group I to the Fifth Assessment Report of the Intergovernmental Panel on Climate Change [Stocker, T.F., D. Qin, G.-K. Plattner, M. Tignor, S.K. Allen, J. Boschung, A. Nauels, Y. Xia, V. Bex and P.M. Midgley (eds.)]. Cambridge University Press, Cambridge, United Kingdom and New York, NY, USA, 1535 pp.

Jacobson, M. Z.: Strong radiative heating due to the mixing state of black carbon in the atmospheric aerosols, Nature, 409, 695–698, 2001.

Karlsson, K.-G., Devasthale, A: Inter-Comparison and Evaluation of the Four Longest Satellite-Derived Cloud Climate Data Records: CLARA-A2, ESA Cloud CCI V3, ISCCP-HGM, and PATMOS-x. Remote Sens. 2018, 10, 1567.

Karlsson, K.-G., Anttila, K., Trentmann, J., Stengel, M., Fokke Meirink, J., Devasthale, A., Hanschmann, T., Kothe, S., Jääskeläinen, E., Sedlar, J., Benas, N., van Zadelhoff, G.-J., Schlundt, C., Stein, D., Finkensieper, S., Håkansson, N., and Hollmann, R.: CLARA-A2: the second edition of the CM SAF cloud and radiation data record from 34 years of global AVHRR data, Atmos. Chem. Phys., 17, 5809–5828, https://doi.org/10.5194/acp-17-5809-2017, 2017.

Karlsson, Karl-Göran; Anttila, Kati; Trentmann, Jörg; Stengel, Martin; Meirink, Jan Fokke; Devasthale, Abhay; Hanschmann, Timo; Kothe, Steffen; Jääskeläinen, Emmihenna; Sedlar, Joseph; Benas, Nikos; van Zadelhoff, Gerd-Jan; Schlundt, Cornelia; Stein, Diana; Finkensieper, Stephan; Håkansson, Nina; Hollmann, Rainer; Fuchs, Petra; Werscheck, Martin (2017): CLARA-A2: CM SAF cLoud, Albedo and surface RAdiation dataset from AVHRR data - Edition 2, Satellite Application Facility on Climate Monitoring, https://doi.org/10.5676/EUM_SAF_CM/CLARA_AVHRR/V002 (last access: October 26th 2020).

Kay, J., and L'Ecuyer, T.: Observational constraints on Arctic Ocean clouds and radiative fluxes during the early 21st century. Journal of Geophysical Research: Atmospheres. 118. 10.1002/jgrd.50489, 2013.

Keil, P., Mauritsen, T., Jungclaus, J. *et al.* Multiple drivers of the North Atlantic warming hole. *Nat. Clim. Chang.* 10, 667–671, https://doi.org/10.1038/s41558-020-0819-8, 2020.

Kelley, M., Schmidt, G. A., Nazarenko, L. S., Bauer, S. E., Ruedy, R., Russell, G. L., et al.: GISS-E2.1: Configurations and climatology. Journal of Advances in Modeling Earth Systems, 12, e2019MS002025. https://doi.org/10.1029/2019MS002025, 2020.

Klimont, Heyes, Rafaj, Schoepp, Purohit, Cofala, Hoglund-Isaksson, Wagner,...et al. Global scenarios of anthropogenic emissions of air pollutants: ECLIPSE (in preparation for GMD)

Klimont, Z., Kupiainen, K., Heyes, C., Purohit, P., Cofala, J., Rafaj, P., Borken-Kleefeld, J., and Schöpp, W.: Global anthropogenic emissions of particulate matter including black carbon, Atmos. Chem. Phys., 17, 8681–8723, https://doi.org/10.5194/acp-17-8681-2017, 2017.

Lamarque, J.-F., Bond, T. C., Eyring, V., Granier, C., Heil, A., Klimont, Z., Lee, D., Liousse, C., Mieville, A., Owen, B., Schultz, M. G., Shindell, D., Smith, S. J., Stehfest, E., Van Aardenne, J., Cooper, O. R., Kainuma, M., Mahowald, N., McConnell, J. R., Naik, V., Riahi, K., and van Vuuren, D. P.: Historical (1850–2000) gridded anthropogenic and biomass burning emissions of reactive gases and aerosols: methodology and application, Atmos. Chem. Phys., 10, 7017–7039, https://doi.org/10.5194/acp-10-7017-2010, 2010.

Lelieveld, J., Klingmüller, K., Pozzer, A., Pöschl, U., Fnais, M., Daiber, A., Münzel, T. Cardiovascular disease burden from ambient air pollution in Europe reassessed using novel hazard ratio functions. European Heart Journal 40, 1590-1596. https://doi.org/10.1093/eurheartj/ehz135, 2019.

Lenssen, N. J. L., Schmidt, G. A., Hansen, J. E., Menne, M. J., Persin, A., Ruedy, R. and Zyss, D.: Improvements in the GISTEMP Uncertainty Model. Journal of Geophysical Research: Atmospheres 124: 6307-6326 10.1029/2018jd029522, 2019.

Lewinschal, A., Ekman, A. M. L., Hansson, H. C., Sand, M., Berntsen, T. K., & Langner, J. (2019). Local and remote temperature response of regional SO2 emissions. Atmospheric Chemistry and Physics, 19, 2385– 2403. https://doi.org/10.5194/acp-19-2385-2019

Lund, M. T., Myhre, G., Haslerud, A. S., Skeie, R. B., Griesfeller, J., Platt, S. M., Kumar, R., Myhre, C. L., and Schulz, M.: Concentrations and radiative forcing of anthropogenic aerosols from 1750 to 2014 simulated with the Oslo CTM3 and CEDS emission inventory, Geosci. Model Dev., 11, 4909–4931, https://doi.org/10.5194/gmd-11-4909-2018, 2018.

Lund, M. T., Berntsen, T. K., and Samset, B. H.: Sensitivity of black carbon concentrations and climate impact to aging and scavenging in OsloCTM2-M7, Atmos. Chem. Phys., 17, 6003–6022, https://doi.org/10.5194/acp-17-6003-2017, 2017.

Mahmood, R., von Salzen, K., Norman, A.-L., Galí, M., and Levasseur, M.: Sensitivity of Arctic sulfate aerosol and clouds to changes in future surface seawater dimethylsulfide concentrations, Atmos. Chem. Phys., 19, 6419–6435, https://doi.org/10.5194/acp-19-6419-2019, 2019.

Markowicz, K.M.,Lisok, J., Xian, P.: Simulation of long-term direct aerosol radiative forcing over the arctic within the framework of the iAREA project. Atmospheric Environment, 244, 117882, 2021.

Menary, M.B., Wood, R.A.: An anatomy of the projected North Atlantic warming hole in CMIP5 models. *Clim Dyn* 50, 3063–3080, https://doi.org/10.1007/s00382-017-3793-8, 2018.

Menon, S., and Rotstayn, L.: The radiative influence of aerosol effects on liquid-phase cumulus and stratus clouds based on sensitivity studies with two climate models, Clim. Dyn., 27, 345– 356, 2006.

Miller, R.L., G.A. Schmidt, L. Nazarenko, S.E. Bauer, M. Kelley, R. Ruedy, G.L. Russell, A. Ackerman, I. Aleinov, M. Bauer, R. Bleck, V. Canuto, G. Cesana, Y. Cheng, T.L. Clune, B. Cook, C.A. Cruz, A.D. Del Genio, G.S. Elsaesser, G. Faluvegi, N.Y. Kiang, D. Kim, A.A. Lacis, A. Leboissetier, A.N. LeGrande, K.K. Lo, J. Marshall, E.E. Matthews, S. McDermid, K. Mezuman, L.T. Murray, V. Oinas, C. Orbe, C. Pérez García-Pando, J.P. Perlwitz, M.J. Puma, D. Rind, A. Romanou, D.T. Shindell, S. Sun, N. Tausnev, K. Tsigaridis, G. Tselioudis, E. Weng, J. Wu, and M.-S. Yao: CMIP6 historical simulations (1850-2014) with GISS-E2.1. J. Adv. Model. Earth Syst., in press, doi:10.1029/2019MS002034, 2020.

Miller, R.L., G.A. Schmidt, and D.T. Shindell: Forced annular variations in the 20th century Intergovernmental Panel on Climate Change Fourth Assessment Report models. J. Geophys. Res., 111, D18101, doi:10.1029/2005JD006323, 2006.

Myhre, G., D. Shindell, F.-M. Bréon, W. Collins, J. Fuglestvedt, J. Huang, D. Koch, J.-F. Lamarque, D. Lee, B. Mendoza, T. Nakajima, A. Robock, G. Stephens, T. Takemura, and H. Zhang: Anthropogenic and natural radiative forcing. In Climate Change 2013: The Physical Science Basis. Contribution of Working Group I to the Fifth Assessment Report of the Intergovernmental Panel on Climate Change. T.F. Stocker, D. Qin, G.-K. Plattner, M. Tignor, S.K. Allen, J. Doschung, A. Nauels, Y. Xia, V. Bex, and P.M. Midgley, Eds. Cambridge University Press, pp. 659-740, doi:10.1017/CBO9781107415324.018, 2013.

Platnick, S., S. A. Ackerman, M. D. King, K. Meyer, W. P. Menzel, R. E. Holz, B. A. Baum, and P. Yang: MODIS atmosphere L2 cloud product (06_L2), NASA MODIS Adaptive Processing System, Goddard Space Flight Center, 2015.

Quinn, P.K., Shaw, G., Andrews, E., Dutton, E.G., Ruoho-Airola, T., Gong, S.L. Arctic haze: current trends and knowledge gaps, Tellus B: Chemical and Physical Meteorology, 59:1, 99-114, DOI: 10.1111/j.1600-0889.2006.00236.x, 2007.

Rao, S., Klimont, Z., Smith, S.J., Van Dingenen, R., Dentener, F., Bouwman, L., Riahia, K., Amann, M., Bodirsky, B.L., van Vuuren, D.P., Reis, L.A., Calvin, K., Drouet, L., Fricko, O., Fujimori, S., Gernaat, D., Havlik, P., Harmsen, M., Hasegawa, T., Heyes, C., Hilaire, J., Luderer, G., Masui, T., Stehfest, E., Strefler, J., van der Slui, S., Tavonil, M.: Future air pollution in the Shared Socio-economic Pathways. Global Environmental Change, 42, 346-358, 2017.

Rayner, N. A., D. E. Parker, E. B. Horton, C. K. Folland, L. V. Alexander, D. P. Rowell, E. C. Kent, and A. Kaplan, Global analyses of sea surface temperature, sea ice, and night marine air temperature since the late nineteenth century, J. Geophys. Res.,108(D14), 4407, doi:10.1029/2002JD002670, 2003.

Formatted: English (US)
Formatted: English (US)
Formatted: English (US)
Formatted: English (US)
Formatted: English (US)
Formatted: English (US)
Formatted: English (US)
Formatted: English (US)
Formatted: English (US)
Formatted
Formatted
Formatted

Ren, L., Yang, Y., Wang, H., Zhang, R., Wang, P., and Liao, H.: Source attribution of Arctic black carbon and sulfate aerosols and associated Arctic surface warming during 1980–2018, Atmos. Chem. Phys., 20, 9067–9085, https://doi.org/10.5194/acp-20-9067-2020, 2020.

Reynolds, R.W., Rayner, N.A., Smith, T.M., Stokes, D.C., and Wang, W. An improved in situ and satellite SST analysis for climate. J. Climate, 15, 1609-1625, 2002.

Riahi, K.,van Vuuren, D.P., Kriegler, E., Edmonds, J., O'Neil, B.C., Fujimori, S., Bauer, N., Calvin, K., Dellink, R., Fricko, O., Lutz, W., Popp, A., Cuaresma, C.J., KC, S., Leimbach, M., Jiang, L., Kram, T., Rao, S., Emmerling, J., Ebi, K., Hasegawa, T., Havlik, P., Humpenöder, F., Da Silva, L.A:, Smith, S., Stehfest, E., Bosetti, V., Eom, J., Gernaat, D., Masui, T., Rogelj, J., Strefler, J., Drouet, L., Krey, V., Luderer, G., Harmsen, M., Takahashi, K., Baumstark, L., Doelman, J.C., Kainuma, M., Klimont, Z., Marangoni, G., Lotze-Campen, H., Obersteiner, M., Tabeau, A., Tavoni, M.: The Shared Socioeconomic Pathways and their energy, land use, and greenhouse gas emissions implications: An overview. Global Environmental Change, 42, 153-168, 2017.

Samset, B. H., Sand, M., Smith, C. J., Bauer, S. E., Forster, P. M., Fuglestvedt, J. S., Osprey, S., & Schleussner, C.-F.: Climate impacts from a removal of anthropogenic aerosol emissions. Geophysical Research Letters, 45. https://doi.org/10.1002/2017GL076079, 2018.

Sand, M., T. K. Berntsen, K. von Salzen, M. G. Flanner, J. Langner, and D. G. Victor: Response of arctic temperature to changes in emissions of short-lived climate forcers, Nat. Clim. Change, 6, 286–289, doi:10.1038/nclimate2880, 2015.

Sayer, A. M., Hsu, N. C., Lee, J., Kim, W. V., Dubovik, O., Dutcher, S. T. et al.: Validation of SOAR VIIRS over-water aerosol retrievals and context within the global satellite aerosol data record. Journal of Geophysical Research: Atmospheres, 123, 13,496–13,526, https://doi.org/10.1029/2018JD029465, 2018.

Sayer, A. M. and Knobelspiesse, K. D.: How should we aggregate data? Methods accounting for the numerical distributions, with an assessment of aerosol optical depth, Atmos. Chem. Phys., 19, 15023–15048, https://doi.org/10.5194/acp-19-15023-2019, 2019.

Schacht, J., Heinold, B., Quaas, J., Backman, J., Cherian, R., Ehrlich, A., Herber, A., Huang, W. T. K., Kondo, Y., Massling, A., Sinha, P. R., Weinzierl, B., Zanatta, M., and Tegen, I.: The importance of the representation of air pollution emissions for the modeled distribution and radiative effects of black carbon in the Arctic, Atmos. Chem. Phys., 19, 11159–11183, https://doi.org/10.5194/acp-19-11159-2019, 2019.

Schmale, J., Zieger, P., Ekman, A.M.L. Aerosols in current and future Arctic climate. Nature Climate Change, 11, 95–105, https://doi.org/10.1038/s41558-020-00969-5, 2021.

Schutgens, N. A. J.: Site representativity of AERONET and GAW remotely sensed aerosol optical thickness and absorbing aerosol optical thickness observations, Atmos. Chem. Phys., 20, 7473–7488, https://doi.org/10.5194/acp-20-7473-2020, 2020a.

Schutgens, N., Sayer, A. M., Heckel, A., Hsu, C., Jethva, H., de Leeuw, G., Leonard, P. J. T., Levy, R. C., Lipponen, A., Lyapustin, A., North, P., Popp, T., Poulson, C., Sawyer, V., Sogacheva, L., Thomas, G., Torres, O., Wang, Y., Kinne, S., Schulz, M., and Stier, P.: An

AeroCom/AeroSat study: Intercomparison of Satellite AOD Datasets for Aerosol Model Evaluation, Atmos. Chem. Phys. Discuss., https://doi.org/10.5194/acp-2019-1193, in review, 2020b.

Semmler, T., Pithan, F., Jung, T.: Quantifying two-way influences between the Arctic and mid-latitudes through regionally increased CO2 concentrations in coupled climate simulations, *Climate Dynamics*, 54, 3307–3321, 2020.

Serreze, M.C., Francis, J.A. The Arctic Amplification Debate. Climatic Change 76, 241–264, https://doi.org/10.1007/s10584-005-9017-y, 2006.

Shindell, D. T., Lamarque, J.-F., Schulz, M., Flanner, M., Jiao, C., Chin, M., Young, P. J., Lee, Y. H., Rotstayn, L., Mahowald, N., Milly, G., Faluvegi, G., Balkanski, Y., Collins, W. J., Conley, A. J., Dalsoren, S., Easter, R., Ghan, S., Horowitz, L., Liu, X., Myhre, G., Nagashima, T., Naik, V., Rumbold, S. T., Skeie, R., Sudo, K., Szopa, S., Takemura, T., Voulgarakis, A., Yoon, J.-H., and Lo, F.: Radiative forcing in the ACCMIP historical and future climate simulations, Atmos. Chem. Phys., 13, 2939–2974, https://doi.org/10.5194/acp-13-2939-2013, 2013.

Shindell, D., J.C.I. Kuylenstierna, E. Vignati, R. van Dingenen, M. Amann, Z. Klimont, S.C. Anenberg, N. Muller, G. Janssens-Maenhout, F. Raes, J. Schwartz, G. Faluvegi, L. Pozzoli, K. Kupiainen, L. Höglund-Isaksson, L. Emberson, D. Streets, V. Ramanathan, K. Hicks, N.T.K. Oanh, G. Milly, M. Williams, V. Demkine, and D. Fowler, Simultaneously mitigating near-term climate change and improving human health and food security. Science, 335, 183-189, doi:10.1126/science.1210026, 2012.

Shindell, D., and G. Faluvegi,: Climate response to regional radiative forcing during the twentieth century. Nature Geosci., 2, 294-300, doi:10.1038/ngeo473, 2009.

Shindell, D.: Local and remote contributions to Arctic warming, Geophysical Research Letters – Climate, 34, L14704, https://doi.org/10.1029/2007GL030221, 2007.

Sogacheva, L., Popp, T., Sayer, A. M., Dubovik, O., Garay, M. J., Heckel, A., Hsu, N. C., Jethva, H., Kahn, R. A., Kolmonen, P., Kosmale, M., de Leeuw, G., Levy, R. C., Litvinov, P., Lyapustin, A., North, P., Torres, O., and Arola, A.: Merging regional and global aerosol optical depth records from major available satellite products, Atmos. Chem. Phys., 20, 2031–2056, https://doi.org/10.5194/acp-20-2031-2020, 2020.

Skeie, R. B., Berntsen, T., Myhre, G., Pedersen, C. A., Ström, J., Gerland, S., and Ogren, J. A.: Black carbon in the atmosphere and snow, from pre-industrial times until present, Atmos. Chem. Phys., 11, 6809–6836, https://doi.org/10.5194/acp-11-6809-2011, 2011.

Stephens, G. L., and Coauthors,: THE CLOUDSAT MISSION AND THE A-TRAIN: A New Dimension of Space-Based Observations of Clouds and Precipitation. Bull. Amer. Meteor. Soc., 83, 1771–1790, https://doi.org/10.1175/BAMS-83-12-1771, 2002.

Stjern, C. W., Samset, B. H., Myhre, G.,Forster, P. M., Hodnebrog, Ø. Andrews,T., Boucher, O., Faluvegi, G., Iversen, T., Kasoar, M., Kharin, V., Kirkevåg, A., Lamarque, J.-F., Olivie, D., Richardson, T, Shawki, D., Shindell, D., Smith, C.J., Takemura, T., Voulgarakis, A. Rapid adjustments cause weak surface temperature response to increased black carbon

Formatted: English (US)

concentrations. Journal of Geophysical Research: Atmospheres, 122,11,462–11,481. https://doi.org/10.1002/2017JD02732, 2017.

Stohl, A., Aamaas, B., Amann, M., Baker, L. H., Bellouin, N., Berntsen, T. K., Boucher, O., Cherian, R., Collins, W., Daskalakis, N., Dusinska, M., Eckhardt, S., Fuglestvedt, J. S., Harju, M., Heyes, C., Hodnebrog, Ø., Hao, J., Im, U., Kanakidou, M., Klimont, Z., Kupiainen, K., Law, K. S., Lund, M. T., Maas, R., MacIntosh, C. R., Myhre, G., Myriokefalitakis, S., Olivié, D., Quaas, J., Quennehen, B., Raut, J.-C., Rumbold, S. T., Samset, B. H., Schulz, M., Seland, Ø., Shine, K. P., Skeie, R. B., Wang, S., Yttri, K. E., and Zhu, T.: Evaluating the climate and air quality impacts of short-lived pollutants, Atmos. Chem. Phys., 15, 10529–10566, https://doi.org/10.5194/acp-15-10529-2015, 2015.

Stuecker, M.F., Bitz, C.M., Armour, K.C., Proistosescu, C., Kang, S.M., Xie, S.-P., Kim, D., McGregor, S., Zhang, W., Zhao, S., Cai, W., Dong, Y., Jin, F.-F.: Polar amplification dominated by local forcing and feedbacks, *Nature Climate Change*, 8, 1076–1081, 2018.

Takemura, T., Suzuki, K. Weak global warming mitigation by reducing black carbon emissions. Scientific Reports, 9, 4419 (2019). https://doi.org/10.1038/s41598-019-41181-6

Thomas, J.L., et al.: Fostering multidisciplinary research on interactions between chemistry, biology, and physics within the coupled cryosphere-atmosphere system. Elem Sci Anth, 7: 58. DOI: https://doi.org/10.1525/elementa.396, 2019.

Tsigaridis, K., and M. Kanakidou,: Secondary organic aerosol importance in the future atmosphere. Atmos. Environ., 41, 4682-4692, doi:10.1016/j.atmosenv.2007.03.045, 2007.

Turnock, S. T., Allen, R. J., Andrews, M., Bauer, S. E., Deushi, M., Emmons, L., Good, P., Horowitz, L., John, J. G., Michou, M., Nabat, P., Naik, V., Neubauer, D., O'Connor, F. M., Olivié, D., Oshima, N., Schulz, M., Sellar, A., Shim, S., Takemura, T., Tilmes, S., Tsigaridis, K., Wu, T., and Zhang, J.: Historical and future changes in air pollutants from CMIP6 models, Atmos. Chem. Phys., 20, 14547–14579, https://doi.org/10.5194/acp-20-14547-2020, 2020.

van Marle, M. J. E., Kloster, S., Magi, B. I., Marlon, J. R., Daniau, A.-L., Field, R. D., Arneth, A., Forrest, M., Hantson, S., Kehrwald, N. M., Knorr, W., Lasslop, G., Li, F., Mangeon, S., Yue, C., Kaiser, J. W., and van der Werf, G. R.: Historic global biomass burning emissions for CMIP6 (BB4CMIP) based on merging satellite observations with proxies and fire models (1750–2015), Geosci. Model Dev., 10, 3329–3357, https://doi.org/10.5194/gmd-10-3329-2017, 2017.

Wei, J., Peng, Y., Mahmood, R., Sun, L., and Guo, J.: Intercomparison in spatial distributions and temporal trends derived from multi-source satellite aerosol products, Atmos. Chem. Phys., 19, 7183–7207, https://doi.org/10.5194/acp-19-7183-2019, 2019.

Westervelt, D. M., Horowitz, L. W., Naik, V., Golaz, J.-C., & Mauzerall, D. L.: Radiative forcing and climate response to projected 21st century aerosol decreases. Atmospheric Chemistry and Physics, 15, 12,681– 12,703. https://doi.org/10.5194/acp-15-12681-2015, 2015.

1999 Willis, M. D., Leaitch, W. R., &Abbatt, J. P.: Processescontrolling the composition
2000 andabundance of Arctic aerosol.Reviews of Geophysics, 56, 621–671.
2001 https://doi.org/10.1029/2018RG000602, 2018.

2002 Willmott, C. J. and K. Matsuura,: Terrestrial Air Temperature and Precipitation: Monthly and
2003 Annual Time Series (1950 - 1999), 2001.
2004 (http://climate.geog.udel.edu/~climate/html_pages/README.ghcn_ts2.html, (last access:
2005 October 26th)

Tables

Table 1. GISS-E2.1 simulations carried out in the Eclipse and CMIP6 ensembles.

Simulations	Description	No. Ensemble	Period
NINT_Cpl	No tracers- Coupled	1	1850-2014
Eclipse_AMIP	AMIP OMA	1	1995-2014
Eclipse_AMIP_NCEP	AMIP OMA – winds nudged to NCEP	1	1995-2014
Eclipse_CplHist	OMA – Coupled	3	1990-2014
Eclipse_Cpl_CLE	OMA – Coupled	3	2015-2050
Eclipse_Cpl_MFR	OMA – Coupled	3	2020-2050
CMIP6_Cpl_Hist	OMA – Coupled	1	1850-2014
CMIP6_Cpl_SSP1-2.6	OMA – Coupled	1	2015-2050
CMIP6_Cpl_SSP2-4.5	OMA – Coupled	1	2015-2050
CMIP6_Cpl_SSP3-7.0	OMA – Coupled	1	2015-2050
CMIP6_Cpl_SSP3-7.0-lowNTCF	OMA – Coupled	1	2015-2050

Table 2. Annual mean normalized mean bias (*NMB:%*) and correlation coefficients (*r*) for the recent past simulations in the GISS-E2.1 model ensemble during 1995-2014 for BC, OA, SO_4^{2-} and 2008/2009-2014 for AOD550 from AERONET and satellites.

	BC		OA		SO_4^{2-}		AOD_aero		AOD_sat	
Model	*NMB*	*r*	*NMB*	*r*	*NMB*	*r*	*NMB*	*r*	*NMB*	*r*
AMAP_OnlyAtm.	-67.32	0.27	-35.46	0.54	-49.83	0.65	-33.28	-0.07	-0.48	0.00
AMAP_OnlyAtm_NCEP	-57.00	0.26	-7.80	0.56	-52.70	0.74	-41.99	0.02	-0.55	0.13
AMAP_CplHist (x3)	-64.11	0.42	-19.07	0.58	-49.39	0.71	-43.28	0.04	-0.56	0.07
CMIP6_Cpl_Hist	-49.90	0.26	13.14	0.69	-39.81	0.70	-39.86	0.05	-0.53	0.11

Deleted: Normalised
Deleted: M
Deleted: B
Deleted: C
Formatted Table
Deleted: C
Formatted: Font: 10 pt
Formatted: Font: 10 pt
Formatted: Font: 10 pt
Formatted: Centred
Formatted: Centred
Formatted: Font: 10 pt
Formatted: Centred
Formatted: Centred
Formatted: Font: 10 pt
Deleted: -62.82
Deleted: 0.21
Formatted: Centred
Deleted: -22.85
Deleted: 0.51
Deleted: -50.13
Deleted: 0.70
Deleted: -47.42
Deleted: 0.03
Formatted: Centred
Deleted: -0.59
Deleted: -0.00
Formatted: Font: 10 pt
Deleted: 1
Formatted: Font: 10 pt
Deleted: AMAP_CplHist2 ... [59]
Formatted: Font: 10 pt
Formatted: Font: 10 pt
Formatted: Centred
Formatted: Centred
Formatted: Font: 10 pt

Table 3a. Annual normalized mean biases (*NMB*; %) and correlation coefficients (*r*) for the recent past simulations in the GISS-E2.1 model ensemble in 1995-2014 for surface air temperature (T_{surf}) and sea surface temperature (SST) in units of °C, and precipitation (Precip), and sea-ice fraction (Sea-ice).

	T_{surf}		Precip		SST		Sea-ice	
Model	*NMB*	*r*	*NMB*	*r*	*NMB*	*r*	*NMB*	*r*
NINT	-0.08	1.00	-52.68	0.88	-88.87	0.99	12.14	1.00
AMAP_OnlyAtm.	-19.73	1.00	-50.33	0.89	-68.00	0.99	-2.56	1.00
AMAP_OnlyAtm_NCEP	-14.74	1.00	-53.19	0.90	-68.00	0.99	-2.56	1.00
AMAP_CplHistx3	-3.35	1.00	-53.06	0.86	-87.51	0.99	11.35	1.00
CMIP6_Cpl_Hist	-1.22	1.00	-53.96	0.85	-88.53	0.98	12.56	0.99

Table 3b. Annual mean normalized mean biases (*NMB*; %) and correlation coefficients (*r*) for the recent past simulations in the GISS-E2.1 model ensemble in 1995-2014 for total cloud fraction (Cld Frac), liquid water path (LWP), and ice water path (IWP) in units of %.

	Cld Frac		LWP		IWP	
Model	*NMB*	*r*	*NMB*	*r*	*NMB*	*r*
NINT	20.95	-0.67	70.55	-0.89	-56.06	0.53
AMAP_OnlyAtm.	23.78	-0.81	57.52	-0.96	-58.53	-0.18
AMAP_OnlyAtm_NCEP	24.83	-0.79	14.19	-0.91	-70.32	-0.64
AMAP_CplHistx3	21.64	-0.65	70.99	-0.91	-55.74	0.48
CMIP6_Cpl_Hist	21.49	-0.65	69.18	-0.91	-56.28	0.40

Formatted ... [60]
Formatted ... [63]
Formatted ... [64]
Formatted ... [65]
Formatted ... [61]
Formatted Table ... [62]
Formatted ... [66]
Formatted ... [67]
Formatted ... [68]
Formatted ... [70]
Formatted ... [69]
Formatted ... [72]
Formatted ... [71]
Formatted ... [74]
Formatted ... [73]
Formatted ... [76]
Formatted ... [77]
Formatted ... [78]
Formatted ... [79]
Formatted ... [80]
Formatted ... [81]
Formatted ... [82]
Formatted ... [83]
Formatted ... [84]
Formatted ... [85]
Formatted ... [75]
Formatted ... [87]
Formatted ... [86]
Formatted ... [88]
Formatted ... [89]
Formatted ... [92]
Formatted ... [93]
Formatted ... [90]
Formatted Table ... [91]
Formatted ... [94]
Formatted ... [95]
Formatted ... [96]
Formatted ... [98]
Formatted ... [97]
Formatted ... [100]
Formatted ... [99]
Formatted ... [102]
Formatted ... [101]
Formatted ... [104]
Formatted ... [105]
Formatted ... [106]
Formatted ... [107]
Formatted ... [108]
Formatted ... [109]
Formatted ... [110]
Formatted ... [111]
Formatted ... [103]
Formatted ... [113]
Formatted ... [112]
Deleted:

Table 4. Trends in Arctic BC, OA and SO_4^{2-} burdens in the near-past (1990-2014) and future (2030-2050) as calculated by the GISS-E2.1. The bold numbers indicate the trends that are statistically significant on a 95% significance level.

	BC		OA		SO_4^{2-}	
	1990-2014	2015-2050	1990-2014	2015-2050	1990-2014	2015-205
Eclipse_AMIP	**-0.026**		0.030		**-0.886**	
Eclipse_AMIP_NCEP	**-0.021**		0.112		**-0.939**	
Eclipse_CplHist_3xEns	**-0.026**		-0.006		**-1.332**	
Eclipse_CplCLE_3xEns		**-0.024**		**-0.201**		**-0.1**
Eclipse_CplMFR_3xEns		**-0.043**		**-0.367**		**-0.1**
CEDS_Cpl_Hist	0.007		0.121		**-1.093**	
CEDS_Cpl_SSP126		**-0.068**		**-0.715**		**-0.9**
CEDS_Cpl_SSP245		**-0.047**		**-0.384**		**-0.4**
CEDS_Cpl_SSP370		**-0.004**		**-0.062**		**0.0**
CEDS_Cpl_SSP370-lowNTCF		**-0.051**		**-0.642**		**-0.5**

Table 5. Arctic BC, OA and SO_4^{2-} burdens in 1990-2010 and 2030-2050 periods as calculated by the GISS-E2.1.

	BC		OA		SO_4^{2-}	
	1990-2010	2030-2050	1990-2010	2030-2050	1990-2010	2030-205
Eclipse_AMIP	3.52		50.70		95.10	
Eclipse_AMIP_NCEP	3.49		57.31		93.93	
Eclipse_CplHist_3xEns	3.75		55.55		93.59	
Eclipse_CplCLE_3xEns		2.58		48.95		63.52
Eclipse_CplMFR_3xEns		1.44		40.39		53.35
CEDS_Cpl_Hist	3.64		67.48		99.11	
CEDS_Cpl_SSP126		2.05		50.41		53.99
CEDS_Cpl_SSP245		2.65		59.43		69.71
CEDS_Cpl_SSP370		4.08		68.81		83.26
CEDS_Cpl_SSP370-lowNTCF		2.94		56.05		69.72

Formatted: English (US)
Formatted: English (US)
Formatted: English (US)
Formatted: English (US)
Deleted: ¶
Formatted: Font: (Default) Times New Roman, 10 pt
Formatted: Font: (Default) Times New Roman, 10 pt, Danish
Formatted: Font: (Default) Times New Roman, 10 pt
Formatted: Font: (Default) Times New Roman, 10 pt, Subscript
Formatted: Superscript
Formatted: Font: (Default) Times New Roman, 10 pt, Danish
Formatted: Font: 10 pt
Formatted Table
Formatted: Font: (Default) Times New Roman, 10 pt
Formatted: Font: (Default) Times New Roman, 10 pt
Formatted: Font: (Default) Times New Roman, 10 pt
Formatted: Font: (Default) Times New Roman, 10 pt
Formatted: Font: (Default) Times New Roman, 10 pt
Formatted: Font: (Default) Times New Roman, 10 pt
Formatted: Font: (Default) Times New Roman, 10 pt
Formatted: Font: (Default) Times New Roman, 10 pt
Formatted: Font: (Default) Times New Roman, 10 pt
Formatted: Font: (Default) Times New Roman, 10 pt
Formatted: Font: (Default) Times New Roman, 10 pt
Deleted: ¶
Formatted: Subscript
Formatted: Superscript
Formatted: English (US)
Formatted: Danish
Formatted Table

Table 6a. RF_{ARI} for BC, OA, SO_4^{2-} and NO_3^- aerosols in 1990-2010 and 2030-2050 periods as calculated by the GISS-E2.1.

	BC		OA		SO_4^{2-}		NO_3^-	
	1990-2010	2030-2050	1990-2010	2030-2050	1990-2010	2030-2050	1990-2010	2030-2050
NINT_Cpl	0.20		-0.05		-0.33		-0.01	
Eclipse_AMIP	0.20		-0.06		-0.39		-0.02	
Eclipse_AMIP_NCEP	0.19		-0.08		-0.39		-0.04	
Eclipse_CplHist_3xEns	0.23		-0.05		-0.38		-0.03	
Eclipse_CplCLE_3xEns		0.17		-0.07		-0.27		-0.07
Eclipse_CplMFR_3xEns		0.09		-0.07		-0.22		-0.04
CEDS_Cpl_Hist	0.23		-0.06		-0.40		-0.04	
CEDS_Cpl_SSP126		0.13		-0.07		-0.22		-0.10
CEDS_Cpl_SSP245		0.19		-0.08		-0.29		-0.09
CEDS_Cpl_SSP370		0.28		-0.09		-0.34		-0.06
CEDS_Cpl_SSP370-lowNTCF		0.20		-0.07		-0.28		-0.09

Table 6b. RF_{ARI} for total and anthropogenic aerosols in 1990-2010 and 2030-2050 periods as calculated by the GISS-E2.1.

	Aerosols Total		Anthropogenic Aerosols	
	1990-2010	2030-2050	1990-2010	2030-2050
NINT_Cpl	-0.35		-0.19	
Eclipse_AMIP	-0.46		-0.27	
Eclipse_AMIP_NCEP	-0.47		-0.32	
Eclipse_CplHist_3xEns	-0.32		-0.22	
Eclipse_CplCLE_3xEns		-0.39		-0.24
Eclipse_CplMFR_3xEns		-0.39		-0.23
CEDS_Cpl_Hist	-0.35		-0.26	
CEDS_Cpl_SSP126		-0.40		-0.26
CEDS_Cpl_SSP245		-0.41		-0.27
CEDS_Cpl_SSP370		-0.35		-0.21
CEDS_Cpl_SSP370-lowNTCF		-0.38		-0.24

Deleted: 4
Formatted: English (US)
Formatted: Subscript
Formatted: Superscript
Formatted: Subscript
Formatted: Superscript
Deleted:
Deleted: C
Formatted: Subscript
Formatted: Superscript
Formatted: Danish
Formatted: Subscript
Formatted: Superscript
Formatted: Danish
Formatted: Font: (Default) Times New Roman, 10 pt
Formatted: Font: (Default) Times New Roman, 10 pt
Formatted: Font: 10 pt
Formatted Table
Formatted: Font: (Default) Times New Roman, 10 pt
Formatted: Font: (Default) Times New Roman, 10 pt
Formatted: Font: (Default) Times New Roman, 10 pt
Formatted: Font: (Default) Times New Roman, 10 pt
Formatted: Font: (Default) Times New Roman, 10 pt
Formatted: Font: (Default) Times New Roman, 10 pt
Formatted: Font: (Default) Times New Roman, 10 pt
Formatted: Font: (Default) Times New Roman, 10 pt
Formatted: Font: (Default) Times New Roman, 10 pt
Formatted: Font: (Default) Times New Roman, 10 pt
Formatted: Font: (Default) Times New Roman, 10 pt
Formatted: Font: (Default) Times New Roman, 10 pt
Formatted: Font: (Default) Times New Roman, 10 pt
Formatted

Table 7. Trends in near surface temperature (T_{surf}) and annual mean sea-ice extent in 1990-2010 and 2030-2050 periods as calculated by the GISS-E2.1. The bold numbers indicate the changes in 2030-2050 mean compared to the 1990-2010 mean that are statistically significant on a 95% significance level.

	T_{surf} (°C decade^{-1})		Sea-ice (10^3 km^2)	
	1990-2010	2030-2050	1990-2010	2030-2050
Observed	**0.19**		**-28.36**	
NINT_Cpl	**0.88**		**-60.10**	
Eclipse_AMIP	**0.52**		**-28.65**	
Eclipse_AMIP_NCEP	**0.62**		**-29.47**	
Eclipse_CplHist_3xEns	**0.52**		**-37.89**	
Eclipse_CplCLE_3xEns		**0.45**		**-37.212**
Eclipse_CplMFR_3xEns		**0.55**		**-41.33**
CEDS_Cpl_Hist	**0.10**		**-69.79**	
CEDS_Cpl_SSP126		**0.31**		**-23.21**
CEDS_Cpl_SSP245		**0.38**		**-24.28**
CEDS_Cpl_SSP370		**0.50**		**-39.18**
CEDS_Cpl_SSP370-lowNTCF		**0.31**		**-21.89**

Table 8. Near surface temperature (T_{surf}) and September-mean sea-ice extent in1990-2010 and 2030-2050 periods as calculated by the GISS-E2.1. The bold numbers indicate the changes in 2030-2050 mean compared to the 1990-2010 mean that are statistically significant on a 95% significance level.

	T_{surf} (°C)		September Sea-ice (10^3 km^2)	
	1990-2010	2030-2050	1990-2010	2030-2050
NINT_Cpl	-8.39			
Eclipse_AMIP	-6.54			
Eclipse_AMIP_NCEP	-7.10			
Eclipse_CplHist_3xEns	-8.13		1.56	
Eclipse_CplCLE_3xEns		**-6.06**		**1.32**
Eclipse_CplMFR_3xEns		**-5.79**		**1.31**
CEDS_Cpl_Hist	-8.52		1.60	
CEDS_Cpl_SSP126		-6.64		1.44
CEDS_Cpl_SSP245		-6.37		1.37
CEDS_Cpl_SSP370		-6.33		1.37
CEDS_Cpl_SSP370-lowNTCF		-6.56		1.38

Formatted ... [114]
Formatted ... [115]
Formatted ... [116]
Formatted ... [117]
Formatted ... [118]
Formatted ... [119]
Formatted ... [120]
Formatted ... [121]
Formatted ... [122]
Formatted ... [123]
Formatted ... [126]
Formatted ... [127]
Formatted ... [124]
Formatted Table ... [125]
Formatted ... [128]
Formatted ... [129]
Formatted ... [130]
Formatted ... [131]
Formatted ... [132]
Formatted ... [133]
Formatted ... [134]
Formatted ... [135]
Formatted ... [136]
Formatted ... [137]
Formatted ... [138]
Formatted ... [139]
Formatted ... [140]
Formatted ... [141]
Formatted ... [142]
Formatted ... [143]
Formatted ... [144]
Formatted ... [145]
Formatted ... [146]
Formatted ... [147]
Formatted ... [148]
Formatted ... [149]
Formatted ... [150]
Formatted ... [151]
Formatted ... [152]
Formatted ... [153]
Formatted ... [154]
Formatted ... [155]
Formatted ... [156]
Formatted ... [157]
Formatted ... [158]
Formatted ... [159]
Formatted ... [160]
Formatted ... [161]
Formatted ... [162]

Figures

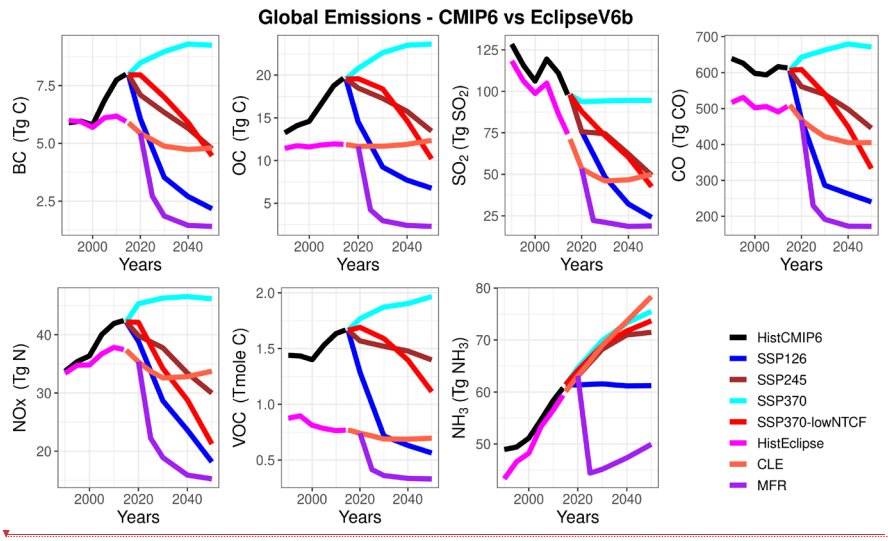

Figure 1. Global recent past and future CMIP6 and Eclipse V6b anthropogenic emissions for different pollutants and scenarios.

Deleted:

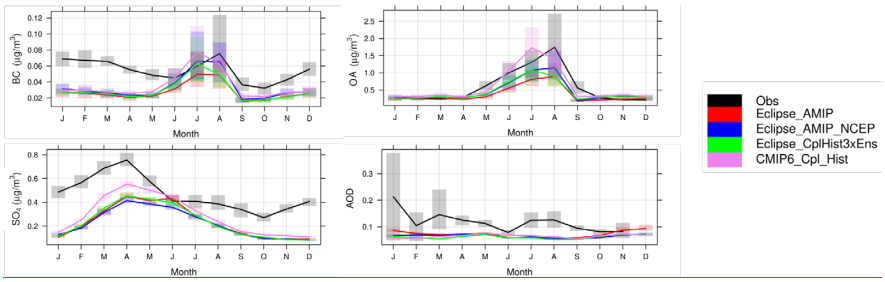

Figure 2. Observed and simulated Arctic climatological (1995-2014) monthly BC, OA, SO_4^{2-}, and AERONET AOD at 550nm (2008/09-14), along with the interannual variation shown in bars. The data presents monthly accumulated timeseries for all stations that are merged together.

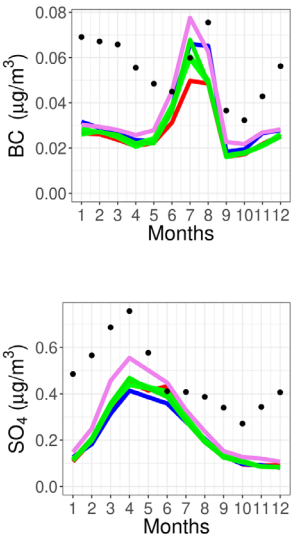

Deleted:

Deleted: C

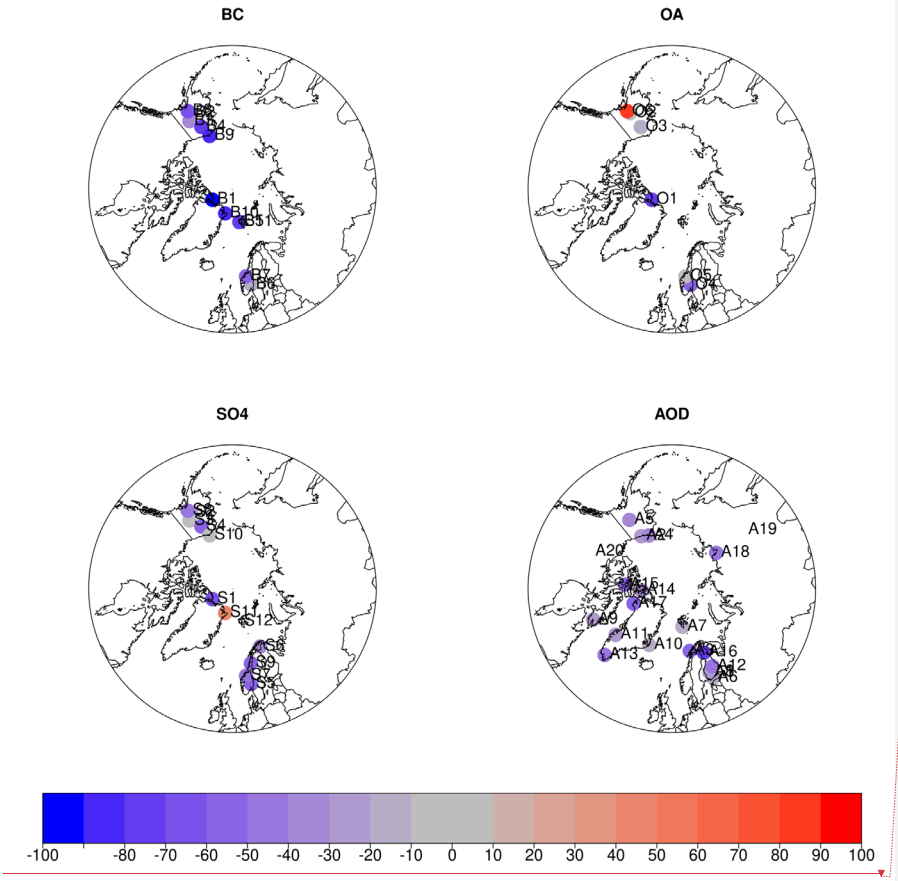

Figure 3. Spatial distribution of normalized mean bias (*NMB*, in %) for climatological mean (1995-2014) BC, OA, SO_4^{2-} and AOD at monitoring stations, calculated as the mean of all recent past simulations.

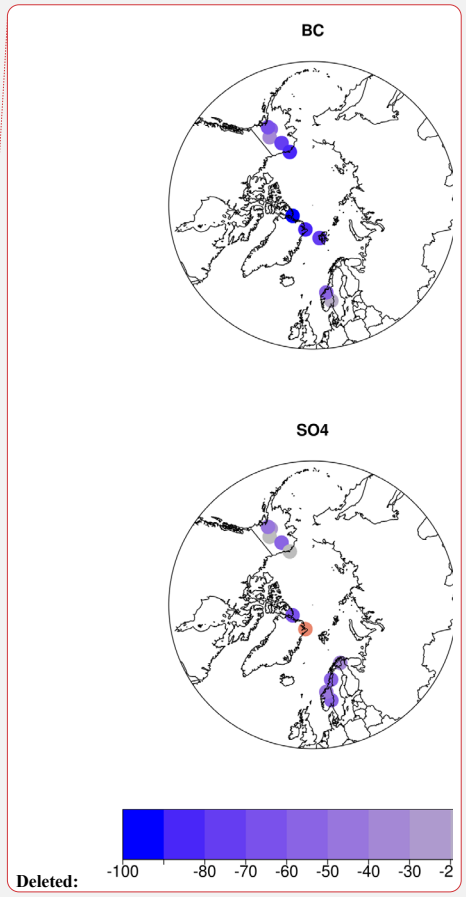

Deleted:

Deleted: C

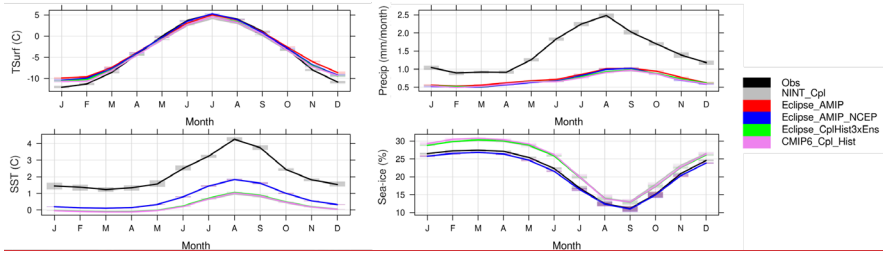

Figure 4. Observed and simulated Arctic climatological (1995-2014) surface air temperature, precipitation, sea surface temperature, and sea-ice, along with the interannual variation shown in bars. Obs denote UDel dataset for surface air temperature and precipitation, and HADISST for sea surface temperature and sea-ice extent. Note that the two AMIP runs (blue and red lines) for the SST and sea-ice are on top of each other as they use that data to run, as input.

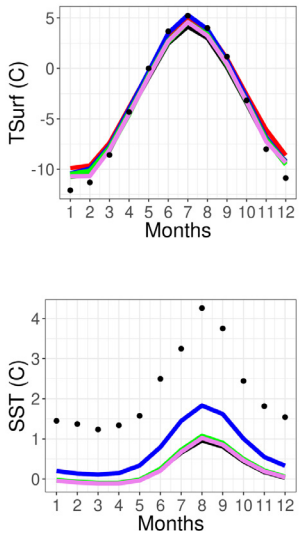

Deleted:

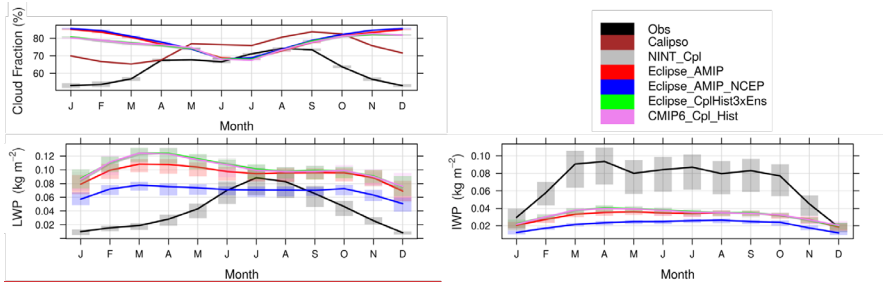

Figure 5. Observed and simulated Arctic climatological total cloud fraction (1995-2014 mean), liquid water path (2007-2014 mean), and ice water path (2007-2014 mean) , along with the interannual variation shown in bars. Obs denote Clara-A2 for the cloud fractions and CloudSat for the LWP and IWP.

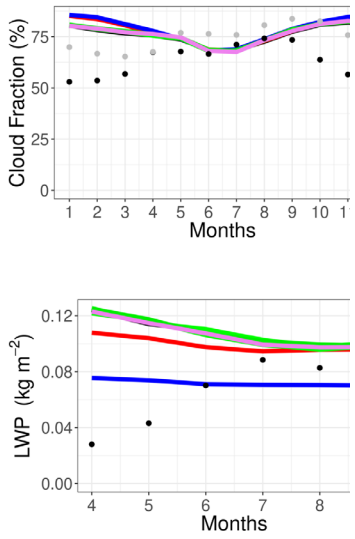

Deleted:

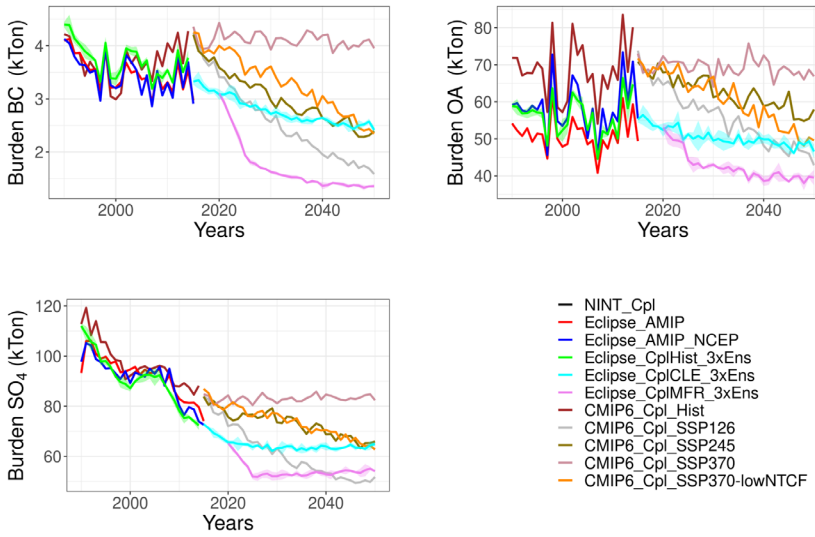

Figure 6. Arctic BC, OA, and SO_4^{2-} burdens in 1990-2050 as calculated by the GISS-E2.1 ensemble.

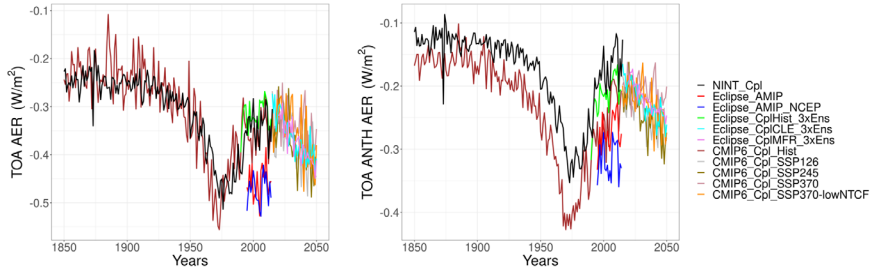

Figure 7. Arctic RF_{ARI} from anthropogenic and natural aerosols (BC+OA+SO_4^{2-}+NO_3^-+Dust+SSA), and only anthropogenic aerosols (BC+OA+SO_4^{2-}+NO_3^-) in 1850-2050 as calculated by the full GISS-E2.1 ensemble.

Formatted: Subscript

Deleted: TOA aerosol radiative forcing

Deleted: C

Deleted: OC

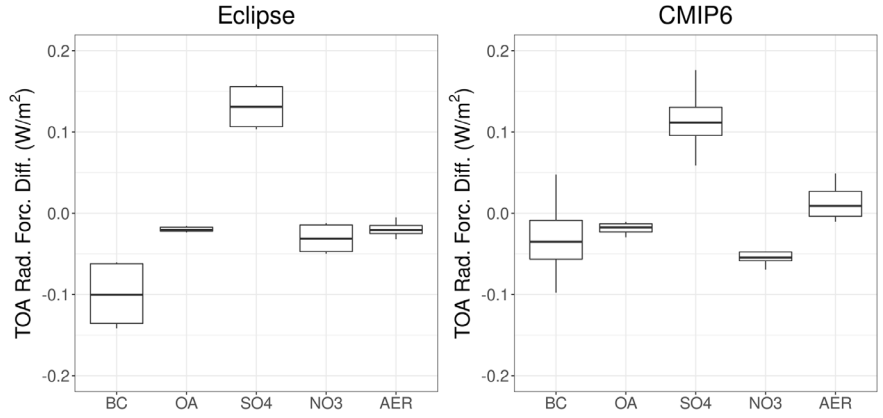

Deleted:

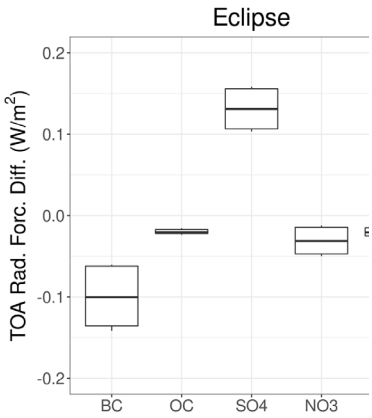

Figure 8. Box-Whisker plot showing the differences between 1990-2010 mean and 2030-2050 mean RF_{ARI} for the anthropogenic aerosol components (BC, OA, SO_4^{2-} and NO_3^-) and their sum (AER) in the Eclipse (left panel) and the CMIP6 (right panel) ensembles. The boxes show the median, the 25th and 75th percentiles. The upper whisker is located at the *smaller* of the maximum value and Q_3 + 1.5 IQR, whereas the lower whisker is located at the *larger* of the smallest x value and Q_1 – 1.5 IQR, where IQR (interquartile range) is the box height (75th percentile - 25th percentile).

Formatted: Subscript

Deleted: TOA radiative forcing

Deleted: C

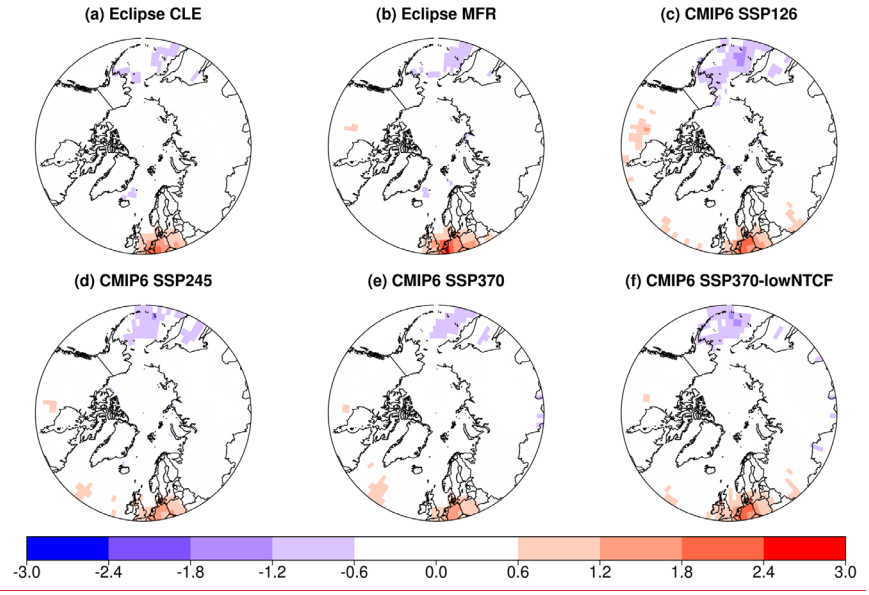

Figure 9. Spatial distribution of the statistically significant annual mean Arctic RF_{ARI} ($W\ m^{-2}$) changes between the 1990-2010 mean and the 2030-2050 mean as calculated by the GISS-E2.1 ensemble.

Formatted: Subscript

Formatted: Superscript

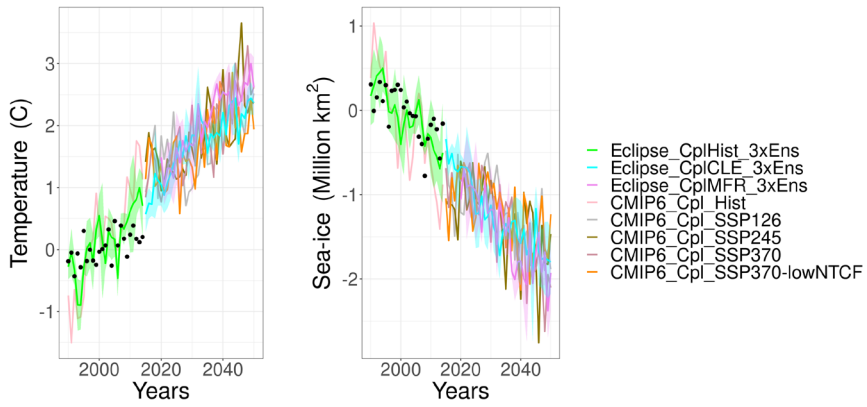

Figure 10. Arctic annual mean surface air temperature and sea-ice extent anomalies in 2015-2050 based on the 1990-2010 mean as calculated by the GISS-E2.1 ensemble.

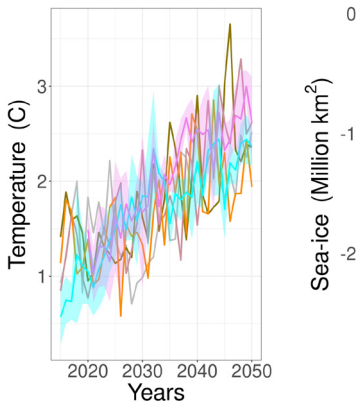

Deleted:

Deleted: 9

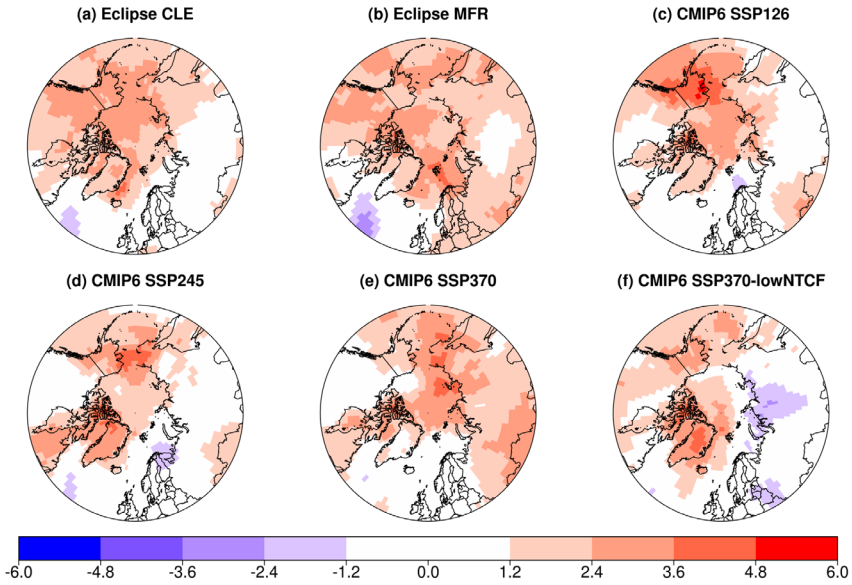

Figure 11. Spatial distribution of the statistically significant annual mean Arctic surface air temperature (°C) changes between the 1990-2010 mean and the 2030-2050 mean as calculated by the GISS-E2.1 ensemble.

Deleted: 0

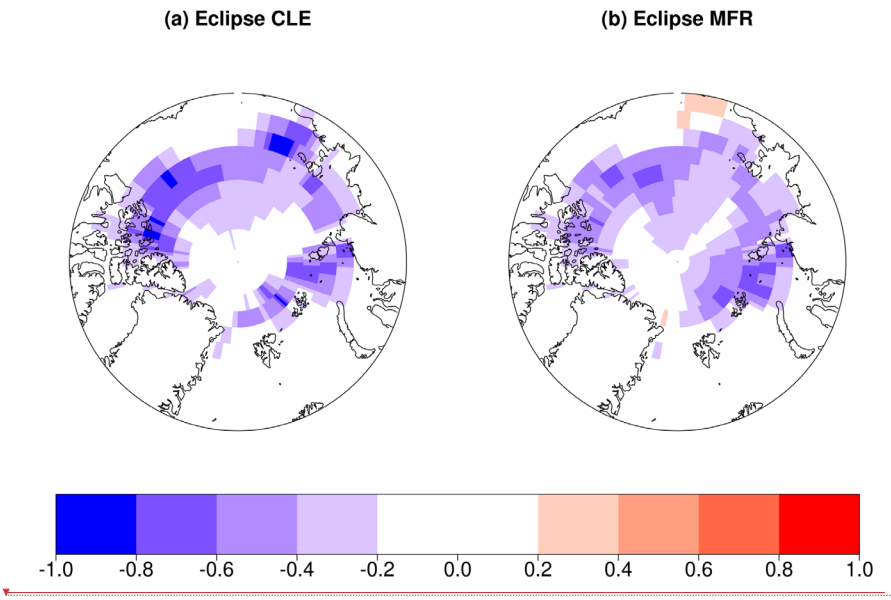

Figure 12. Spatial distribution of the statistically significant September Arctic sea-ice fraction change between the 1990-2010 mean and the 2030-2050 mean as calculated by the GISS-E2.1 Eclipse ensemble (CMIP6 ensemble is not shown due to statistically insignificant changes calculated by the student t-test).

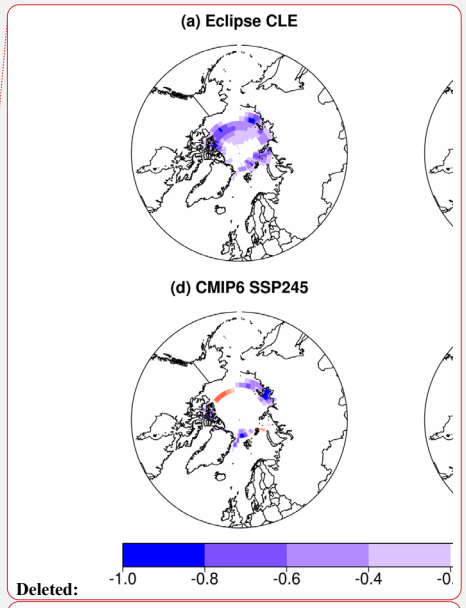

Deleted:

Deleted: 1

Page 15: [1] Formatted	**Ulas Im**	**23/05/2021 17:20:00**

Highlight

Page 15: [2] Formatted	**Ulas Im**	**23/05/2021 17:20:00**

Subscript, Highlight

Page 15: [3] Formatted	**Ulas Im**	**23/05/2021 17:20:00**

Highlight

Page 15: [4] Formatted	**Ulas Im**	**23/05/2021 17:20:00**

Subscript, Highlight

Page 15: [5] Formatted	**Ulas Im**	**23/05/2021 17:20:00**

Highlight

Page 15: [6] Formatted	**Ulas Im**	**23/05/2021 17:20:00**

Subscript, Highlight

Page 15: [7] Formatted	**Ulas Im**	**23/05/2021 17:20:00**

Highlight

Page 15: [8] Formatted	**Ulas Im**	**23/05/2021 17:20:00**

Subscript, Highlight

Page 15: [9] Formatted	**Ulas Im**	**23/05/2021 17:20:00**

Highlight

Page 15: [10] Formatted	**Ulas Im**	**23/05/2021 17:20:00**

Subscript, Highlight

Page 15: [11] Formatted	**Ulas Im**	**23/05/2021 17:20:00**

Highlight

Page 15: [12] Formatted	**Ulas Im**	**03/05/2021 11:26:00**

Font: Italic

Page 15: [13] Deleted	**Ulas Im**	**29/04/2021 09:51:00**
Page 15: [14] Formatted	**Ulas Im**	**23/05/2021 17:20:00**

Highlight

Page 15: [15] Deleted	**Ulas Im**	**03/05/2021 10:41:00**
Page 15: [16] Deleted	**Ulas Im**	**03/05/2021 10:50:00**
Page 15: [17] Deleted	**Ulas Im**	**03/05/2021 10:57:00**
Page 15: [18] Deleted	**Ulas Im**	**03/05/2021 10:58:00**
Page 15: [19] Deleted	**Ulas Im**	**03/05/2021 11:05:00**
Page 15: [20] Deleted	**Ulas Im**	**03/05/2021 11:06:00**

Page 15: [21] Formatted	**Ulas Im**	**23/05/2021 17:20:00**

Highlight

Page 15: [22] Formatted	**Ulas Im**	**23/05/2021 17:20:00**

Subscript, Highlight

Page 15: [23] Formatted	**Ulas Im**	**23/05/2021 17:20:00**

Highlight

Page 15: [24] Formatted	**Ulas Im**	**23/05/2021 17:20:00**

Subscript, Highlight

Page 15: [25] Formatted	**Ulas Im**	**23/05/2021 17:20:00**

Highlight

Page 15: [26] Formatted	**Ulas Im**	**23/05/2021 17:20:00**

Subscript, Highlight

Page 15: [27] Formatted	**Ulas Im**	**23/05/2021 17:20:00**

Highlight

Page 15: [28] Formatted	**Ulas Im**	**23/05/2021 17:20:00**

Subscript, Highlight

Page 15: [29] Formatted	**Ulas Im**	**23/05/2021 17:20:00**

Highlight

Page 15: [30] Formatted	**Ulas Im**	**23/05/2021 17:20:00**

Superscript, Highlight

Page 15: [31] Formatted	**Ulas Im**	**23/05/2021 17:20:00**

Highlight

Page 15: [32] Formatted	**Ulas Im**	**23/05/2021 17:20:00**

Not Superscript/ Subscript, Highlight

Page 16: [33] Deleted	**Ulas Im**	**03/05/2021 14:19:00**
Page 16: [33] Deleted	**Ulas Im**	**03/05/2021 14:19:00**
Page 16: [33] Deleted	**Ulas Im**	**03/05/2021 14:19:00**
Page 16: [33] Deleted	**Ulas Im**	**03/05/2021 14:19:00**
Page 16: [33] Deleted	**Ulas Im**	**03/05/2021 14:19:00**
Page 16: [33] Deleted	**Ulas Im**	**03/05/2021 14:19:00**
Page 16: [33] Deleted	**Ulas Im**	**03/05/2021 14:19:00**

Page 16: [33] Deleted	Ulas Im	03/05/2021 14:19:00
Page 16: [33] Deleted	Ulas Im	03/05/2021 14:19:00
Page 16: [33] Deleted	Ulas Im	03/05/2021 14:19:00
Page 16: [34] Formatted	Ulas Im	23/05/2021 17:20:00

Highlight

Page 16: [34] Formatted	Ulas Im	23/05/2021 17:20:00

Highlight

Page 16: [35] Deleted	Ulas Im	03/05/2021 14:23:00
Page 16: [35] Deleted	Ulas Im	03/05/2021 14:23:00
Page 16: [35] Deleted	Ulas Im	03/05/2021 14:23:00
Page 16: [35] Deleted	Ulas Im	03/05/2021 14:23:00
Page 16: [35] Deleted	Ulas Im	03/05/2021 14:23:00
Page 16: [35] Deleted	Ulas Im	03/05/2021 14:23:00
Page 16: [35] Deleted	Ulas Im	03/05/2021 14:23:00
Page 16: [35] Deleted	Ulas Im	03/05/2021 14:23:00
Page 16: [35] Deleted	Ulas Im	03/05/2021 14:23:00
Page 16: [35] Deleted	Ulas Im	03/05/2021 14:23:00
Page 16: [35] Deleted	Ulas Im	03/05/2021 14:23:00
Page 16: [35] Deleted	Ulas Im	03/05/2021 14:23:00
Page 16: [35] Deleted	Ulas Im	03/05/2021 14:23:00

Page 16: [35] Deleted	Ulas Im	03/05/2021 14:23:00

Page 16: [35] Deleted	Ulas Im	03/05/2021 14:23:00

Page 16: [35] Deleted	Ulas Im	03/05/2021 14:23:00

Page 16: [35] Deleted	Ulas Im	03/05/2021 14:23:00

Page 16: [35] Deleted	Ulas Im	03/05/2021 14:23:00

Page 16: [36] Formatted	Ulas Im	23/05/2021 17:21:00

Highlight

Page 16: [36] Formatted	Ulas Im	23/05/2021 17:21:00

Highlight

Page 16: [36] Formatted	Ulas Im	23/05/2021 17:21:00

Highlight

Page 16: [36] Formatted	Ulas Im	23/05/2021 17:21:00

Highlight

Page 16: [36] Formatted	Ulas Im	23/05/2021 17:21:00

Highlight

Page 16: [36] Formatted	Ulas Im	23/05/2021 17:21:00

Highlight

Page 16: [36] Formatted	Ulas Im	23/05/2021 17:21:00

Highlight

Page 16: [36] Formatted	Ulas Im	23/05/2021 17:21:00

Highlight

Page 16: [36] Formatted	Ulas Im	23/05/2021 17:21:00

Highlight

Page 16: [36] Formatted	Ulas Im	23/05/2021 17:21:00

Highlight

Page 16: [36] Formatted	Ulas Im	23/05/2021 17:21:00

Highlight

Page 16: [36] Formatted	Ulas Im	23/05/2021 17:21:00

Highlight

Page 16: [36] Formatted	Ulas Im	23/05/2021 17:21:00

Highlight

Page 16: [36] Formatted	Ulas Im	23/05/2021 17:21:00

Highlight

Page 16: [36] Formatted	Ulas Im	23/05/2021 17:21:00

Highlight

Page 16: [36] Formatted **Ulas Im** **23/05/2021 17:21:00**

Highlight

Page 16: [36] Formatted **Ulas Im** **23/05/2021 17:21:00**

Highlight

Page 16: [36] Formatted **Ulas Im** **23/05/2021 17:21:00**

Highlight

Page 16: [36] Formatted **Ulas Im** **23/05/2021 17:21:00**

Highlight

Page 16: [37] Deleted **Ulas Im** **03/05/2021 14:43:00**

Page 16: [37] Deleted **Ulas Im** **03/05/2021 14:43:00**

Page 16: [38] Formatted **Ulas Im** **23/05/2021 17:21:00**

Subscript, Highlight

Page 16: [38] Formatted **Ulas Im** **23/05/2021 17:21:00**

Subscript, Highlight

Page 16: [38] Formatted **Ulas Im** **23/05/2021 17:21:00**

Subscript, Highlight

Page 16: [39] Deleted **Ulas Im** **03/05/2021 14:48:00**

Page 16: [39] Deleted **Ulas Im** **03/05/2021 14:48:00**

Page 16: [40] Formatted **Ulas Im** **23/05/2021 17:21:00**

Subscript, Highlight

Page 16: [40] Formatted **Ulas Im** **23/05/2021 17:21:00**

Subscript, Highlight

Page 16: [40] Formatted **Ulas Im** **23/05/2021 17:21:00**

Subscript, Highlight

Page 17: [41] Deleted **Ulas Im** **03/05/2021 14:50:00**

Page 17: [41] Deleted **Ulas Im** **03/05/2021 14:50:00**

Page 17: [41] Deleted **Ulas Im** **03/05/2021 14:50:00**

Page 17: [41] Deleted **Ulas Im** **03/05/2021 14:50:00**

Page 17: [41] Deleted **Ulas Im** **03/05/2021 14:50:00**

Page 17: [41] Deleted **Ulas Im** **03/05/2021 14:50:00**

Page 17: [42] Formatted	Ulas Im	23/05/2021 17:21:00

Subscript, Highlight

Page 17: [42] Formatted	Ulas Im	23/05/2021 17:21:00

Subscript, Highlight

Page 17: [42] Formatted	Ulas Im	23/05/2021 17:21:00

Subscript, Highlight

Page 17: [43] Formatted	Ulas Im	23/05/2021 17:21:00

Highlight

Page 17: [43] Formatted	Ulas Im	23/05/2021 17:21:00

Highlight

Page 17: [43] Formatted	Ulas Im	23/05/2021 17:21:00

Highlight

Page 17: [43] Formatted	Ulas Im	23/05/2021 17:21:00

Highlight

Page 17: [43] Formatted	Ulas Im	23/05/2021 17:21:00

Highlight

Page 17: [43] Formatted	Ulas Im	23/05/2021 17:21:00

Highlight

Page 17: [43] Formatted	Ulas Im	23/05/2021 17:21:00

Highlight

Page 17: [43] Formatted	Ulas Im	23/05/2021 17:21:00

Highlight

Page 17: [43] Formatted	Ulas Im	23/05/2021 17:21:00

Highlight

Page 17: [43] Formatted	Ulas Im	23/05/2021 17:21:00

Highlight

Page 17: [43] Formatted	Ulas Im	23/05/2021 17:21:00

Highlight

Page 17: [43] Formatted	Ulas Im	23/05/2021 17:21:00

Highlight

Page 17: [43] Formatted	Ulas Im	23/05/2021 17:21:00

Highlight

Page 17: [43] Formatted	Ulas Im	23/05/2021 17:21:00

Highlight

Page 17: [43] Formatted	Ulas Im	23/05/2021 17:21:00

Highlight

Page 17: [43] Formatted	Ulas Im	23/05/2021 17:21:00

Highlight

Page 17: [43] Formatted	Ulas Im	23/05/2021 17:21:00

Highlight

Page 17: [43] Formatted **Ulas Im** **23/05/2021 17:21:00**

Highlight

Page 17: [43] Formatted **Ulas Im** **23/05/2021 17:21:00**

Highlight

Page 17: [43] Formatted **Ulas Im** **23/05/2021 17:21:00**

Highlight

Page 17: [43] Formatted **Ulas Im** **23/05/2021 17:21:00**

Highlight

Page 17: [43] Formatted **Ulas Im** **23/05/2021 17:21:00**

Highlight

Page 17: [43] Formatted **Ulas Im** **23/05/2021 17:21:00**

Highlight

Page 17: [43] Formatted **Ulas Im** **23/05/2021 17:21:00**

Highlight

Page 17: [43] Formatted **Ulas Im** **23/05/2021 17:21:00**

Highlight

Page 17: [43] Formatted **Ulas Im** **23/05/2021 17:21:00**

Highlight

Page 17: [43] Formatted **Ulas Im** **23/05/2021 17:21:00**

Highlight

Page 17: [43] Formatted **Ulas Im** **23/05/2021 17:21:00**

Highlight

Page 17: [43] Formatted **Ulas Im** **23/05/2021 17:21:00**

Highlight

Page 17: [43] Formatted **Ulas Im** **23/05/2021 17:21:00**

Highlight

Page 17: [43] Formatted **Ulas Im** **23/05/2021 17:21:00**

Highlight

Page 17: [43] Formatted **Ulas Im** **23/05/2021 17:21:00**

Highlight

Page 17: [44] Deleted **Ulas Im** **03/05/2021 14:54:00**

Page 17: [44] Deleted **Ulas Im** **03/05/2021 14:54:00**

Page 17: [44] Deleted **Ulas Im** **03/05/2021 14:54:00**

Page 17: [44] Deleted **Ulas Im** **03/05/2021 14:54:00**

Page 17: [44] Deleted **Ulas Im** **03/05/2021 14:54:00**

Page 17: [45] Formatted **Ulas Im** **23/05/2021 17:21:00**

Superscript, Highlight

Page 17: [45] Formatted **Ulas Im** **23/05/2021 17:21:00**

Superscript, Highlight

Page 17: [45] Formatted **Ulas Im** **23/05/2021 17:21:00**

Superscript, Highlight

Page 17: [45] Formatted **Ulas Im** **23/05/2021 17:21:00**

Superscript, Highlight

Page 17: [46] Deleted **Ulas Im** **04/05/2021 10:16:00**

Page 17: [46] Deleted **Ulas Im** **04/05/2021 10:16:00**

Page 17: [47] Formatted **Ulas Im** **23/05/2021 17:21:00**

Font: Not Italic, Highlight

Page 17: [47] Formatted **Ulas Im** **23/05/2021 17:21:00**

Font: Not Italic, Highlight

Page 17: [48] Deleted **Ulas Im** **04/05/2021 10:02:00**

Page 17: [48] Deleted **Ulas Im** **04/05/2021 10:02:00**

Page 17: [48] Deleted **Ulas Im** **04/05/2021 10:02:00**

Page 17: [48] Deleted **Ulas Im** **04/05/2021 10:02:00**

Page 17: [48] Deleted **Ulas Im** **04/05/2021 10:02:00**

Page 17: [48] Deleted **Ulas Im** **04/05/2021 10:02:00**

Page 17: [48] Deleted **Ulas Im** **04/05/2021 10:02:00**

Page 17: [49] Formatted **Ulas Im** **23/05/2021 17:21:00**

Superscript, Highlight

Page 17: [49] Formatted **Ulas Im** **23/05/2021 17:21:00**

Superscript, Highlight

Page 17: [49] Formatted **Ulas Im** **23/05/2021 17:21:00**

Superscript, Highlight

Page 17: [49] Formatted **Ulas Im** **23/05/2021 17:21:00**

Superscript, Highlight

Page 17: [50] Deleted	**Ulas Im**	**04/05/2021 11:26:00**
Page 17: [51] Deleted	**Ulas Im**	**03/05/2021 14:54:00**
Page 17: [52] Deleted	**Ulas Im**	**27/04/2021 23:09:00**
Page 17: [52] Deleted	**Ulas Im**	**27/04/2021 23:09:00**
Page 17: [52] Deleted	**Ulas Im**	**27/04/2021 23:09:00**
Page 17: [52] Deleted	**Ulas Im**	**27/04/2021 23:09:00**
Page 17: [52] Deleted	**Ulas Im**	**27/04/2021 23:09:00**
Page 18: [53] Deleted	**Ulas Im**	**07/05/2021 09:07:00**
Page 19: [54] Deleted	**Ulas Im**	**10/05/2021 11:11:00**
Page 19: [55] Deleted	**Ulas Im**	**10/05/2021 23:35:00**
Page 19: [56] Deleted	**Ulas Im**	**10/05/2021 23:37:00**
Page 19: [57] Deleted	**Ulas Im**	**10/05/2021 23:07:00**
Page 19: [58] Deleted	**Ulas Im**	**10/05/2021 14:17:00**
Page 1: [59] Deleted	**Ulas Im**	**20/05/2021 14:10:00**
Page 2: [60] Formatted	**Ulas Im**	**29/04/2021 09:16:00**

English (US)

Page 2: [60] Formatted	**Ulas Im**	**29/04/2021 09:16:00**

English (US)

Page 2: [60] Formatted	**Ulas Im**	**29/04/2021 09:16:00**

English (US)

Page 2: [60] Formatted	**Ulas Im**	**29/04/2021 09:16:00**

English (US)

Page 2: [60] Formatted	**Ulas Im**	**29/04/2021 09:16:00**

English (US)

Page 2: [60] Formatted	**Ulas Im**	**29/04/2021 09:16:00**

English (US)

Page 2: [61] Formatted **Ulas Im** **10/05/2021 23:47:00**

Font: 10 pt

Page 2: [62] Formatted Table **Ulas Im** **10/05/2021 23:47:00**

Formatted Table

Page 2: [63] Formatted **Ulas Im** **10/05/2021 23:47:00**

Font: (Default) Times New Roman, 10 pt

Page 2: [64] Formatted **Ulas Im** **29/04/2021 09:17:00**

Centred

Page 2: [65] Formatted **Ulas Im** **10/05/2021 23:47:00**

Font: (Default) Times New Roman, 10 pt, Subscript

Page 2: [65] Formatted **Ulas Im** **10/05/2021 23:47:00**

Font: (Default) Times New Roman, 10 pt, Subscript

Page 2: [66] Formatted **Ulas Im** **10/05/2021 23:47:00**

Font: (Default) Times New Roman, 10 pt

Page 2: [67] Formatted **Ulas Im** **10/05/2021 23:47:00**

Font: (Default) Times New Roman, 10 pt, Italic

Page 2: [68] Formatted **Ulas Im** **29/04/2021 09:15:00**

Centred

Page 2: [69] Formatted **Ulas Im** **10/05/2021 23:47:00**

Font: (Default) Times New Roman, 10 pt

Page 2: [70] Formatted **Ulas Im** **20/05/2021 14:14:00**

Centred

Page 2: [71] Formatted **Ulas Im** **10/05/2021 23:47:00**

Font: (Default) Times New Roman, 10 pt

Page 2: [72] Formatted **Ulas Im** **20/05/2021 14:14:00**

Centred

Page 2: [73] Formatted **Ulas Im** **10/05/2021 23:47:00**

Font: (Default) Times New Roman, 10 pt

Page 2: [74] Formatted **Ulas Im** **20/05/2021 14:14:00**

Centred

Page 2: [75] Formatted **Ulas Im** **10/05/2021 23:47:00**

Font: (Default) Times New Roman, 10 pt

Page 2: [75] Formatted **Ulas Im** **10/05/2021 23:47:00**

Font: (Default) Times New Roman, 10 pt

Page 2: [76] Formatted **Ulas Im** **20/05/2021 14:14:00**

Font: 10 pt

Page 2: [77] Formatted **Ulas Im** **20/05/2021 14:14:00**

Centred

Page 2: [78] Formatted **Ulas Im** **20/05/2021 14:14:00**

Font: (Default) Times New Roman, 10 pt

Page 2: [79] Formatted	**Ulas Im**	**20/05/2021 14:14:00**

Font: 10 pt

Page 2: [79] Formatted	**Ulas Im**	**20/05/2021 14:14:00**

Font: 10 pt

Page 2: [80] Formatted	**Ulas Im**	**20/05/2021 14:14:00**

Font: 10 pt

Page 2: [80] Formatted	**Ulas Im**	**20/05/2021 14:14:00**

Font: 10 pt

Page 2: [81] Formatted	**Ulas Im**	**20/05/2021 14:14:00**

Font: 10 pt

Page 2: [81] Formatted	**Ulas Im**	**20/05/2021 14:14:00**

Font: 10 pt

Page 2: [82] Formatted	**Ulas Im**	**20/05/2021 14:14:00**

Font: 10 pt

Page 2: [82] Formatted	**Ulas Im**	**20/05/2021 14:14:00**

Font: 10 pt

Page 2: [83] Formatted	**Ulas Im**	**20/05/2021 14:14:00**

Font: 10 pt

Page 2: [83] Formatted	**Ulas Im**	**20/05/2021 14:14:00**

Font: 10 pt

Page 2: [84] Formatted	**Ulas Im**	**20/05/2021 14:14:00**

Font: 10 pt

Page 2: [84] Formatted	**Ulas Im**	**20/05/2021 14:14:00**

Font: 10 pt

Page 2: [85] Formatted	**Ulas Im**	**20/05/2021 14:14:00**

Font: 10 pt

Page 2: [85] Formatted	**Ulas Im**	**20/05/2021 14:14:00**

Font: 10 pt

Page 2: [86] Formatted	**Ulas Im**	**10/05/2021 23:47:00**

Font: (Default) Times New Roman, 10 pt

Page 2: [87] Formatted	**Ulas Im**	**20/05/2021 14:14:00**

Centred

Page 2: [88] Formatted	**Ulas Im**	**29/04/2021 09:13:00**

Formatted

Page 2: [89] Formatted	**Ulas Im**	**10/05/2021 23:48:00**

English (US)

Page 2: [89] Formatted	**Ulas Im**	**10/05/2021 23:48:00**

English (US)

Page 2: [89] Formatted	**Ulas Im**	**10/05/2021 23:48:00**

English (US)

Page 2: [89] Formatted	**Ulas Im**	**10/05/2021 23:48:00**

English (US)

Page 2: [90] Formatted	**Ulas Im**	**10/05/2021 23:47:00**

Font: 10 pt

Page 2: [91] Formatted Table	**Ulas Im**	**10/05/2021 23:47:00**

Formatted Table

Page 2: [92] Formatted	**Ulas Im**	**10/05/2021 23:47:00**

Font: (Default) Times New Roman, 10 pt

Page 2: [93] Formatted	**Ulas Im**	**29/04/2021 09:18:00**

Centred

Page 2: [94] Formatted	**Ulas Im**	**10/05/2021 23:47:00**

Font: (Default) Times New Roman, 10 pt

Page 2: [95] Formatted	**Ulas Im**	**10/05/2021 23:47:00**

Font: (Default) Times New Roman, 10 pt, Italic

Page 2: [96] Formatted	**Ulas Im**	**29/04/2021 09:18:00**

Centred

Page 2: [97] Formatted	**Ulas Im**	**10/05/2021 23:47:00**

Font: (Default) Times New Roman, 10 pt

Page 2: [98] Formatted	**Ulas Im**	**20/05/2021 14:15:00**

Centred

Page 2: [99] Formatted	**Ulas Im**	**10/05/2021 23:47:00**

Font: (Default) Times New Roman, 10 pt

Page 2: [100] Formatted	**Ulas Im**	**20/05/2021 14:15:00**

Centred

Page 2: [101] Formatted	**Ulas Im**	**10/05/2021 23:47:00**

Font: (Default) Times New Roman, 10 pt

Page 2: [102] Formatted	**Ulas Im**	**20/05/2021 14:15:00**

Centred

Page 2: [103] Formatted	**Ulas Im**	**10/05/2021 23:47:00**

Font: (Default) Times New Roman, 10 pt

Page 2: [103] Formatted	**Ulas Im**	**10/05/2021 23:47:00**

Font: (Default) Times New Roman, 10 pt

Page 2: [104] Formatted	**Ulas Im**	**20/05/2021 14:14:00**

Font: 10 pt

Page 2: [105] Formatted	**Ulas Im**	**20/05/2021 14:15:00**

Centred

Page 2: [106] Formatted	**Ulas Im**	**20/05/2021 14:14:00**

Font: (Default) Times New Roman, 10 pt

Page 2: [107] Formatted	**Ulas Im**	**20/05/2021 14:14:00**

Font: 10 pt

Page 2: [107] Formatted **Ulas Im** **20/05/2021 14:14:00**

Font: 10 pt

Page 2: [108] Formatted **Ulas Im** **20/05/2021 14:14:00**

Font: 10 pt

Page 2: [108] Formatted **Ulas Im** **20/05/2021 14:14:00**

Font: 10 pt

Page 2: [109] Formatted **Ulas Im** **20/05/2021 14:14:00**

Font: 10 pt

Page 2: [109] Formatted **Ulas Im** **20/05/2021 14:14:00**

Font: 10 pt

Page 2: [110] Formatted **Ulas Im** **20/05/2021 14:14:00**

Font: 10 pt

Page 2: [110] Formatted **Ulas Im** **20/05/2021 14:14:00**

Font: 10 pt

Page 2: [111] Formatted **Ulas Im** **20/05/2021 14:14:00**

Font: 10 pt

Page 2: [111] Formatted **Ulas Im** **20/05/2021 14:14:00**

Font: 10 pt

Page 2: [112] Formatted **Ulas Im** **10/05/2021 23:47:00**

Font: (Default) Times New Roman, 10 pt

Page 2: [113] Formatted **Ulas Im** **20/05/2021 14:15:00**

Centred

Page 5: [114] Formatted **Ulas Im** **11/05/2021 00:07:00**

Danish

Page 5: [115] Formatted **Ulas Im** **11/05/2021 00:27:00**

Font: Bold

Page 5: [115] Formatted **Ulas Im** **11/05/2021 00:27:00**

Font: Bold

Page 5: [116] Formatted **Ulas Im** **11/05/2021 00:12:00**

Danish

Page 5: [117] Formatted **Ulas Im** **11/05/2021 00:11:00**

Danish

Page 5: [118] Formatted **Ulas Im** **11/05/2021 00:11:00**

Danish

Page 5: [119] Formatted **Ulas Im** **11/05/2021 00:12:00**

Danish

Page 5: [120] Formatted **Ulas Im** **11/05/2021 00:12:00**

Danish

Page 5: [121] Formatted **Ulas Im** **11/05/2021 00:12:00**

Danish

Page 5: [122] Formatted **Ulas Im** **11/05/2021 00:12:00**

Danish

Page 5: [123] Formatted **Ulas Im** **10/05/2021 14:42:00**

Font: Not Bold

Page 5: [123] Formatted **Ulas Im** **10/05/2021 14:42:00**

Font: Not Bold

Page 5: [123] Formatted **Ulas Im** **10/05/2021 14:42:00**

Font: Not Bold

Page 5: [123] Formatted **Ulas Im** **10/05/2021 14:42:00**

Font: Not Bold

Page 5: [124] Formatted **Ulas Im** **04/05/2021 14:22:00**

Font: 10 pt

Page 5: [125] Formatted Table **Ulas Im** **10/05/2021 14:40:00**

Formatted Table

Page 5: [126] Formatted **Ulas Im** **04/05/2021 14:22:00**

Font: (Default) Times New Roman, 10 pt

Page 5: [126] Formatted **Ulas Im** **04/05/2021 14:22:00**

Font: (Default) Times New Roman, 10 pt

Page 5: [126] Formatted **Ulas Im** **04/05/2021 14:22:00**

Font: (Default) Times New Roman, 10 pt

Page 5: [127] Formatted **Ulas Im** **04/05/2021 14:22:00**

Font: (Default) Times New Roman, 10 pt

Page 5: [127] Formatted **Ulas Im** **04/05/2021 14:22:00**

Font: (Default) Times New Roman, 10 pt

Page 5: [127] Formatted **Ulas Im** **04/05/2021 14:22:00**

Font: (Default) Times New Roman, 10 pt

Page 5: [127] Formatted **Ulas Im** **04/05/2021 14:22:00**

Font: (Default) Times New Roman, 10 pt

Page 5: [128] Formatted **Ulas Im** **04/05/2021 14:22:00**

Font: (Default) Times New Roman, 10 pt

Page 5: [129] Formatted **Ulas Im** **04/05/2021 14:22:00**

Font: (Default) Times New Roman, 10 pt

Page 5: [130] Formatted **Ulas Im** **04/05/2021 14:22:00**

Font: (Default) Times New Roman, 10 pt

Page 5: [131] Formatted **Ulas Im** **04/05/2021 14:22:00**

Font: (Default) Times New Roman, 10 pt

Page 5: [132] Formatted **Ulas Im** **04/05/2021 14:22:00**

Font: (Default) Times New Roman, 10 pt

Page 5: [133] Formatted **Ulas Im** **10/05/2021 14:40:00**

Font: (Default) Times New Roman, 10 pt, Danish

Page 5: [134] Formatted **Ulas Im** **04/05/2021 14:22:00**

Font: (Default) Times New Roman, 10 pt

Page 5: [135] Formatted **Ulas Im** **04/05/2021 14:22:00**

Font: (Default) Times New Roman, 10 pt

Page 5: [136] Formatted **Ulas Im** **10/05/2021 14:39:00**

Font: (Default) Times New Roman, 10 pt, Bold

Page 5: [137] Formatted **Ulas Im** **04/05/2021 14:22:00**

Font: (Default) Times New Roman, 10 pt

Page 5: [138] Formatted **Ulas Im** **10/05/2021 14:40:00**

Font: (Default) Times New Roman, 10 pt, Bold

Page 5: [138] Formatted **Ulas Im** **10/05/2021 14:40:00**

Font: (Default) Times New Roman, 10 pt, Bold

Page 5: [139] Formatted **Ulas Im** **04/05/2021 14:22:00**

Font: (Default) Times New Roman, 10 pt

Page 5: [140] Formatted **Ulas Im** **10/05/2021 14:39:00**

Font: (Default) Times New Roman, 10 pt, Bold

Page 5: [141] Formatted **Ulas Im** **04/05/2021 14:22:00**

Font: (Default) Times New Roman, 10 pt

Page 5: [142] Formatted **Ulas Im** **10/05/2021 14:41:00**

Font: (Default) Times New Roman, 10 pt, Bold, Danish

Page 5: [143] Formatted **Ulas Im** **04/05/2021 14:22:00**

Font: (Default) Times New Roman, 10 pt

Page 5: [144] Formatted **Ulas Im** **10/05/2021 14:39:00**

Font: (Default) Times New Roman, 10 pt, Bold

Page 5: [145] Formatted **Ulas Im** **10/05/2021 14:40:00**

Font: (Default) Times New Roman, 10 pt, Danish

Page 5: [146] Formatted **Ulas Im** **04/05/2021 14:22:00**

Font: (Default) Times New Roman, 10 pt

Page 5: [147] Formatted **Ulas Im** **04/05/2021 14:22:00**

Font: (Default) Times New Roman, 10 pt

Page 5: [148] Formatted **Ulas Im** **10/05/2021 14:39:00**

Font: (Default) Times New Roman, 10 pt, Bold

Page 5: [149] Formatted **Ulas Im** **04/05/2021 14:22:00**

Font: (Default) Times New Roman, 10 pt

Page 5: [150] Formatted **Ulas Im** **10/05/2021 14:41:00**

Font: (Default) Times New Roman, 10 pt, Danish

Page 5: [151] Formatted **Ulas Im** **04/05/2021 14:22:00**

Font: (Default) Times New Roman, 10 pt

Page 5: [152] Formatted **Ulas Im** **10/05/2021 14:39:00**

Font: (Default) Times New Roman, 10 pt, Bold

Page 5: [153] Formatted **Ulas Im** **04/05/2021 14:22:00**

Font: (Default) Times New Roman, 10 pt

Page 5: [154] Formatted **Ulas Im** **10/05/2021 14:41:00**

Font: (Default) Times New Roman, 10 pt, Danish

Page 5: [155] Formatted **Ulas Im** **04/05/2021 14:22:00**

Font: (Default) Times New Roman, 10 pt

Page 5: [156] Formatted **Ulas Im** **10/05/2021 14:39:00**

Font: (Default) Times New Roman, 10 pt, Bold

Page 5: [157] Formatted **Ulas Im** **04/05/2021 14:22:00**

Font: (Default) Times New Roman, 10 pt

Page 5: [158] Formatted **Ulas Im** **10/05/2021 14:41:00**

Font: (Default) Times New Roman, 10 pt, Danish

Page 5: [159] Formatted **Ulas Im** **04/05/2021 14:22:00**

Font: (Default) Times New Roman, 10 pt

Page 5: [160] Formatted **Ulas Im** **10/05/2021 14:39:00**

Font: (Default) Times New Roman, 10 pt, Bold

Page 5: [161] Formatted **Ulas Im** **04/05/2021 14:22:00**

Font: (Default) Times New Roman, 10 pt

Page 5: [162] Formatted **Ulas Im** **10/05/2021 14:41:00**

Font: (Default) Times New Roman, 10 pt, Danish

Supplementary Material

Historical and future Arctic aerosol burdens and impacts on radiative forcing and climate change as simulated by the GISS-E2.1 earth system model

Ulas Im[1,2,*], Kostas Tsigaridis[3,4], Gregory Faluvegi[3,4], Peter L. Langen[1,2], Joshua P. French[5], Rashed Mahmood[6], Manu A. Thomas[7], Knut von Salzen[8], Daniel C. Thomas[1,2], Cynthia H. Whaley[8], Zbigniew Klimont[9], Henrik Skov[1,2], Jørgen Brandt[1,2]

[1]Department of Environmental Science, Aarhus University, Roskilde, Denmark.
[2] Interdisciplinary Centre for Climate Change, Aarhus University, Roskilde, Denmark.
[3] Center for Climate Systems Research, Columbia University, New York, NY, USA.
[4] NASA Goddard Institute for Space Studies, New York, NY, USA.
[5] Barcelona Supercomputing Center, Barcelona, Spain.
[6] Swedish Meteorological and Hydrological Institute, Norrköping, Sweden.
[7] Candian Centre for Climate Modelling and Analysis, Environment and Climate Change Canada, Victoria, British Columbia, Canada.
[8] International Institute for Applied Systems Analysis (IIASA), Laxenburg, Austria.

Formatted: Superscript

Deleted: Thomas Manu[7]

Measurement Techniques

Black carbon

Measurements of elemental carbon (EC, which is a "type" of BC) uses a thermal/ or thermal-optical method (Chow et al, 1993) after collecting particulate matter on a Quartz filter for the EMEP, IMPROVE (including Fairbanks), and CABM datasets (Torseth et al, 2012; EMEP manual, 2014; Huang et al, 2006; Sharma et al, 2017; Huang et al, 2020). This method determines the total carbon in the particulate material and then splits this measurement into OC and EC based on an optical correction via thermal-optical protocol or only using stepwise temperature to separate OC from EC (Huang et al., 2020). These are reported for $PM_{2.5}$ and PM_{10} in the EMEP dataset, and for total suspended particles (TSP) in the Alert (CABM) dataset for the years 2005-2011. From 2011 to present, the Alert measurements of EC are for PM_1. Alert sampling frequency is a weekly integration. The overall uncertainty for Alert EC measurements is approximately upto 30%, and the IMPROVE EC measurements have 0.002 μg C m^{-3} method detection limit.

Measurements of equivalent black carbon (eBC, which is another "type" of BC) can be done via aethalometer (e.g. complementary measurements at Alert and at Zeppelin), or via particle soot absorption photometer (PSAP, Bond et al, 1999) at Gruvebadet, Zeppelin, and at Utqiagvik (Barrow), and these are for PM_1. Both use the light absorption method where the change in light

transmission through the filter over time is related to the concentration of eBC. These eBC measurements from different instruments may be systematically offset unless scaled by a third type of measurement (e.g., Continuous Soot Monitoring System, COSMOS; Kondo et al, 2011). While each of these BC measurement methods are different, and none of them fully represent BC, they have been shown to provide a range of the "true" BC concentrations, and typically agree with each other within a factor of two (2021 AMAP SLCF report, chapter 4).

Sulfate

For the IMPROVE and CABM networks, water soluble inorganic ions, like $SO4^{2-}$, are measured with ion chromatography. The particulates are caught on nylon filters, then the samples are dissolved in deionized water, separated by ion chromatography and detected by changes in conductivity (Harris, 2003). For EMEP SO_4^{2-} measurements are made daily, particulate matter is collected for 24 hours on Teflon filters kept at ambient conditions. The samples are prepared via water extraction after ultrasonic treatment. The reported concentrations are blank corrected, and the method has a detection limit of 0.01-0.02 **µ**g S m^{-3}. At Gruvebadet lab, SO_4^{2-} is by TECORA SKYPOST sampler, with a PM_{10} particle size cutoff. FTFE filters. These SO_4^{2-} measurements have up to 20% analytical uncertainty (2021 AMAP SLCF report, chapter 4).

Organic carbon

As mentioned above, OC is also measured via a thermal/or thermal- optical method (Chow et al, 1993; Huang et al., 2006; Huang e al., 2020) after being collected on a quartz filter, using the same thermal/ or thermal-optical instrumentation as EC in the IMPROVE, NAPS, EMEP and CABM measurement networks. These OC measurements have approximately 20% uncertainty (Sharma et al, 2017).

Table S1. Arctic monitoring stations and the observed aerosol species used in model evaluation

Stations	Latitude	Longitude	Aerosol Species
Alert (B1, O1, S1)	82.47	-62.5	BC, OC, $SO4^{2-}$
Denali (B2, O2, S2)	63.11	-151.19	BC, OC, $SO4^{2-}$
Fairbanks (B3, S3)	64.84	-147.72	BC, $SO4^{2-}$
Gates of the Arctic (B4, O3, S4)	67.91	-153.46	BC, OC, $SO4^{2-}$
Gruvebadet (B5)	79.00	12.00	BC
Hurdal (B6, O4, S5)	60.44	11.07	BC, OC, $SO4^{2-}$
Karasjok (S6)	69.47	25.51	$SO4^{2-}$
Karvatn (B7, O5, S7)	62.78	8.88	BC, OC, $SO4^{2-}$
TrapperCreek (B8, O6, S8)	62.32	-150.23	BC, OC, $SO4^{2-}$
Utqiagvik (B9, S10)	71.29	-156.79	BC, $SO4^{2-}$
Villum Research Station (B10, S11)	81.60	-16.67	EC, $SO4^{2-}$
ZeppelinMountain (B11, S12)	78.91	11.89	BC, $SO4^{2-}$

Formatted Table

Table S2. Arctic Aeronet stations used in model evaluation

Stations	Latitude	Longitude
Andenes (A1)	69.28	16.01
ARM_Oliktok_AK (A2)	70.50	210.12
Barrow (A3)	71.31	203.34
Bonanza Creek (A4)	64.74	211.68
Helsinki (A5)	60.20	24.96
Hornsund (A6)	77.00	15.54
Hyytiala (A7)	61.85	24.30
Iqaluit (A8)	63.75	291.46
Ittoqqortoormiit (A9)	70.48	338.05
Kangerlussuaq (A10)	67.00	309.38
Kuopio (A11)	62.89	27.63
Narsarsuaq (A12)	61.16	314.58
Opal (A13)	79.99	274.06
Pearl (A14)	80.05	273.58
Resolute_Bay (A15)	74.71	265.03
Sodankyla (A16)	67.37	26.63
Thule (A17)	76.52	291.23
Tiksi (A18)	71.59	128.92
Yakutsk (A19)	61.66	129.37
Yellowknife_Aurora (A20)	62.45	245.62

Formatted Table

Formatted Table

Formatted Table

Formatted Table

Formatted Table

Formatted Table

Deleted: ARM_Oliktok_AK ... [1]

Table S3. Model evaluation over the individual monitoring stations for black carbon (BC). Statistics used are mean bias (*MB*), mean gross error (*MGE*), normalized mean bias (*NMB*), normalized mean gross error (*NMGE*), root mean square error (*RMSE*), and Pearson's correlation (*r*).

Station	*MB*	*MGE*	*NMB*	*NMGE*	*RMSE*	*r*	Simulation
Alert	-0.04	0.04	-0.95	0.96	0.05	0.01	Eclipse_AMIP
Alert	-0.04	0.04	-0.96	0.96	0.05	0.43	Eclipse_AMIP_NCEP
Alert	-0.04	0.04	-0.95	0.95	0.05	0.13	Eclipse_CplHist1
Alert	-0.04	0.04	-0.95	0.95	0.05	0.37	Eclipse_CplHist2
Alert	-0.04	0.04	-0.95	0.95	0.05	0.30	Eclipse_CplHist3
Alert	-0.04	0.04	-0.94	0.94	0.05	0.09	CMIP6_Cpl_Hist
Denali	-0.06	0.06	-0.73	0.74	0.11	0.70	Eclipse_AMIP
Denali	-0.05	0.05	-0.62	0.66	0.09	0.77	Eclipse_AMIP_NCEP
Denali	-0.05	0.06	-0.70	0.72	0.11	0.60	Eclipse_CplHist1
Denali	-0.05	0.05	-0.68	0.70	0.11	0.60	Eclipse_CplHist2
Denali	-0.05	0.05	-0.68	0.70	0.10	0.71	Eclipse_CplHist3
Denali	-0.05	0.05	-0.65	0.69	0.10	0.65	CMIP6_Cpl_Hist
Fairbanks	-0.02	0.14	-0.19	1.28	0.33	-0.09	Eclipse_AMIP
Fairbanks	0.03	0.16	0.31	1.50	0.49	-0.08	Eclipse_AMIP_NCEP
Fairbanks	0.00	0.16	0.04	1.50	0.46	-0.09	Eclipse_CplHist1
Fairbanks	-0.02	0.14	-0.16	1.31	0.32	-0.10	Eclipse_CplHist2
Fairbanks	-0.01	0.15	-0.06	1.39	0.39	-0.09	Eclipse_CplHist3
Fairbanks	0.00	0.16	-0.04	1.44	0.40	-0.10	CMIP6_Cpl_Hist
GatesoftheArctic	-0.05	0.05	-0.74	0.77	0.13	0.84	Eclipse_AMIP

GatesoftheArctic	-0.05	0.05	-0.68	0.69	0.12	0.74	Eclipse_AMIP_NCEP
GatesoftheArctic	-0.04	0.04	-0.66	0.66	0.12	0.80	Eclipse_CplHist1
GatesoftheArctic	-0.04	0.04	-0.64	0.65	0.11	0.84	Eclipse_CplHist2
GatesoftheArctic	-0.04	0.04	-0.64	0.66	0.12	0.76	Eclipse_CplHist3
GatesoftheArctic	-0.04	0.04	-0.59	0.61	0.14	0.53	CMIP6_Cpl_Hist
Gruvebadet	-0.04	0.04	-0.93	0.93	0.06	0.43	Eclipse_AMIP
Gruvebadet	-0.05	0.05	-0.94	0.94	0.06	0.42	Eclipse_AMIP_NCEP
Gruvebadet	-0.04	0.04	-0.93	0.93	0.06	0.34	Eclipse_CplHist1
Gruvebadet	-0.04	0.04	-0.91	0.91	0.05	0.23	Eclipse_CplHist2
Gruvebadet	-0.05	0.05	-0.94	0.94	0.06	0.43	Eclipse_CplHist3
Gruvebadet	-0.04	0.04	-0.87	0.87	0.05	0.25	CMIP6_Cpl_Hist
Hurdal	-0.06	0.06	-0.43	0.44	0.07	0.64	Eclipse_AMIP
Hurdal	-0.06	0.06	-0.45	0.46	0.08	0.63	Eclipse_AMIP_NCEP
Hurdal	-0.06	0.06	-0.45	0.45	0.08	0.62	Eclipse_CplHist1
Hurdal	-0.06	0.06	-0.42	0.46	0.08	0.54	Eclipse_CplHist2
Hurdal	-0.06	0.06	-0.45	0.45	0.08	0.66	Eclipse_CplHist3
Hurdal	-0.03	0.04	-0.21	0.28	0.05	0.61	CMIP6_Cpl_Hist
Karvatn	-0.02	0.03	-0.35	0.52	0.04	-0.09	Eclipse_AMIP
Karvatn	-0.02	0.02	-0.29	0.41	0.03	0.36	Eclipse_AMIP_NCEP
Karvatn	-0.02	0.03	-0.36	0.47	0.03	-0.05	Eclipse_CplHist1
Karvatn	-0.02	0.03	-0.28	0.50	0.03	-0.13	Eclipse_CplHist2
Karvatn	-0.02	0.03	-0.37	0.47	0.03	0.08	Eclipse_CplHist3
Karvatn	-0.02	0.02	-0.31	0.43	0.03	0.04	CMIP6_Cpl_Hist

TrapperCreek	-0.03	0.04	-0.61	0.69	0.05	0.69	Eclipse_AMIP
TrapperCreek	-0.02	0.04	-0.42	0.66	0.05	0.72	Eclipse_AMIP_NCEP
TrapperCreek	-0.03	0.04	-0.57	0.70	0.05	0.57	Eclipse_CplHist1
TrapperCreek	-0.03	0.04	-0.54	0.70	0.06	0.47	Eclipse_CplHist2
TrapperCreek	-0.03	0.04	-0.52	0.69	0.05	0.62	Eclipse_CplHist3
TrapperCreek	-0.03	0.04	-0.46	0.76	0.07	0.53	CMIP6_Cpl_Hist
Utqiagvik	-0.02	0.03	-0.74	0.90	0.04	-0.23	Eclipse_AMIP
Utqiagvik	-0.02	0.03	-0.67	0.88	0.04	-0.12	Eclipse_AMIP_NCEP
Utqiagvik	-0.02	0.03	-0.67	0.94	0.04	-0.23	Eclipse_CplHist1
Utqiagvik	-0.02	0.03	-0.69	0.92	0.04	-0.21	Eclipse_CplHist2
Utqiagvik	-0.02	0.03	-0.69	0.93	0.04	-0.21	Eclipse_CplHist3
Utqiagvik	0.00	0.03	0.10	0.83	0.04	-0.04	CMIP6_Cpl_Hist
ZeppelinMountain	-0.02	0.02	-0.83	0.83	0.03	0.38	Eclipse_AMIP
ZeppelinMountain	-0.02	0.02	-0.84	0.84	0.03	0.48	Eclipse_AMIP_NCEP
ZeppelinMountain	-0.02	0.02	-0.80	0.81	0.03	0.32	Eclipse_CplHist1
ZeppelinMountain	-0.02	0.02	-0.81	0.82	0.03	0.40	Eclipse_CplHist2
ZeppelinMountain	-0.02	0.02	-0.81	0.82	0.03	0.39	Eclipse_CplHist3
ZeppelinMountain	-0.02	0.02	-0.74	0.77	0.03	0.23	CMIP6_Cpl_Hist

Table S4. Model evaluation over the individual monitoring stations for organic carbon (OC). Statistics used are mean bias (*MB*), mean gross error (*MGE*), normalized mean bias (*NMB*), normalized mean gross error (*NMGE*), root mean square error (*RMSE*), and Pearson's correlation (*r*).

Station	*MB*	*MGE*	*NMB*	*NMGE*	*RMSE*	*r*	Simulation
Alert	-0.13	0.14	-0.83	0.88	0.16	0.01	Eclipse_AMIP
Alert	-0.13	0.13	-0.83	0.84	0.15	0.24	Eclipse_AMIP_NCEP
Alert	-0.12	0.13	-0.79	0.81	0.15	0.04	Eclipse_CplHist1
Alert	-0.12	0.13	-0.79	0.82	0.15	0.11	Eclipse_CplHist2
Alert	-0.12	0.12	-0.79	0.81	0.15	0.21	Eclipse_CplHist3
Alert	-0.11	0.12	-0.72	0.77	0.14	0.09	CMIP6_Cpl_Hist
Denali	-0.20	0.44	-0.31	0.66	1.59	0.69	Eclipse_AMIP
Denali	0.03	0.46	0.05	0.69	1.34	0.77	Eclipse_AMIP_NCEP
Denali	-0.10	0.49	-0.15	0.74	1.68	0.59	Eclipse_CplHist1
Denali	-0.07	0.48	-0.11	0.73	1.76	0.52	Eclipse_CplHist2
Denali	-0.05	0.45	-0.07	0.68	1.55	0.67	Eclipse_CplHist3
Denali	0.17	0.56	0.26	0.84	1.74	0.62	CMIP6_Cpl_Hist
GatesOfTheArctic	-0.28	0.38	-0.44	0.59	0.68	0.90	Eclipse_AMIP
GatesOfTheArctic	-0.18	0.30	-0.29	0.47	0.55	0.93	Eclipse_AMIP_NCEP
GatesOfTheArctic	-0.16	0.30	-0.25	0.46	0.52	0.94	Eclipse_CplHist1
GatesOfTheArctic	-0.13	0.23	-0.20	0.37	0.41	0.96	Eclipse_CplHist2
GatesOfTheArctic	-0.12	0.26	-0.19	0.41	0.43	0.95	Eclipse_CplHist3
GatesOfTheArctic	-0.06	0.38	-0.10	0.59	1.01	0.84	CMIP6_Cpl_Hist

Hurdal	-0.60	0.73	-0.52	0.64	0.98	-0.50	Eclipse_AMIP
Hurdal	-0.65	0.77	-0.57	0.67	0.98	-0.26	Eclipse_AMIP_NCEP
Hurdal	-0.59	0.69	-0.51	0.61	0.93	-0.54	Eclipse_CplHist1
Hurdal	-0.58	0.72	-0.50	0.63	0.92	-0.48	Eclipse_CplHist2
Hurdal	-0.66	0.74	-0.57	0.65	0.97	-0.49	Eclipse_CplHist3
Hurdal	-0.44	0.65	-0.39	0.57	0.87	-0.62	CMIP6_Cpl_Hist
Karvatn	-0.67	0.67	-0.82	0.83	0.89	-0.24	Eclipse_AMIP
Karvatn	-0.64	0.66	-0.79	0.80	0.88	-0.25	Eclipse_AMIP_NCEP
Karvatn	-0.68	0.68	-0.83	0.83	0.89	-0.35	Eclipse_CplHist1
Karvatn	-0.66	0.67	-0.81	0.82	0.88	-0.23	Eclipse_CplHist2
Karvatn	-0.68	0.69	-0.84	0.84	0.89	-0.20	Eclipse_CplHist3
Karvatn	-0.62	0.63	-0.76	0.77	0.85	-0.36	CMIP6_Cpl_Hist
TrapperCreek	0.06	0.32	0.13	0.73	0.71	0.74	Eclipse_AMIP
TrapperCreek	0.33	0.49	0.76	1.12	1.17	0.80	Eclipse_AMIP_NCEP
TrapperCreek	0.14	0.39	0.32	0.88	0.86	0.63	Eclipse_CplHist1
TrapperCreek	0.20	0.44	0.45	1.00	1.05	0.52	Eclipse_CplHist2
TrapperCreek	0.23	0.41	0.53	0.92	0.99	0.68	Eclipse_CplHist3
TrapperCreek	0.50	0.61	1.13	1.39	1.97	0.63	CMIP6_Cpl_Hist

Table S5. Model evaluation over the individual monitoring stations for sulfate ($SO4^{2-}$). Statistics used are mean bias (*MB*), mean gross error (*MGE*), normalized mean bias (*NMB*), normalized mean gross error (*NMGE*), root mean square error (*RMSE*), and Pearson's correlation (*r*).

Station	*MB*	*MGE*	*NMB*	*NMGE*	*RMSE*	*r*	Simulation
Alert	-0.34	0.37	-0.72	0.77	0.48	0.38	Eclipse_AMIP
Alert	-0.37	0.37	-0.77	0.78	0.49	0.50	Eclipse_AMIP_NCEP
Alert	-0.34	0.36	-0.72	0.76	0.48	0.44	Eclipse_CplHist1
Alert	-0.34	0.35	-0.72	0.75	0.47	0.48	Eclipse_CplHist2
Alert	-0.34	0.36	-0.72	0.75	0.47	0.46	Eclipse_CplHist3
Alert	-0.32	0.34	-0.68	0.72	0.45	0.51	CMIP6_Cpl_Hist
Denali	-0.15	0.17	-0.46	0.53	0.24	0.38	Eclipse_AMIP
Denali	-0.16	0.17	-0.50	0.52	0.23	0.67	Eclipse_AMIP_NCEP
Denali	-0.14	0.16	-0.45	0.50	0.23	0.48	Eclipse_CplHist1
Denali	-0.14	0.16	-0.43	0.49	0.23	0.46	Eclipse_CplHist2
Denali	-0.14	0.16	-0.42	0.48	0.22	0.51	Eclipse_CplHist3
Denali	-0.09	0.14	-0.28	0.43	0.20	0.54	CMIP6_Cpl_Hist
Fairbanks	0.00	0.19	0.02	1.04	0.24	-0.36	Eclipse_AMIP
Fairbanks	0.02	0.20	0.09	1.07	0.25	-0.28	Eclipse_AMIP_NCEP
Fairbanks	0.00	0.19	0.03	1.05	0.24	-0.35	Eclipse_CplHist1
Fairbanks	0.01	0.19	0.06	1.02	0.23	-0.34	Eclipse_CplHist2
Fairbanks	0.01	0.19	0.06	1.02	0.23	-0.31	Eclipse_CplHist3
Fairbanks	0.08	0.23	0.46	1.22	0.27	-0.32	CMIP6_Cpl_Hist
GatesoftheArctic	-0.25	0.26	-0.64	0.66	0.36	0.53	Eclipse_AMIP

GatesoftheArctic	-0.26	0.26	-0.65	0.66	0.36	0.64	Eclipse_AMIP_NCEP
GatesoftheArctic	-0.25	0.26	-0.64	0.66	0.37	0.49	Eclipse_CplHist1
GatesoftheArctic	-0.24	0.25	-0.61	0.63	0.36	0.48	Eclipse_CplHist2
GatesoftheArctic	-0.25	0.25	-0.63	0.64	0.36	0.52	Eclipse_CplHist3
GatesoftheArctic	-0.20	0.22	-0.51	0.55	0.31	0.64	CMIP6_Cpl_Hist
Hurdal	-0.55	0.57	-0.60	0.62	0.72	0.28	Eclipse_AMIP
Hurdal	-0.54	0.55	-0.59	0.59	0.65	0.69	Eclipse_AMIP_NCEP
Hurdal	-0.55	0.58	-0.60	0.63	0.72	0.29	Eclipse_CplHist1
Hurdal	-0.52	0.55	-0.57	0.60	0.69	0.34	Eclipse_CplHist2
Hurdal	-0.54	0.57	-0.59	0.62	0.72	0.27	Eclipse_CplHist3
Hurdal	-0.49	0.53	-0.53	0.57	0.68	0.29	CMIP6_Cpl_Hist
Karasjok	-0.48	0.52	-0.58	0.61	0.67	0.24	Eclipse_AMIP
Karasjok	-0.50	0.50	-0.60	0.60	0.63	0.55	Eclipse_AMIP_NCEP
Karasjok	-0.46	0.49	-0.55	0.58	0.65	0.28	Eclipse_CplHist1
Karasjok	-0.47	0.48	-0.56	0.57	0.65	0.29	Eclipse_CplHist2
Karasjok	-0.46	0.48	-0.55	0.57	0.64	0.34	Eclipse_CplHist3
Karasjok	-0.38	0.42	-0.46	0.50	0.59	0.35	CMIP6_Cpl_Hist
Karvatn	-0.16	0.26	-0.29	0.49	0.39	0.39	Eclipse_AMIP
Karvatn	-0.19	0.20	-0.35	0.38	0.30	0.76	Eclipse_AMIP_NCEP
Karvatn	-0.19	0.25	-0.35	0.47	0.38	0.44	Eclipse_CplHist1
Karvatn	-0.16	0.24	-0.31	0.46	0.37	0.45	Eclipse_CplHist2
Karvatn	-0.18	0.24	-0.34	0.45	0.36	0.50	Eclipse_CplHist3
Karvatn	-0.13	0.23	-0.24	0.42	0.35	0.48	CMIP6_Cpl_Hist

TrapperCreek	-0.16	0.17	-0.49	0.52	0.25	0.52	Eclipse_AMIP
TrapperCreek	-0.17	0.17	-0.52	0.52	0.23	0.75	Eclipse_AMIP_NCEP
TrapperCreek	-0.16	0.17	-0.49	0.50	0.24	0.61	Eclipse_CplHist1
TrapperCreek	-0.15	0.17	-0.46	0.51	0.24	0.51	Eclipse_CplHist2
TrapperCreek	-0.15	0.16	-0.46	0.49	0.23	0.60	Eclipse_CplHist3
TrapperCreek	-0.11	0.14	-0.32	0.42	0.21	0.60	CMIP6_Cpl_Hist
Tustervatn	-0.22	0.29	-0.39	0.52	0.40	0.37	Eclipse_AMIP
Tustervatn	-0.26	0.27	-0.46	0.47	0.35	0.72	Eclipse_AMIP_NCEP
Tustervatn	-0.25	0.29	-0.44	0.52	0.42	0.36	Eclipse_CplHist1
Tustervatn	-0.23	0.29	-0.40	0.51	0.40	0.38	Eclipse_CplHist2
Tustervatn	-0.24	0.28	-0.43	0.50	0.40	0.41	Eclipse_CplHist3
Tustervatn	-0.18	0.26	-0.32	0.46	0.38	0.40	CMIP6_Cpl_Hist
Utqiagvik	-0.25	0.29	-0.61	0.70	0.37	0.16	Eclipse_AMIP
Utqiagvik	-0.23	0.28	-0.56	0.68	0.35	0.24	Eclipse_AMIP_NCEP
Utqiagvik	-0.24	0.29	-0.59	0.69	0.37	0.13	Eclipse_CplHist1
Utqiagvik	-0.24	0.29	-0.59	0.69	0.37	0.15	Eclipse_CplHist2
Utqiagvik	-0.25	0.28	-0.60	0.68	0.36	0.22	Eclipse_CplHist3
Utqiagvik	-0.20	0.26	-0.48	0.63	0.33	0.27	CMIP6_Cpl_Hist
VillumNord	-0.26	0.30	-0.64	0.72	0.41	0.41	Eclipse_AMIP
VillumNord	-0.28	0.30	-0.68	0.72	0.41	0.49	Eclipse_AMIP_NCEP
VillumNord	-0.26	0.29	-0.63	0.72	0.41	0.41	Eclipse_CplHist1
VillumNord	-0.26	0.29	-0.64	0.70	0.40	0.48	Eclipse_CplHist2
VillumNord	-0.26	0.29	-0.64	0.70	0.40	0.50	Eclipse_CplHist3

VillumNord	-0.24	0.27	-0.59	0.67	0.38	0.51	CMIP6_Cpl_Hist
ZeppelinMountain	0.04	0.11	0.29	0.80	0.16	0.34	Eclipse_AMIP
ZeppelinMountain	0.03	0.08	0.18	0.62	0.11	0.59	Eclipse_AMIP_NCEP
ZeppelinMountain	0.05	0.11	0.39	0.80	0.15	0.49	Eclipse_CplHist1
ZeppelinMountain	0.05	0.11	0.37	0.79	0.15	0.47	Eclipse_CplHist2
ZeppelinMountain	0.05	0.10	0.33	0.74	0.15	0.52	Eclipse_CplHist3
ZeppelinMountain	0.08	0.12	0.56	0.89	0.17	0.52	CMIP6_Cpl_Hist

Table S6. Model evaluation over the individual Aeronet monitoring stations for aerosol optical depth at 550 nm. Statistics used are mean bias (*MB*), mean gross error (*MGE*), normalized mean bias (*NMB*), normalized mean gross error (*NMGE*), root mean square error (*RMSE*), and Pearson's correlation (*r*).

Station	*MB*	*MGE*	*NMB*	*NMGE*	*RMSE*	*r*	Simulation
Andenes	-0.02	0.05	-0.22	0.49	0.06	0.03	Eclipse_AMIP
Andenes	-0.03	0.04	-0.30	0.36	0.04	0.35	Eclipse_AMIP_NCEP
Andenes	-0.04	0.05	-0.43	0.46	0.05	0.04	Eclipse_CplHist1
Andenes	-0.03	0.04	-0.32	0.43	0.05	0.22	Eclipse_CplHist2
Andenes	-0.01	0.05	-0.13	0.47	0.06	-0.09	Eclipse_CplHist3
Andenes	-0.03	0.04	-0.29	0.36	0.04	0.20	CMIP6_Cpl_Hist
ARM_HyytialaFinland	0.00	0.06	0.00	0.65	0.07	-0.73	Eclipse_AMIP
ARM_HyytialaFinland	-0.02	0.04	-0.23	0.46	0.04	-0.51	Eclipse_AMIP_NCEP
ARM_HyytialaFinland	-0.02	0.05	-0.21	0.55	0.05	-0.68	Eclipse_CplHist1
ARM_HyytialaFinland	-0.02	0.05	-0.18	0.62	0.05	-0.88	Eclipse_CplHist2
ARM_HyytialaFinland	-0.03	0.04	-0.30	0.42	0.04	-0.46	Eclipse_CplHist3
ARM_HyytialaFinland	-0.02	0.04	-0.20	0.44	0.04	-0.73	CMIP6_Cpl_Hist
Barrow	-0.08	0.08	-0.55	0.58	0.10	0.34	Eclipse_AMIP
Barrow	-0.09	0.09	-0.62	0.63	0.11	0.44	Eclipse_AMIP_NCEP
Barrow	-0.09	0.09	-0.65	0.66	0.12	0.22	Eclipse_CplHist1
Barrow	-0.09	0.09	-0.64	0.66	0.11	0.35	Eclipse_CplHist2
Barrow	-0.08	0.09	-0.62	0.63	0.11	0.28	Eclipse_CplHist3
Barrow	-0.08	0.08	-0.56	0.59	0.11	0.02	CMIP6_Cpl_Hist

Bonanza_Creek	-0.08	0.09	-0.57	0.61	0.16	0.13	Eclipse_AMIP
Bonanza_Creek	-0.08	0.08	-0.56	0.57	0.15	0.52	Eclipse_AMIP_NCEP
Bonanza_Creek	-0.10	0.10	-0.67	0.70	0.17	0.00	Eclipse_CplHist1
Bonanza_Creek	-0.10	0.10	-0.66	0.66	0.17	0.28	Eclipse_CplHist2
Bonanza_Creek	-0.09	0.09	-0.64	0.66	0.17	0.31	Eclipse_CplHist3
Bonanza_Creek	-0.09	0.09	-0.59	0.62	0.17	0.09	CMIP6_Cpl_Hist
Helsinki	0.00	0.06	-0.05	0.64	0.08	-0.51	Eclipse_AMIP
Helsinki	-0.02	0.04	-0.25	0.47	0.05	-0.35	Eclipse_AMIP_NCEP
Helsinki	0.00	0.07	0.02	0.75	0.10	-0.54	Eclipse_CplHist1
Helsinki	-0.03	0.04	-0.27	0.39	0.04	-0.14	Eclipse_CplHist2
Helsinki	-0.02	0.05	-0.19	0.50	0.05	-0.68	Eclipse_CplHist3
Helsinki	-0.01	0.06	-0.10	0.59	0.07	-0.66	CMIP6_Cpl_Hist
Hornsund	-0.04	0.04	-0.38	0.42	0.05	0.40	Eclipse_AMIP
Hornsund	-0.05	0.05	-0.48	0.48	0.06	0.31	Eclipse_AMIP_NCEP
Hornsund	-0.04	0.05	-0.43	0.49	0.06	0.07	Eclipse_CplHist1
Hornsund	-0.04	0.05	-0.39	0.48	0.06	0.14	Eclipse_CplHist2
Hornsund	-0.03	0.04	-0.31	0.41	0.06	0.25	Eclipse_CplHist3
Hornsund	-0.04	0.05	-0.43	0.48	0.06	-0.07	CMIP6_Cpl_Hist
Hyytiala	-0.02	0.04	-0.23	0.44	0.05	-0.31	Eclipse_AMIP
Hyytiala	-0.03	0.05	-0.26	0.50	0.06	-0.50	Eclipse_AMIP_NCEP
Hyytiala	0.00	0.06	-0.03	0.61	0.10	-0.32	Eclipse_CplHist1
Hyytiala	-0.02	0.03	-0.22	0.35	0.04	0.09	Eclipse_CplHist2
Hyytiala	-0.03	0.04	-0.32	0.44	0.05	-0.09	Eclipse_CplHist3

Hyytiala	-0.02	0.05	-0.18	0.49	0.06	-0.31	CMIP6_Cpl_Hist
Iqaluit	-0.01	0.04	-0.10	0.42	0.06	0.01	Eclipse_AMIP
Iqaluit	-0.02	0.05	-0.20	0.49	0.07	0.07	Eclipse_AMIP_NCEP
Iqaluit	-0.03	0.04	-0.35	0.45	0.06	-0.13	Eclipse_CplHist1
Iqaluit	-0.02	0.04	-0.18	0.47	0.06	0.18	Eclipse_CplHist2
Iqaluit	-0.02	0.05	-0.21	0.52	0.07	-0.17	Eclipse_CplHist3
Iqaluit	-0.02	0.04	-0.22	0.39	0.06	0.14	CMIP6_Cpl_Hist
Ittoqqortoormiit	-0.01	0.02	-0.20	0.24	0.02	0.71	Eclipse_AMIP
Ittoqqortoormiit	-0.03	0.03	-0.35	0.35	0.03	0.72	Eclipse_AMIP_NCEP
Ittoqqortoormiit	-0.03	0.04	-0.43	0.49	0.04	-0.07	Eclipse_CplHist1
Ittoqqortoormiit	-0.03	0.03	-0.41	0.44	0.03	0.02	Eclipse_CplHist2
Ittoqqortoormiit	-0.02	0.03	-0.34	0.39	0.03	0.43	Eclipse_CplHist3
Ittoqqortoormiit	-0.02	0.03	-0.26	0.35	0.03	0.01	CMIP6_Cpl_Hist
Kangerlussuaq	0.03	0.05	0.37	0.64	0.09	0.50	Eclipse_AMIP
Kangerlussuaq	0.01	0.04	0.08	0.49	0.05	0.22	Eclipse_AMIP_NCEP
Kangerlussuaq	-0.02	0.03	-0.32	0.36	0.03	0.04	Eclipse_CplHist1
Kangerlussuaq	-0.02	0.02	-0.24	0.29	0.03	0.35	Eclipse_CplHist2
Kangerlussuaq	-0.01	0.03	-0.07	0.41	0.04	0.40	Eclipse_CplHist3
Kangerlussuaq	0.00	0.03	-0.05	0.38	0.03	0.06	CMIP6_Cpl_Hist
Kuopio	-0.04	0.04	-0.41	0.44	0.05	-0.19	Eclipse_AMIP
Kuopio	-0.04	0.04	-0.43	0.46	0.05	-0.18	Eclipse_AMIP_NCEP
Kuopio	-0.04	0.04	-0.46	0.46	0.05	-0.16	Eclipse_CplHist1
Kuopio	-0.04	0.04	-0.40	0.41	0.05	0.23	Eclipse_CplHist2

Kuopio	-0.04	0.04	-0.40	0.41	0.05	-0.06	Eclipse_CplHist3
Kuopio	-0.04	0.04	-0.40	0.41	0.05	0.10	CMIP6_Cpl_Hist
Narsarsuaq	-0.01	0.02	-0.10	0.24	0.02	-0.22	Eclipse_AMIP
Narsarsuaq	0.00	0.02	-0.03	0.30	0.03	-0.18	Eclipse_AMIP_NCEP
Narsarsuaq	-0.02	0.03	-0.23	0.35	0.03	-0.99	Eclipse_CplHist1
Narsarsuaq	-0.01	0.02	-0.14	0.23	0.02	-0.79	Eclipse_CplHist2
Narsarsuaq	-0.02	0.02	-0.33	0.33	0.03	-0.15	Eclipse_CplHist3
Narsarsuaq	0.02	0.04	0.34	0.52	0.06	-0.03	CMIP6_Cpl_Hist
OPAL	-0.03	0.03	-0.41	0.45	0.04	0.57	Eclipse_AMIP
OPAL	-0.03	0.03	-0.44	0.46	0.04	0.30	Eclipse_AMIP_NCEP
OPAL	-0.03	0.04	-0.47	0.57	0.05	-0.39	Eclipse_CplHist1
OPAL	-0.03	0.04	-0.44	0.49	0.04	0.23	Eclipse_CplHist2
OPAL	-0.03	0.04	-0.45	0.50	0.04	0.18	Eclipse_CplHist3
OPAL	-0.02	0.04	-0.29	0.56	0.05	-0.69	CMIP6_Cpl_Hist
PEARL	-0.03	0.03	-0.41	0.42	0.04	0.54	Eclipse_AMIP
PEARL	-0.03	0.04	-0.43	0.51	0.05	0.04	Eclipse_AMIP_NCEP
PEARL	-0.03	0.04	-0.47	0.50	0.05	-0.01	Eclipse_CplHist1
PEARL	-0.03	0.03	-0.44	0.46	0.04	0.19	Eclipse_CplHist2
PEARL	-0.03	0.03	-0.35	0.42	0.04	0.12	Eclipse_CplHist3
PEARL	-0.03	0.04	-0.35	0.49	0.05	-0.28	CMIP6_Cpl_Hist
Resolute_Bay	-0.04	0.04	-0.46	0.47	0.06	0.39	Eclipse_AMIP
Resolute_Bay	-0.04	0.04	-0.43	0.43	0.05	0.56	Eclipse_AMIP_NCEP
Resolute_Bay	-0.04	0.05	-0.49	0.50	0.06	0.24	Eclipse_CplHist1

Resolute_Bay	-0.04	0.04	-0.48	0.48	0.06	0.45	Eclipse_CplHist2
Resolute_Bay	-0.04	0.04	-0.45	0.47	0.05	0.48	Eclipse_CplHist3
Resolute_Bay	-0.03	0.04	-0.36	0.40	0.05	0.05	CMIP6_Cpl_Hist
Sodankyla	-0.03	0.05	-0.35	0.55	0.05	-0.60	Eclipse_AMIP
Sodankyla	-0.03	0.04	-0.38	0.50	0.05	-0.62	Eclipse_AMIP_NCEP
Sodankyla	-0.04	0.05	-0.48	0.54	0.06	-0.93	Eclipse_CplHist1
Sodankyla	-0.03	0.06	-0.36	0.68	0.06	-0.81	Eclipse_CplHist2
Sodankyla	-0.03	0.04	-0.36	0.50	0.05	-0.76	Eclipse_CplHist3
Sodankyla	-0.03	0.04	-0.40	0.45	0.05	-0.29	CMIP6_Cpl_Hist
Thule	-0.04	0.04	-0.43	0.49	0.05	0.07	Eclipse_AMIP
Thule	-0.04	0.04	-0.47	0.51	0.05	0.36	Eclipse_AMIP_NCEP
Thule	-0.04	0.05	-0.52	0.56	0.05	0.05	Eclipse_CplHist1
Thule	-0.04	0.04	-0.48	0.51	0.05	0.20	Eclipse_CplHist2
Thule	-0.03	0.04	-0.41	0.49	0.05	0.15	Eclipse_CplHist3
Thule	-0.03	0.04	-0.35	0.49	0.05	-0.26	CMIP6_Cpl_Hist
Tiksi	-0.14	0.14	-0.67	0.67	0.23	0.00	Eclipse_AMIP
Tiksi	-0.15	0.15	-0.72	0.72	0.24	-0.02	Eclipse_AMIP_NCEP
Tiksi	-0.16	0.16	-0.78	0.78	0.24	0.30	Eclipse_CplHist1
Tiksi	-0.16	0.16	-0.76	0.76	0.24	0.03	Eclipse_CplHist2
Tiksi	-0.14	0.14	-0.68	0.68	0.23	0.00	Eclipse_CplHist3
Tiksi	-0.15	0.15	-0.74	0.74	0.23	0.67	CMIP6_Cpl_Hist
Yakutsk	-0.13	0.13	-0.66	0.66	0.15	0.44	Eclipse_AMIP
Yakutsk	-0.11	0.11	-0.55	0.56	0.14	0.45	Eclipse_AMIP_NCEP

Yakutsk	-0.12	0.12	-0.60	0.62	0.15	0.38	Eclipse_CplHist1
Yakutsk	-0.13	0.13	-0.66	0.66	0.15	0.49	Eclipse_CplHist2
Yakutsk	-0.12	0.12	-0.65	0.65	0.15	0.34	Eclipse_CplHist3
Yakutsk	-0.10	0.11	-0.54	0.57	0.14	0.36	CMIP6_Cpl_Hist
Yellowknife_Aurora	-0.07	0.10	-0.46	0.63	0.17	-0.35	Eclipse_AMIP
Yellowknife_Aurora	-0.07	0.10	-0.47	0.61	0.17	-0.09	Eclipse_AMIP_NCEP
Yellowknife_Aurora	-0.10	0.10	-0.62	0.62	0.18	-0.27	Eclipse_CplHist1
Yellowknife_Aurora	-0.08	0.09	-0.51	0.60	0.16	0.14	Eclipse_CplHist2
Yellowknife_Aurora	-0.09	0.10	-0.55	0.63	0.18	-0.30	Eclipse_CplHist3
Yellowknife_Aurora	-0.08	0.11	-0.51	0.67	0.18	-0.31	CMIP6_Cpl_Hist

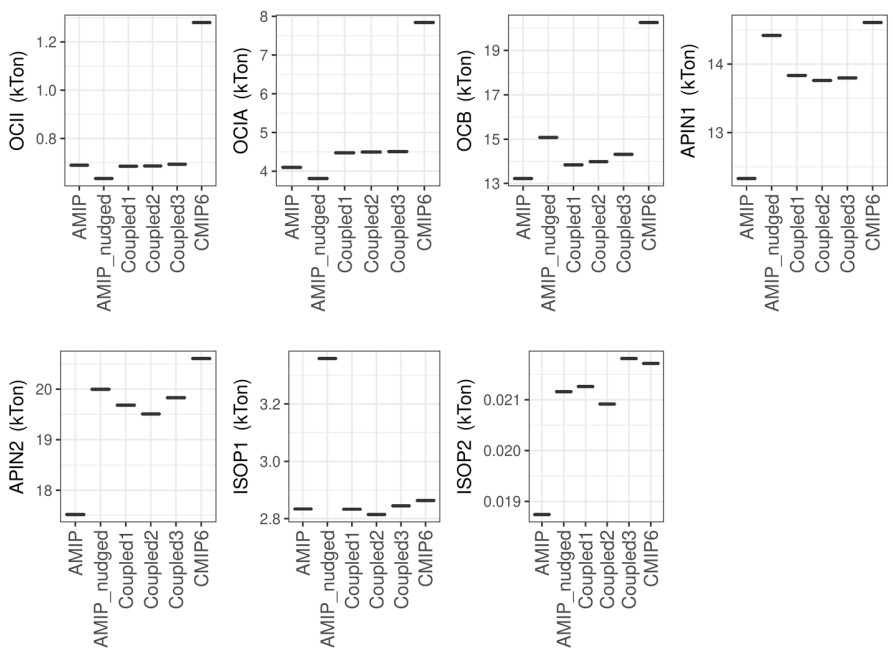

Figure S1. Present day SOA burdens in the Eclipse and CMIP6 ensemble.

Deleted:

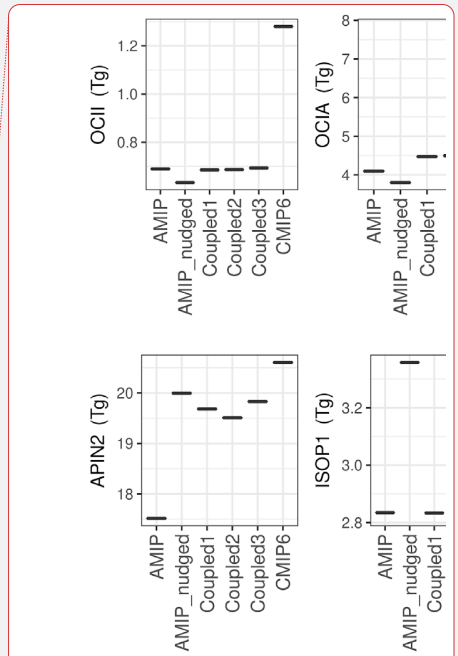

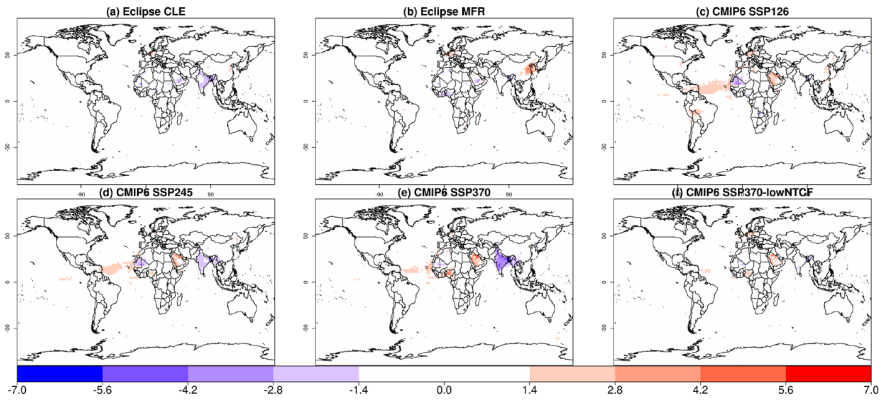

Figure S2. Spatial distribution of the statistically significant annual mean global RF_{ARI} ($W\ m^{-2}$) changes between the 1990-2010 mean and the 2030-2050 mean as calculated by the GISS-E2.1 ensemble.

Formatted: Subscript

Formatted: Superscript

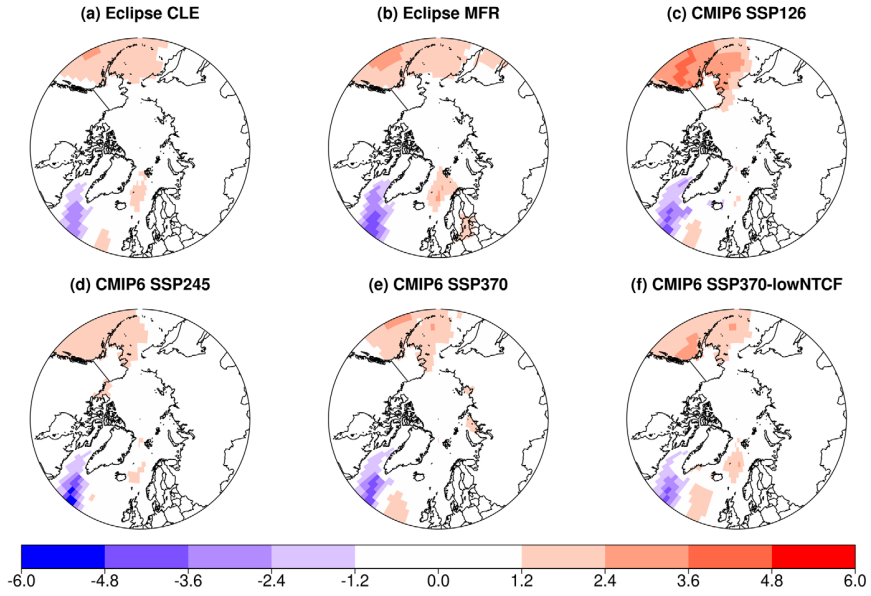

Figure S3. Spatial distribution of the annual mean Arctic sea surface temperature (°C) change between the 1990-2010 mean and the 2030-2050 mean as calculated by the GISS-E2.1 ensemble.

Deleted: 2

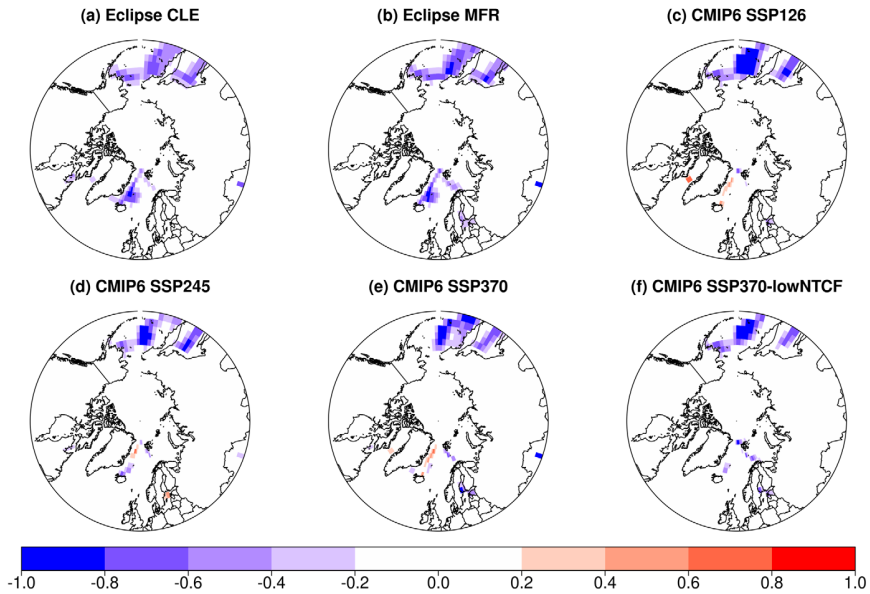

Figure S4. Spatial distribution of the March Arctic sea-ice fraction change between the 1990-2010 mean and the 2030-2050 mean as calculated by the GISS-E2.1 ensemble.

Deleted: 3

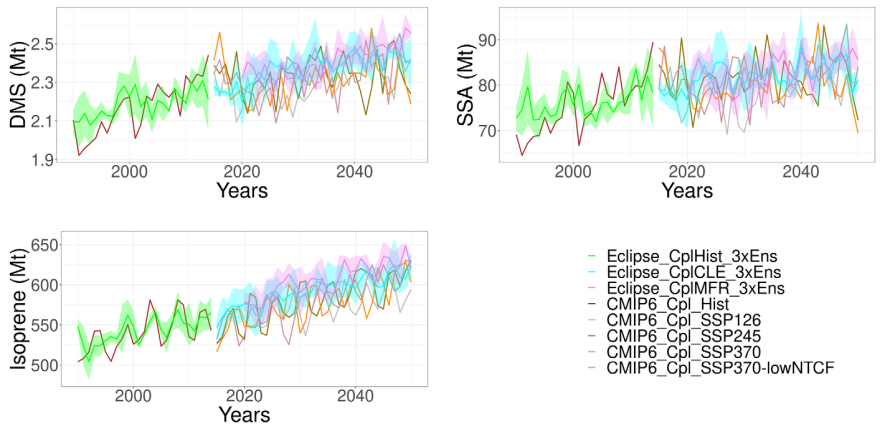

Figure S5. Arctic DMS and sea-salt and global isoprene emissions anomalies in 1900-2050 based on the 1990-2010 mean, simulated by the Eclipse and CMIP6 ensembles.

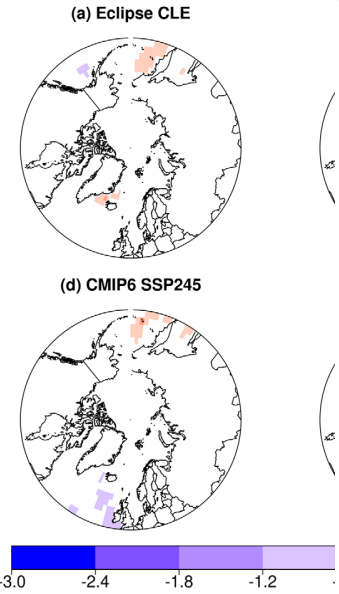

Deleted: Figure S4. Spatial distribution of the March Arctic DMS emissions (Tg) change between the 1990-2010 mean and the 2030-2050 mean as calculated by the GISS-E2.1 ensemble.

Page Break

¶ ... [2]

Deleted: 8

References

Bauguitte, S., *Facility for airborne atmospheric measurements: Science instruments*, Available at http://www.faam.ac.uk/index.php/science-instruments/chemistry/64-instruments , 2014.

Biraud, S. C., *Carbon Monoxide Mixing Ratio System Handbook*, U.S. Dept. of Energy, ARM Clim. Res. Facil., Washington, D. C., 2011.

Bottenheim, J.W., J.D. Fuentes, D.W. Tarasick and K.G. Anlauf (2002), *Ozone in the Arctic lower troposphere during winter and spring 2000 (ALERT2000),* Atmospheric Environment, 36, 2535-2544.

Chow, J. C., Watson, J. G., Pritchett, L. C., Pierson, W. R., Frazier, C. a. and Purcell, R. G.: *The dri thermal/optical reflectance carbon analysis system: description, evaluation and applications in U.S. Air quality studies*, Atmos. Environ. Part A. Gen. Top., 27(8), 11851201, doi:10.1016/0960-1686(93)90245-T, 1993

Betty Croft, R. V. Martin, W. Richard Leaitch, J Burkart, R.Y.-W. Chang, D. B. Collins, P. L. Hayes, A. L. Hodshire6, L. Huang, J. K. Kodros, A. Moravek4, E. L. Mungall, J. G. Murphy, S. Sharma, S. Tremblay, G. R. Wentworth, M. D. Willis, J. P. D. Abbatt, and J. R. Pierce, *Arctic*

marine secondary organic aerosol contributes significantly to summertime particle size distributions in the Canadian Arctic Archipelago, Atmos. Chem. Phys., 19, 2787–2812, 2019, https://doi.org/10.5194/acp-19-2787-2019.

Dabek-Zlotorzynska, E., Dann, T. F., Martinelango, P. K., Celo, V. Brook, J. R., Mathieu, D., Ding, L., Austin, C. C., *Canadian National Air Pollution Surveillance (NAPS) PM2.5 speciation program: Methodology and PM2.5 chemical composition for the years 2003–2008*, Atmospheric Environment,45,3, 2011,673-686, https://doi.org/10.1016/j.atmosenv.2010.10.024.

EMEP manual, https://projects.nilu.no/ccc/manual/ , 2014.

Galbally, I.E., Schultz, M.G., Buchmann, B., Gilge, S., Guenther, F., Koide, H., Oltmans, S., Patrick, L., Scheel, H.-E., Smit, H., Steinbacher, M., Steinbrecht, W., Tarasova, O., Viallon, J., Volz-Thomas, A., Weber, M., Wielgosz R. and Zellweger C. *Guidelines for Continuous Measurement of Ozone in the Troposphere*, GAW Report No 209, Publication WMO-No. 1110, ISBN 978-92-63-11110-4, World Meteorological Organisation, Geneva Switzerland, 76 pp., 2013. http://www.wmo.int/pages/prog/arep/gaw/gaw-reports.html

Harris, D.: *Quantitative Chemical Analysis, 6th ed*., edited by M. L. Byrd, Michelle Russel Julet, New York., 2003.

Kondo, Y., L. Sahu, N. Moteki, F. Khan, N. Takegawa, X. Liu, M. Koike, T. Miyakawa (2011), *Consistency and traceability of black carbon measurements made by laser-induced incandescence, thermal-optical transmittance, and filter-based photo-absorption techniques*, Aerosol Sci. Tech., 45, 295-312, DOI: 10.1080/02786826.2010.533215.

Leaitch, W. R., Sharma,s., Huang, L., Toom-Sauntry, D., Chivulescu, A., Macdonald, A.A., von Salzen, K., *Dimethyl Sulfide Control of the Clean Summertime Arctic Aerosol and Cloud*, Elementa Science of the Anthropocene 1: 000017, 2013, doi:10.12952/journal.elementa.000017dlementascience.org

Malm, W. C., Sisler, J. F., Huffman, D., Eldred, R. A., and Cahill, T. A.: *Spatial and seasonal trends in particle concentration and optical extinction in the United States*, J. Geophys. Res., 99, 1347–1370, 1994.

Nattinger, Kristian C. *Temporal and Spatial Trends of Fine Particulate Matter Composition in Fairbanks, Alaska*, PhD thesis, University of Alaska, Fairbanks, 2016.

Sharma, S., W. R. Leaitch, L. Huang, Daniel Veber, Felicia Kolonjari, Wendy Zhang, Sarah J. Hanna, Allan K. Bertram, and John A. Ogren, *An evaluation of three methods for measuring*

black carbon in Alert, Canada, Atmos. Chem. Phys., 17, 15225–15243, 2017, https://doi.org/10.5194/acp-17-15225-2017.

Sharma, S., Barrie, L.A., Magnusson, E., Brattstrom , G., Leaitch, W. R., Steffen, A., and Landsberger, S., *A factor and trends analysis of multidecadal lower tropospheric observations of arctic aerosol composition, black carbon, ozone, and mercury at Alert, Canada*. J.Geophys. Res.:Atmospheres, 124, 14,133-14,161, 2019, http://doi.org/10.1029/2019JD030844.

Skov, H. Christensen, J. Goodsite, M.E. Heidam, N.Z. Jensen, B. Wåhlin, P. and Geernaert, G.: *The fate of elemental mercury in Arctic during atmospheric mercury depletion episodes and the load of atmospheric mercury to Arctic*. ES & T, 38, 2373-2382, 2004.

Tørseth, K., Aas, W., Breivik, K., Fjæraa, A. M., Fiebig, M., Hjellbrekke, A. G., Lund Myhre, C., Solberg, S., and Yttri, K. E.: *Introduction to the European Monitoring and Evaluation Programme (EMEP) and observed atmospheric composition change during 1972–2009*, Atmos. Chem. Phys., 12, 5447–5481, doi:10.5194/acp-12-5447-2012, 2012.

Page 4: [1] Deleted	**Ulas Im**	**21/05/2021 12:32:00**
Page 23: [2] Deleted	**Ulas Im**	**18/05/2021 11:03:00**